November 2012

contact: qualif@mercator-ocean.fr

QuO Va Dis?
Quarterly Ocean Validation Display #9

Validation bulletin for April-May-June (AMJ) 2012

Edition:
Charles Desportes, Marie Drévillon, Bruno Levier, Charly Régnier
(MERCATOR OCEAN/Production Dep./Products Quality)

Contributions :
Eric Greiner (CLS)
Elisabeth Rémy, Anne Daudin, Jean-Michel Lellouche, Olivier Le Galloudec (MERCATOR OCEAN/ Production Dep./R&D)

Credits for validation methodology and tools:
Eric Greiner, Mounir Benkiran, Nathalie Verbrugge, Hélène Etienne (CLS)
Fabrice Hernandez, Laurence Crosnier (MERCATOR OCEAN)
Nicolas Ferry, Gilles Garric, Jean-Michel Lellouche, Olivier Le Galloudec (MERCATOR OCEAN)
Jean-Marc Molines (CNRS), Sébastien Theeten (Ifremer), Mélanie Juza (IMEDEA), the DRAKKAR and NEMO groups.
Nicolas Pene (ex-AKKA), Silvana Buarque (Météo-France), the BCG group (Météo-France, CERFACS)

Information on input data:
Christine Boone, Stéphanie Guinehut, Gaël Nicolas (CLS/ARMOR team)

Abstract

*This bulletin gives an estimate of the accuracy of MERCATOR OCEAN's analyses and forecast for the season of April-May-June **2012**. It also provides a summary of useful information on the context of the production for this period. Diagnostics will be displayed for the global 1/12° (PSY4), global ¼° (PSY3) and the Atlantic and Mediterranean zoom at 1/12° (PSY2) monitoring and forecasting systems currently producing daily 3D temperature salinity and current products.*

Table of contents

I Executive summary

The Mercator Ocean global monitoring and forecasting system (MyOcean V1 global MFC) is evaluated for the **period April-May-June 2012**. The system's description of the **ocean water masses is very accurate on global average** and almost everywhere between the bottom and 200m. Between 0 and 500m departures from *in situ* observations **rarely exceed 1 °C and 0.2 psu** (mostly in high variability regions like the Gulf Stream or the Eastern Tropical Pacific). During this northern hemisphere spring season the systems display stratification weaknesses in the North Atlantic and North Pacific (resulting in cold biases in the surface layer especially in the global ¼° PSY3V3R1).

A **cold SST** (and 3DT) bias of 0.1 °C on average is observed all year long in the **high resolution global at 1/12°** (PSY4V1R3) which does not yet benefit from the bias correction scheme that is implemented in PSY3V3R1 and PSY2V4R2.

The temperature and salinity forecast have **significant skill** in many regions of the ocean in the 0-500m layer, but the signal is noisy.

The monitoring systems are generally very close to altimetric observations (global average of 6 cm residual RMS error). Future updates of the Mean Dynamic Topography will correct the local biases that are currently observed for instance in the Banda Sea, and hopefully will prevent the **degradation of the subsurface currents at the Equator**. The latter are unrealistic in both global systems, especially in the warm pools in the western equatorial Pacific and Atlantic.

The **surface currents** are underestimated in the mid latitudes and overestimated at the equator with respect to *in situ* measurements of drifting buoys (drifter velocities are corrected of windage and slippage with a method developed by Mercator Océan). The underestimation ranges from 20% in strong currents up to 60% in weak currents. On the contrary the orientation of the current vectors is well represented**. The 1/12° global currents are slightly closer to drifters' observations than ¼° global currents**, especially in equatorial countercurrents.

The high resolution North East Atlantic at 1/36° (IBI36V1) with no data assimilation is accurate on average. **Tidal and residual sea surface elevations are well represented**. Zones of intense tidal mixing are less accurate. The mixed layer is too shallow in the Bay of Biscay (the thermocline is too diffusive). The upwelling along the Iberian coasts is underestimated.

The sea ice concentrations are overestimated in the Arctic all year round in the global 1/12° PSY4V1R3 (unrealistic rheology). PSY3V3R1 **global ¼° sea ice concentrations are realistic** but there is still too much accumulation of ice in the Arctic, especially in the Beaufort Sea. The sea ice concentration is underestimated in the Barents Sea. Antarctic sea ice concentration is underestimated in austral autmun (including AMJ 2012) due to atmospheric forcing problems in PSY3V3R1. The global 1/12° PSY4V1R3 sea ice concentration is overestimated all year round in the Antarctic because of rheology problems.

The **large scale structures corresponding to specific biogeographic regions** (double-gyres, ACC, etc…) **are well reproduced** by the global biogeochemical model at 1° BIOMER. However there are **serious discrepancies especially in the Tropical band** due to overestimated vertical velocities. The latter are the source of anomalous levels of nitrates in the equatorial surface layer. O2, however, is close to climatological estimations. The seasonal cycle is realistic in most parts of the ocean. However **the timing of the blooms is not yet in phase with observations**. This season the South Atlantic bloom is underestimated.

II Status and evolutions of the systems

II.1. Short description and current status of the systems

PSY3V3R1 and PSY2V4R1 systems have been operated at MERCATOR OCEAN since 2010 December, 15th. These systems provide the version 1 products of the MyOcean global monitoring and forecasting centre. As reminded in Table 1 (and illustrated for PSY2 in Figure 1) the atmospheric forcing is updated daily with the latest ECMWF analysis and forecast, and a new oceanic forecast is run every day for both PSY3V3R1 and PSY2V4R1. This daily update of the forcing (referred to as PSY3QV3R1 and PSY2QV4R1) is not broadcasted by MyOcean (it will be for V2).
An updated version (or release) of PSY2 called PSY2V4R2 is operated since the end of June 2011 and replaces PSY2V4R1. The PSY2QV4R2 system also replaces the PSY2QV4R1 system. The improvements of this version have been described in *QuOVaDis?* #5 and are reminded in Table 1.

The latest scientific evolutions of the systems (in red in Table 1) were described in *QuOVaDis?* #2 and #5 and will not be detailed here. The PSY3V3R1 system is started in October 2006 from a 3D climatology of temperature and salinity (World Ocean Atlas Levitus 2005) while the PSY2V4R2 is started in October 2009. After a short 3-month spin up of the model and data assimilation, the performance of PSY3V3R1 has been evaluated on the 2007-2009 period (MyOcean internal calibration report, which results are synthesised in *QuOVaDis?* #2).

System name	Domain	resolution	Model version	Assimilation software version	Assimilated observations	Inter dependencies	Status of production
PSY3V3R1	Global	¼° on the horizontal, 50 levels on the vertical	ORCA025 LIM2 EVP NEMO 3.1 3-hourly atmospheric forcing from ECMWF, bulk CORE	SAM2 (SEEK Kernel) + IAU and bias correction	RTG-SST, SLA from Jason 1, Jason 2 and Envisat, in situ profile from CORIOLIS		Weekly 14-days forecast Daily update of atmospheric forcings for daily 7-day forecast PSY3QV3
PSY4V1R3	Global	1/12° on the horizontal, 50 levels on the vertical	ORCA12 LIM2 NEMO 1.09 Daily atmospheric forcing from ECMWF, bulk CLIO	SAM2 (SEEK Kernel) + IAU	RTG-SST, SLA from Jason 1, Jason 2 and Envisat, in situ profile from CORIOLIS		Weekly 7-day forecast
PSY2V4R2	Tropical, North Atlantic and Mediterranean Sea region	1/12° on the horizontal, 50 levels on the	NATL12 LIM2 EVP NEMO 3.1 3-hourly atmospheric	SAM2 (SEEK Kernel) + IAU and bias correction +	AVHRR-AMSR Reynold ¼° SST, SLA from Jason	Open boundary conditions from PSY3V3R1	Weekly Daily update of atmospheric forcings

		vertical	forcing from ECMWF, bulk CORE	new MDT CNES/CLS09 bias corrected + more observation error near coasts	1, Jason 2 and Envisat, in situ profile from CORIOLIS		PSY2QV4
IBI36V2	North East Atlantic and West Mediterranean Sea (Iberian, Biscay and Ireland) region	1/36° on the horizontal, 50 levels on the vertical	NEATL36 NEMO 2.3 3-hourly atmospheric forcing from ECMWF, bulk CORE, tides, time-splitting, GLS vertical mixing, corrected bathymetry, river runoffs from SMHI & Prévimer	none	none	Two weeks spin up initialized with PSY2V4R1 and open boundary conditions from PSY2V4R1	Weekly spin up two weeks back in time. Daily update of atmospheric forcings for daily 5-day forecast IBI36QV1 To be broadcasted starting from June 2011.
BIOMER	Global	1° on the horizontal, 50 levels on the vertical	PISCES, NEMO 2.3, offline	none	none	Two weeks hindcast with IR global forcing degraded at 1°	1-week average two weeks back in time.

Table 1 : Synthetic description of the Mercator Ocean operational systems. In red, the major upgrades with respect to previous versions (when existing).

The PSY4V1R3 system is delivering operational products since the beginning of 2010. It does not yet benefit from the latest scientific improvements of PSY3V3R1 and PSY2V4R2. The update of PSY4 is planned for the version 3 of MyOcean 2, which will be available in April 2013. This system delivers 7-day forecast (and not 14-day like PSY3V3R1 and PSY2V4R2).

The IBI36V1 system is described in QuO Va Dis? #5 and #6 (see also Table 1 and Figure 1). The nominal MyOcean production unit for IBI is Puertos Del Estado (Spain) while Mercator Océan produces the back up products. The Mercator Océan IBI system is officially operational since June 2011.

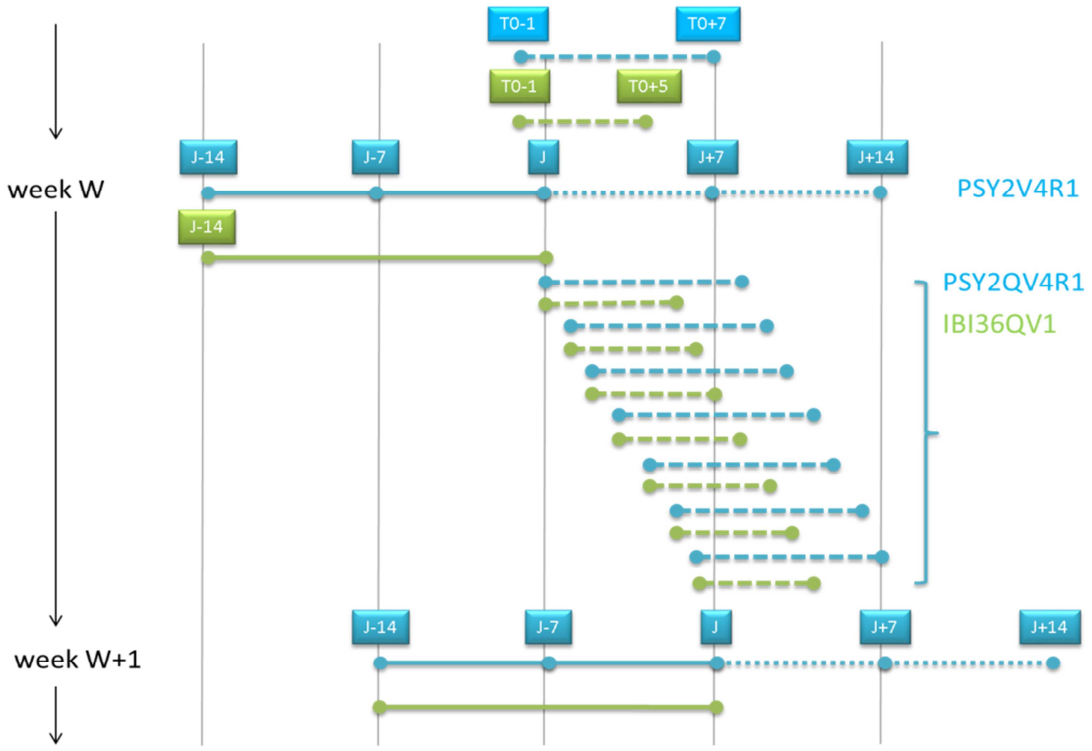

Figure 1: schematic of the operational forecast scenario for IBI36QV1 (green) and PSY2QV4R1 (blue). Solid lines are the PSY2V4R1 weekly hindcast and nowcast experiments, and the IBI36V1 spin up. Dotted lines are the weekly 14-day forecast, dashed lines are daily updates of the ocean forecast forced with the latest ECMWF atmospheric analysis and forecast. The operational scenario of PSY3V3R1 and PSY3QV3R1 is similar to PSY2's scenario. In the case of PSY4V1R3, only weekly hindcast, nowcast and 7-day forecast are performed.

The BIOMER system is described in QuO Va Dis? #6 (see also Table 1 and Figure 2). It is a global hindcast biogeochemical model forced by physical ocean fields. The biogeochemical model used is PISCES. The coupling between ocean physics and biogeochemistry is performed offline. The physical fields from PSY3V3R1 are "degraded" to 1° horizontal resolution and 7-day time resolution.

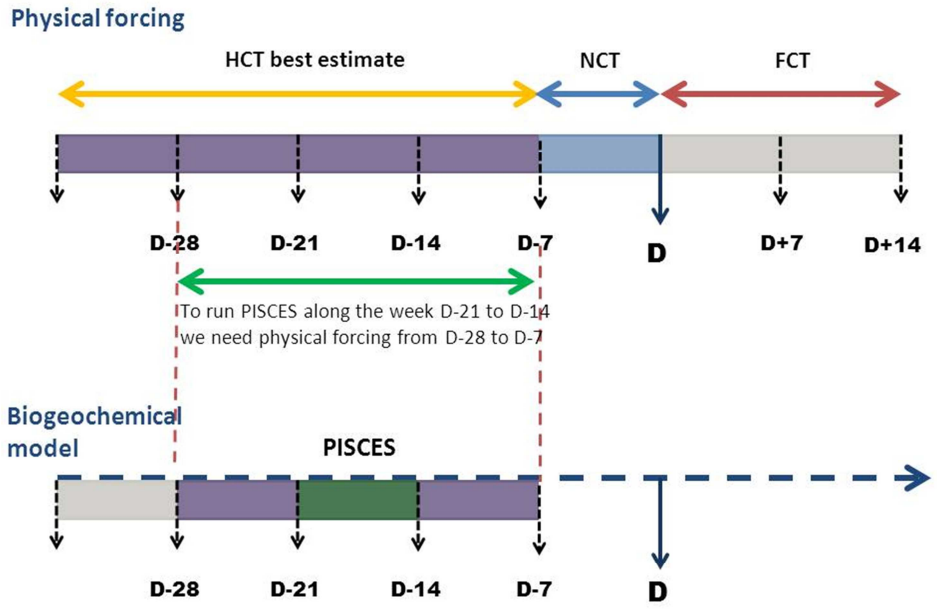

Figure 2: schematic of the operational forecast scenario for BIOMER..

An upgrade of the data assimilation systems was performed in March 2012 in order to assimilate MyOcean V2 altimetric observations and in situ observations (instead of respectively AVISO and CORIOLIS observations, corresponding to MyOcean V0 observations). In consequence, more in situ observations are assimilated in the European seas since March 2012.

II.2. Incidents in the course of AMJ 2012

The main incident during this spring season AMJ 2012 was the absence of Jason 1 observations since the analysis of February 22nd, followed by the end of the ENVISAT mission in April (see Figure 4).

Observations from Jason2, as well as observations of SST and vertical profiles of temperature and salinity, were still assimilated in real time, which maintained a good level of performance in the systems. A degradation of the quality of surface fields by 5 to 10 % is expected by the end of March, especially in the high resolution systems PSY2V4R2 and PSY4V1R3, as suggested by the impact study of Benkiran et al (2005)[1]. Figure 3 shows the scores (RMS error) when one, two, three, four satellites data are assimilated, and when no altimeter data are assimilated. In all experiments, in situ temperature and salinity, and RTG surface temperature are assimilated.

[1] *CLS_DOS_NT_08_139_GIP_V1 Contrat de recherche SHOM n°CA 2006/10/CMO « Etude d'impact de la perte des capacités d'observation par altimétrie spatiale sur la production SOAP » Rapport de synthèse à T0+10*

- Exp0 (black): Jason 1 + Envisat + GFO
- Exp1 (light blue): Jason 1
- Exp2 (orange): Jason 1 + Envisat
- Exp3 (green): No altimetry
- Exp4 (blue): Jason 1 + Envisat + GFO + T/P
- Exp5 (green dots): Progressive loss

The transition from 3 to 2 satellites causes an increase of the RMS error of 5 to 10%.

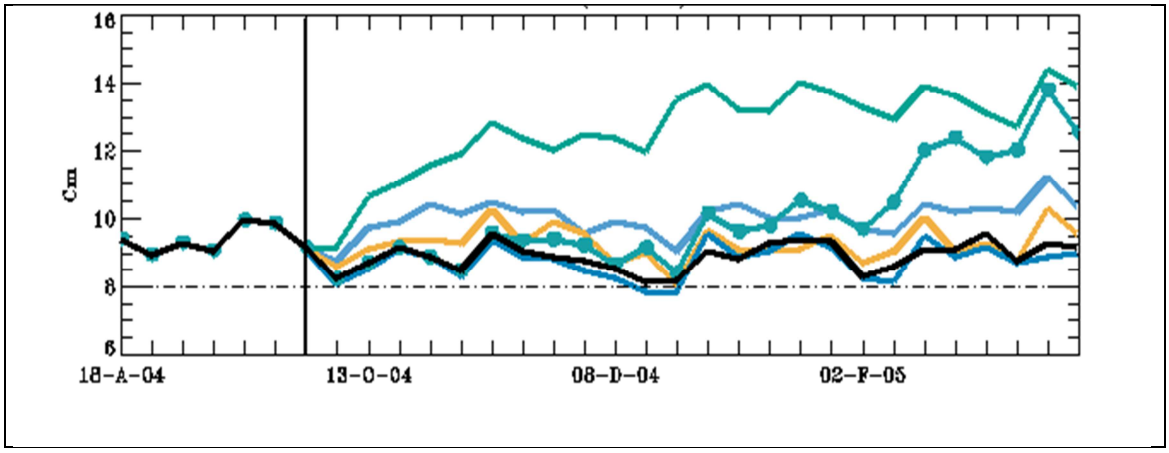

Figure 3: RMS misfit, full domain (psy2). Exp0 (black): Jason 1 + Envisat + GFO, Exp1 (light blue): Jason 1, Exp2 (orange): Jason 1 + Envisat, Exp3 (green): No altimetry, Exp4 (blue): Jason 1 + Envisat + GFO + T/P, Exp5 (green dots): Progressive loss

However, in real time no specific change in the quality of the products could be attributed without doubt to the absence of Jason 1 observations, as no reference experiment could be performed. For this reason a series of Observations Sensitivity Experiments were performed on the year 2010.

III Summary of the availability and quality control of the input data

III.1. Observations available for data assimilation

III.1.1. In situ observations of T/S profiles

System	PSY3V3R1	PSY4V1R3	PSY2V4R2
Min/max number of T profiles per DA cycle	2000/3600	2000/3600	250/800
Min/max number of S profiles per DA cycle	2000/2700	2000/2700	250/400

Table 2: minimum and maximum number of observations (orders of magnitude of vertical profiles) of subsurface temperature and salinity assimilated weekly in AMJ 2012 by the Mercator Ocean monitoring and forecasting systems.

As shown in Table 2 the maximum number of in situ observations was lower this AMJ 2012 season than during the previous OND 2011 season (see *QuO Va Dis?*#7). The minimum

number of T profiles has dropped to 2000 instead of 2300. At the end of December, part of the moorings was not delivered in real time (no significant impact was measured at that time). The number of observations increases over the quarter (not shown) and the maximum number of observations is reached in March.

The mooring observations (including TAO) were not available for assimilation during the month of March, as they were provided by Oceansite (since the beginning of March) and were flagged as bad with respect to the common standard. No impact was measured as argo observations were still assimilated.

III.1.2. Sea Surface Temperature

System	PSY3V3R1	PSY4V1R3	PSY2V4R2
Min/max number (in 10^3) of SST observations	174/185q	174/185	25/26

Table 3: minimum and maximum number (orders of magnitude in thousands) of SST observations (from RTG-SST) assimilated weekly in AMJ 2012 by the Mercator Ocean monitoring and forecasting systems.

RTG-SST is assimilated in PSY3V3R1 and PSY4V1R3, while the Reynolds ¼° "AVHRR only" product is assimilated in PSY2V4R2 in AMJ 2012.

III.1.3. Sea level anomalies along track

As shown in Table 4 and Figure 4 there was no more Jason 1 data since the end of February (see section II.2) and Jason 1 G (for Geodetic) data started to be available in the end of June. Envisat stopped delivering data in the beginning of April, after 10 years of service.

system	PSY3V3R1	PSY4V1R3	PSY2V4R1
Min/max number (in 10^3) of Jason 2 SLA observations	88/97	88/97	14/15
Min/max number (in 10^3) of Jason 1 G SLA observations	93/94	93/94	0/16
Min/max number (in 10^3) of Envisat SLA observations	0/77	0/77	0/13
Min/max number (in 10^3) of Cryosat 2 SLA observations	69/82	69/82	12/15

Table 4: minimum and maximum number (orders of magnitude in thousands) of SLA observations from Jason 2, Envisat and Jason 1 assimilated weekly in AMJ 2012 by the Mercator Ocean monitoring and forecasting systems.

Note that depending on the satellite, the number of observations in the Antarctic circumpolar region is very different. For instance for PSY4V1R3, the median of the number of Jason 2 observations in this region is 30.10^3 while the median of Envisat observations was

22.10^3, that of Jason 1 G is 27.10^3 and that of Cryosat 2 is 20.10^3. In the Antarctic region, the number of Cryosat2 SLA observations is thus 30% lower than for contemporaneous SLA observations with other satellites (Jason 2 or Jason 1 G).

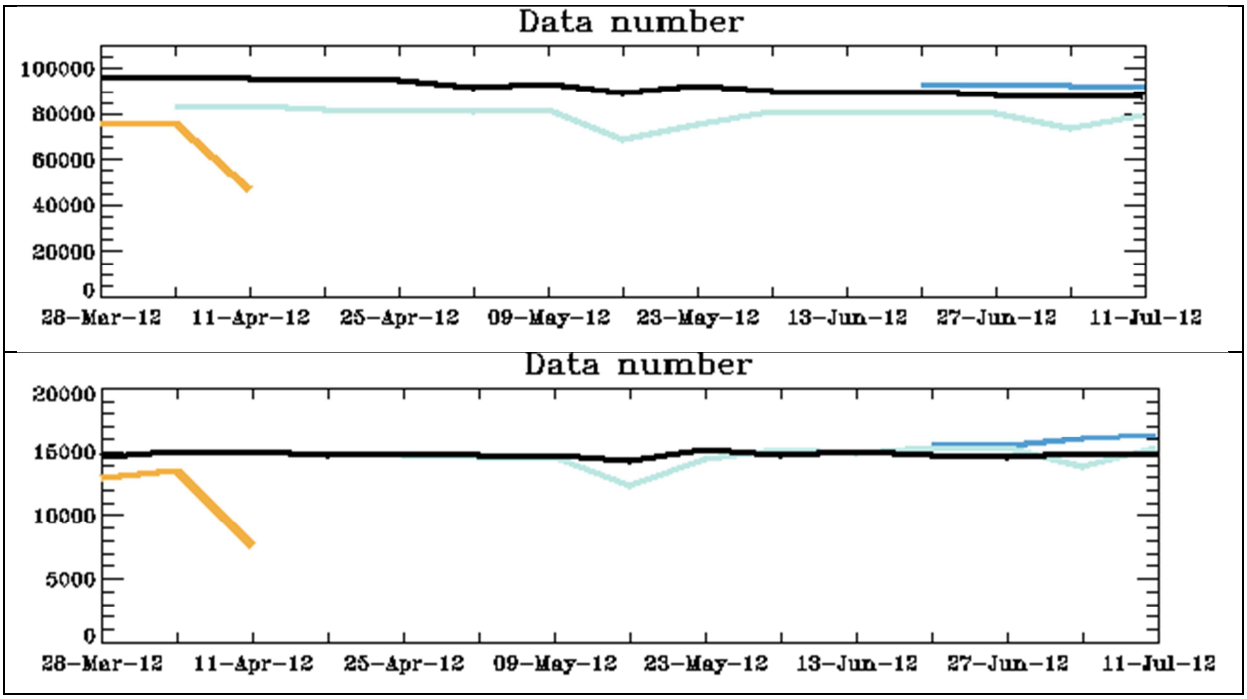

Figure 4: Number of altimetric observations from Jason 2 (black line), Jason 1 (blue line), Envisat new orbit (orange line) and Cryosat 2 (cyan line) assimilated for each weekly hindcast analysis of PSY3V3R1 (upper panel) and PSY2V4R2 (lower panel) during the AMJ 2012 season. *NB: from 4 Apr 2012 to 9 May 2012 cryosat 2 observations were loaded but not assimilated in PSY3V3R1*.

III.2. Observations available for validation

Both observational data and statistical combinations of observations are used for the real time validation of the products. All were available in real time during the AMJ 2012 season:

- T/S profiles from CORIOLIS
- OSTIA SST (with one problem on July 21st) from UKMO
- Arctic sea ice concentration and drift from CERSAT (with some delay on November 2nd)
- SURCOUF surface currents from CLS
- ARMOR-3D 3D temperature and salinity fields from CLS
- Drifters velocities from Météo-France reprocessed by CLS
- Tide gauges

Grodsky et al (GRL, May 2011) show that drifters velocities overestimate current velocities in regions and periods of strong winds due to undetected undrogued drifters. This information will be taken into account for comparisons with Mercator Ocean currents.

IV Information on the large scale climatic conditions

Mercator Ocean participates in the monthly seasonal forecast expertise at Météo France. This chapter summarizes the state of the ocean and atmosphere during the AMJ 2012 season, as discussed in the "Bulletin Climatique Global" of Météo France.

This AMJ 2012 season was characterized by neutral ENSO conditions in the equatorial Pacific Ocean (Figure 5). The equatorial Tropical Pacific Ocean was warmer than the climatology with positive temperature anomalies at depth (we show here the 0-300m layer) extending from the dateline to 90°W, especially in May and June (not shown). Consistently with this warming, a kelvin wave (downwelling) leaves the western tropical pacific in March and arrives in the eastern part of the basin in May (not shown). However, the heat content is still lower than normal in the subtropics of the eastern Tropical Pacific. In the atmosphere the teleconnexions are very weak.

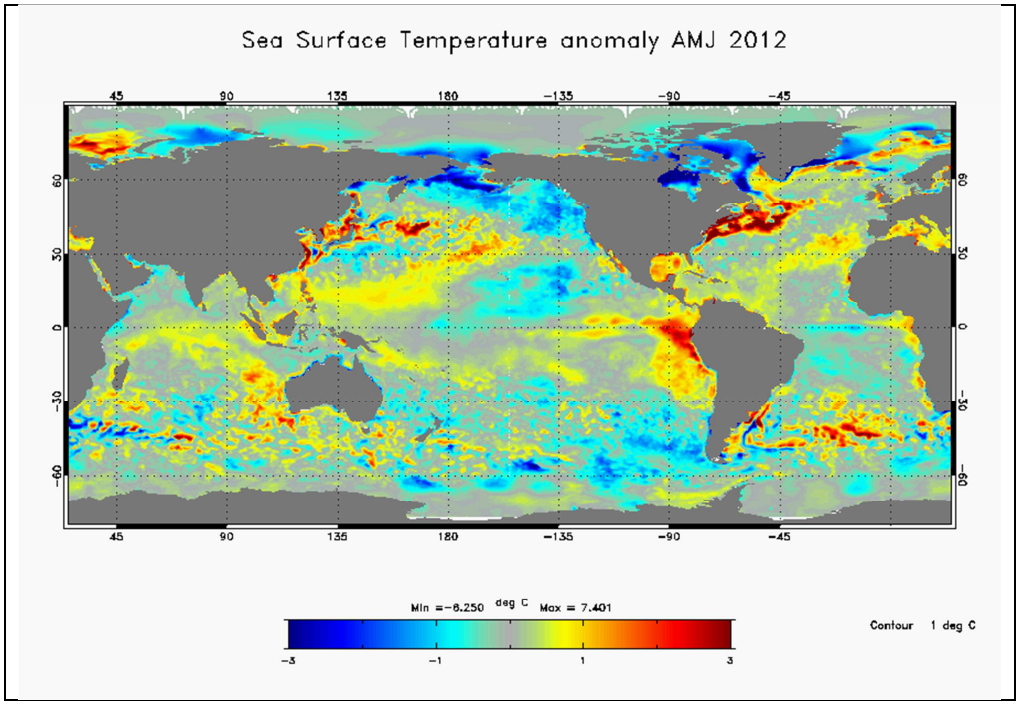

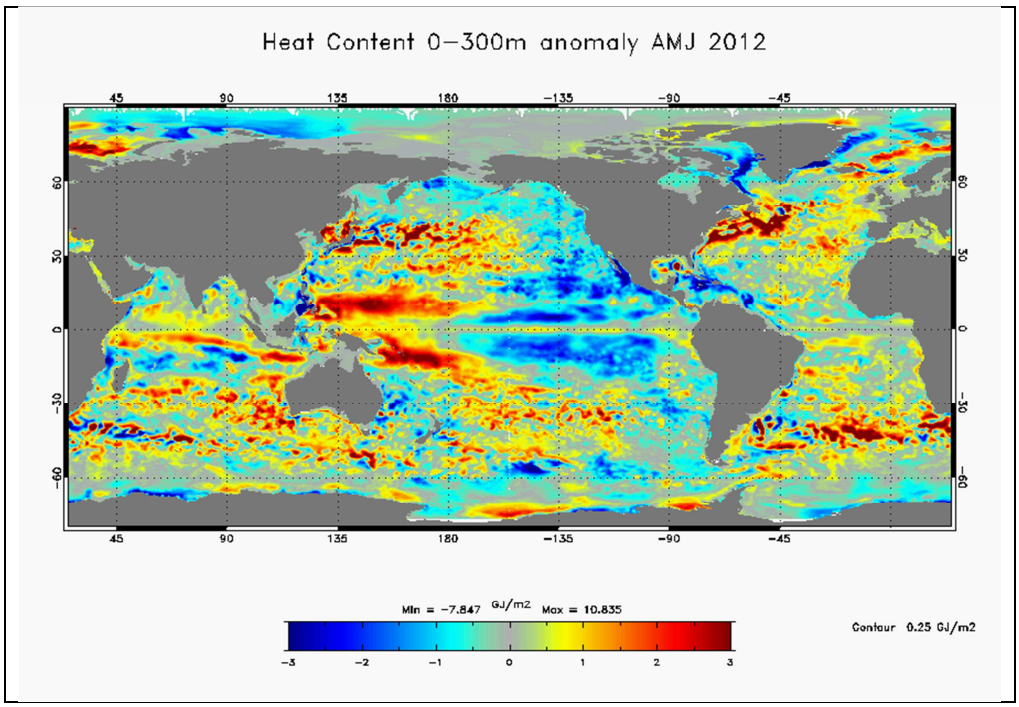

Figure 5: Seasonal AMJ 2012 temperature anomalies with respect to WOA05 (World Ocean Atlas from Levitus 2005) climatology. Upper panel: SST anomaly (°C) at the global scale from the 1/4° ocean monitoring and forecasting system PSY3V3R1. Lower panel heat content anomaly ($\rho_0 C_p \Delta T$, with constant ρ_0=1020 kg/m3) from the surface to 300m.

The equator is also warmer than the climatology in the Atlantic and Indian Oceans, which was not the case in JFM 2012. The Indian Ocean heat content anomaly at the equator is now positive in AMJ 2012 while it was neutral in JFM 2012. The Atlantic upwelling in the Gulf of Guinea seems to slow down.

The strong negative NAO atmospheric forcing in June (not shown) results in colder subtropics and a warmer subpolar gyre in the North Atlantic than in JFM 2012. South of 40°S in the southern ocean the SST conditions are closer to the climatology this austral autumn than during JFM, the austral summer.

As can be seen in Figure 6, the sea ice extent in the Arctic Ocean in June is lower than the observed minima of 2007.

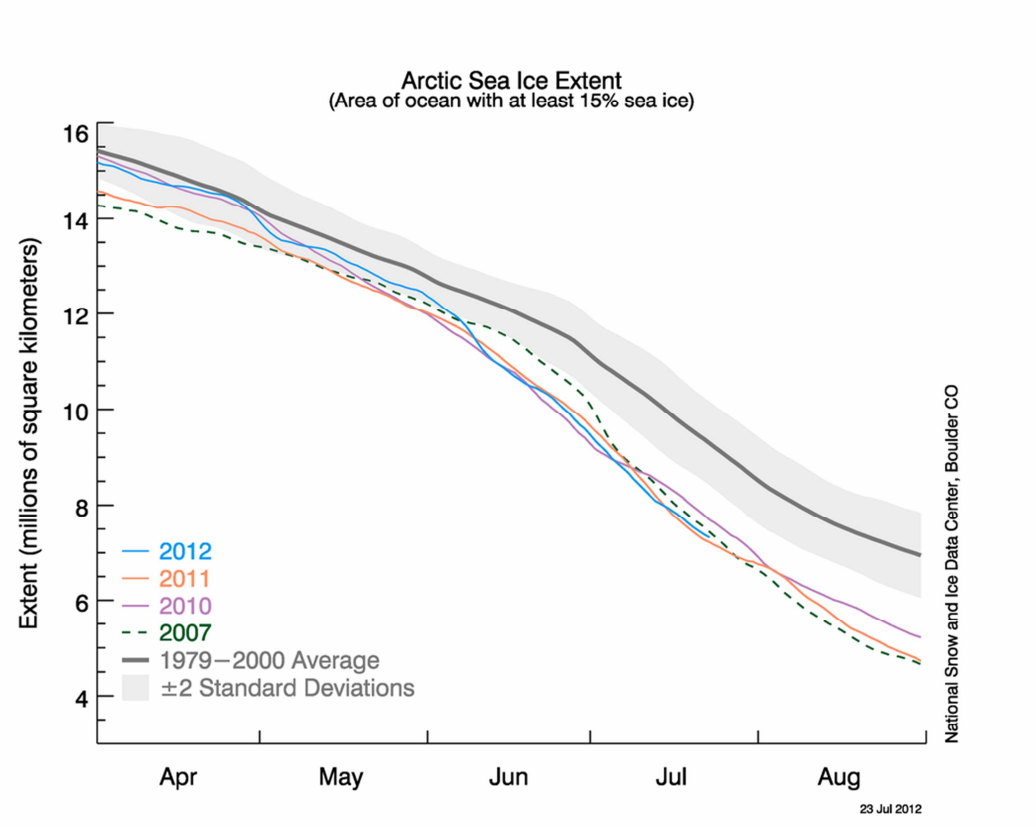

Figure 6: Arctic sea ice extent from the NSIDC: http://nsidc.org/arcticseaicenews/files/2012/07/N_stddev_timeseries.png

V Accuracy of the products

V.1. Data assimilation performance

V.1.1. Sea surface height

V.1.1.1. North Atlantic Ocean and Mediterranean Sea

The Tropical and North Atlantic Ocean SLA assimilation scores for all systems in AMJ 2012 are displayed in Figure 7. The different systems (PSY4V1R3, PSY3V3R1, and PSY2V4R2) reach identical levels of performance on average. The biases are generally small during this spring season. Note that prescribed errors are different in PSY2V4R2 and PSY4V1R3 which can explain different behaviours in spite of identical resolution. PSY2V4R2 assimilated fewer observations near the coasts, like in the Florida Strait region. Part of the biases can be attributed to local errors in the current mean dynamical topography (MDT). The RMS errors are almost identical in all systems, and stay below 5 cm in most regions, except regions of high mesoscale variability.

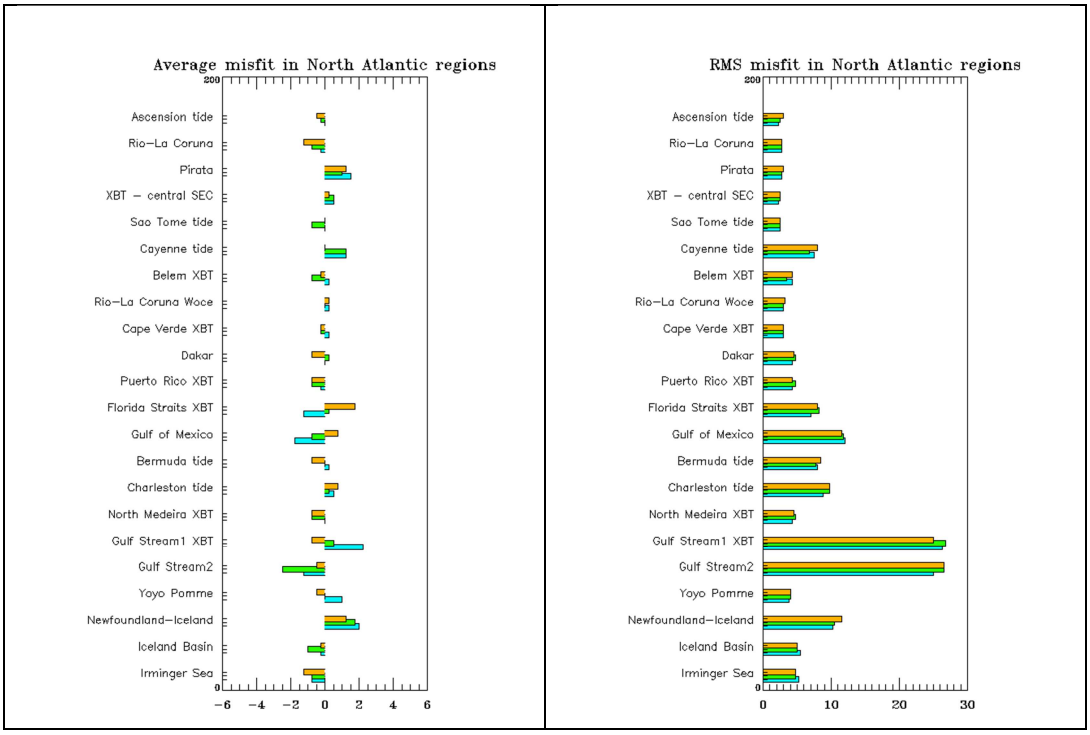

Figure 7: Comparison of SLA data assimilation scores (left: average misfit in cm, right: RMS misfit in cm) in AMJ 2012 and between all available Mercator Ocean systems in the Tropical and North Atlantic. The scores are averaged for all available satellite along track data (Jason 1 G, Jason 2, Cryosat 2 and Envisat). For each region the bars refer respectively to PSY2V4R2 (cyan), PSY3V3R1 (green), PSY4V1R3 (orange). The geographical location of regions is displayed in annex A.

In the Mediterranean Sea a bias of more than 6 cm is present in PSY2V4R2 in the Adriatic Sea, while it is less than 2 cm in other regions, as can be seen in Figure 8. This bias is generally higher in summer and autumn seasons (from 6 to 8 cm). These regions are circled by coasts, and consequently few observations are assimilated. The RMS of the innovation

(misfit) of PSY2V4R2 is generally less than 8 cm. The western Mediterranean exhibits slightly better performance than the eastern Mediterranean. However in the eastern part of the basin, most of the RMS error is linked with the bias, and thus the variability is well represented.
The system still shows overall good performance as the RMS of the innovation is generally lower than the intrinsic variability of the observations in the North Atlantic and Mediterranean (not shown).

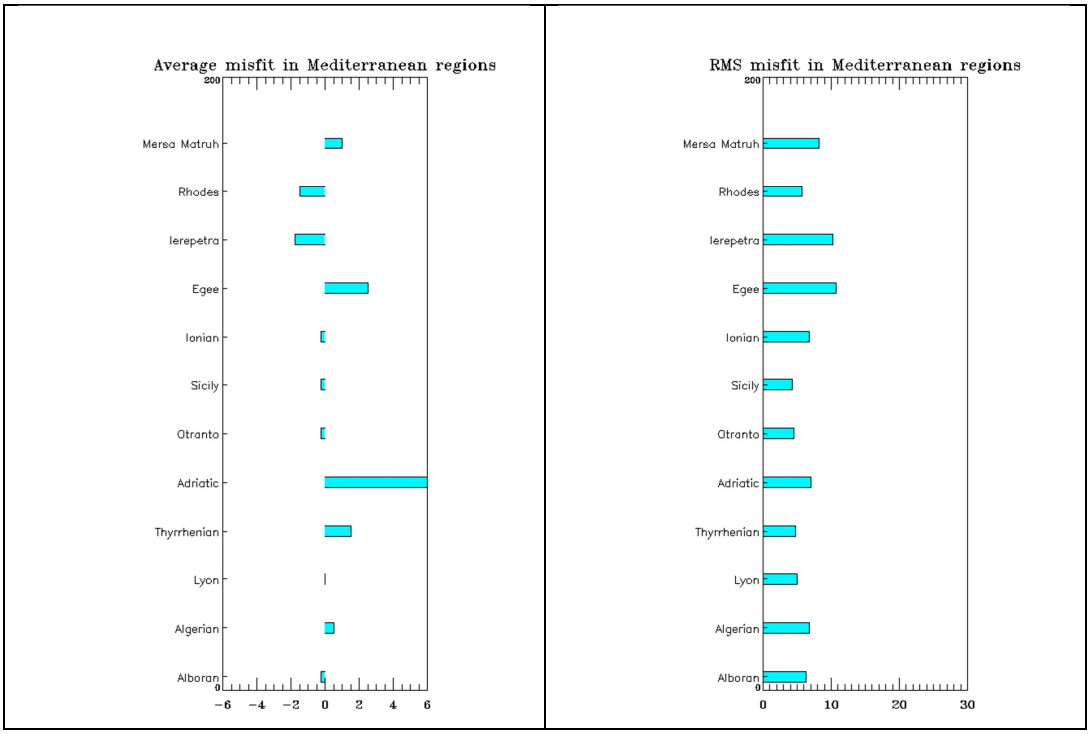

Figure 8: Comparison of SLA data assimilation scores (left: average misfit in cm, right: RMS misfit in cm) in AMJ 2012 for PSY2V4R2. The scores are averaged for all available satellite along track data (Jason 1 G, Jason 2, Cryosat 2 and Envisat). See annex B for geographical location of regions.

V.1.1.2. Performance at global scale in PSY3 (1/4°) and PSY4 (1/12°)

As can be seen in Figure 9 the performance of intermediate resolution global PSY3V3R1 and the performance of high resolution global PSY4V1R3 in terms of SLA assimilation are of the same order of magnitude. The bias is small except in the “Nino 5” box centred on the Banda Sea in Indonesia which corresponds to a MDT problem. These problems disappear when using the MDT updated with GOCE and bias correction (tests made by E. Greiner, B. Tranchant, O. Le Galloudec, this MDT is used in the PSY2V4R2 release in the Atlantic and Mediterranean). The RMS error reaches its highest values in the Agulhas and Falkland Currents where the variability is high during this austral autumn season.

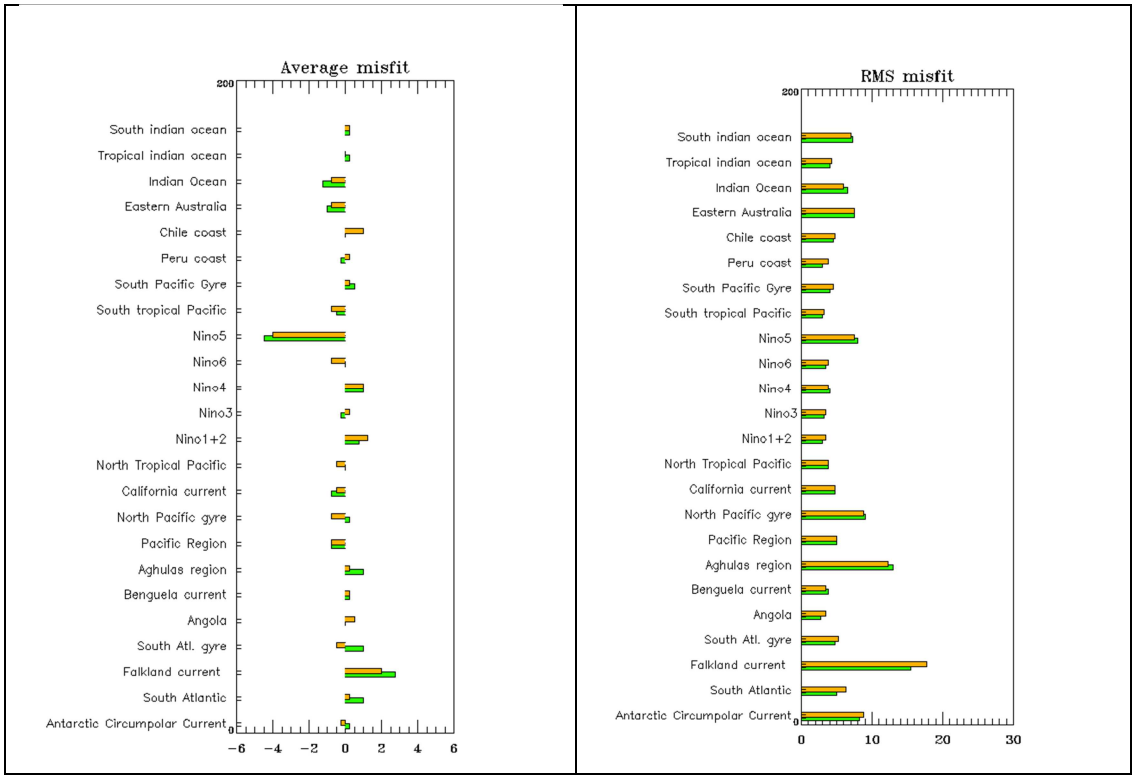

Figure 9: Comparison of SLA data assimilation scores (left: average misfit in cm, right: RMS misfit in cm) in AMJ 2012 and between all available global Mercator Ocean systems in all basins but the Atlantic and Mediterranean: PSY3V3R1 (green) and PSY4V1R3 (orange). The scores are averaged for all available satellite along track data (Jason 1 G, Jason 2, Cryosat 2 and Envisat). The geographical location of regions is displayed in annex B.

V.1.2. Sea surface temperature

V.1.2.1. North and Tropical Atlantic Ocean and Mediterranean Sea in all systems

In the Atlantic the three systems display different regional behaviours in terms of SST bias as illustrated in Figure 10. A cold bias of around 0.1°C is usually diagnosed in most regions of high resolution global PSY4V1R3. This season the bias reaches higher values (around 0.2 °C to 0.5°C). The bias is reduced in PSY3V3R1 with respect to PSY4V1R3 but it is still higher than in PSY2V4R2 which assimilates a better SST product (Reynolds ¼° AVHRR instead of RTG-SST), except in the south Equatorial current. A warm bias appears for all systems in some regions, for instance in the Gulf Stream and Dakar regions. In the Gulf Stream the accuracy of the mesoscale activity may be the main explanation of the bias. The mesoscale activity is more accurate in AVHRR products, which could explain the difference between PSY4V1R3, PSY3V3R1 and PSY2V4R2 results. In the Dakar region, the upwelling is underestimated. Note that as for SLA, prescribed SST errors are higher in PSY2V4R2 within 50km off the coast.

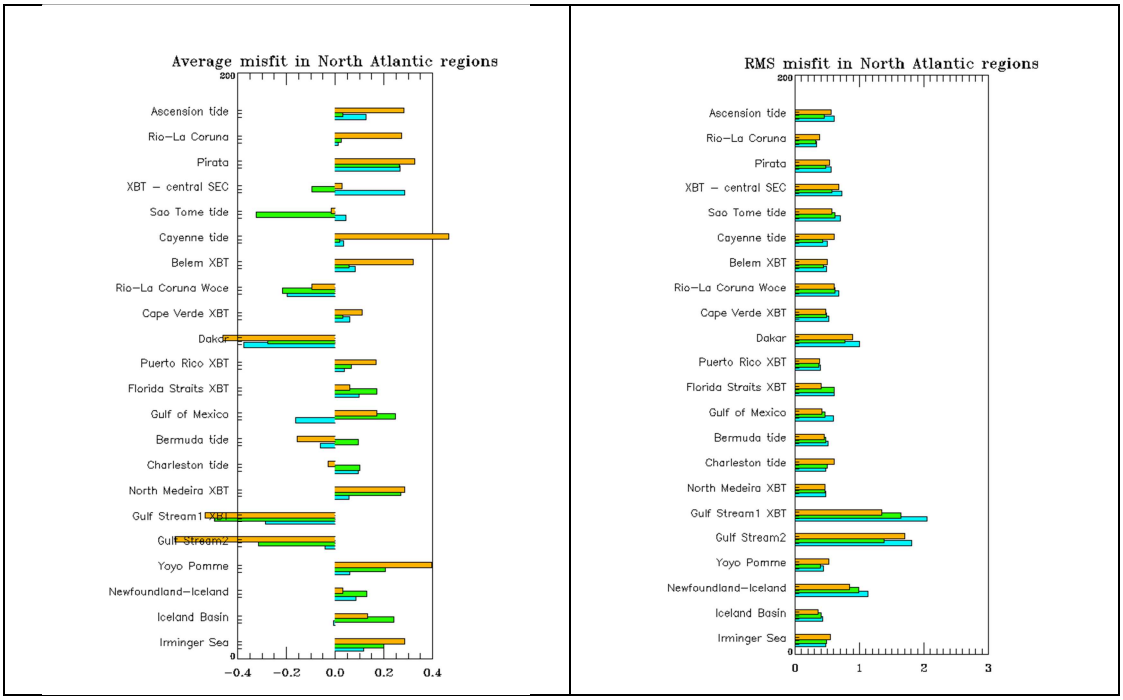

Figure 10: Comparison of RTG-SST data assimilation scores (left: average misfit in °C, right: RMS misfit in °C) in AMJ 2012 and between all available Mercator Ocean systems in the Tropical and North Atlantic: PSY4V1R3 (orange), PSY3V3R1 (green). In cyan: Reynolds ¼°AVHRR-AMSR-E data assimilation scores for PSY2V4R2. The geographical location of regions is displayed in annex B.

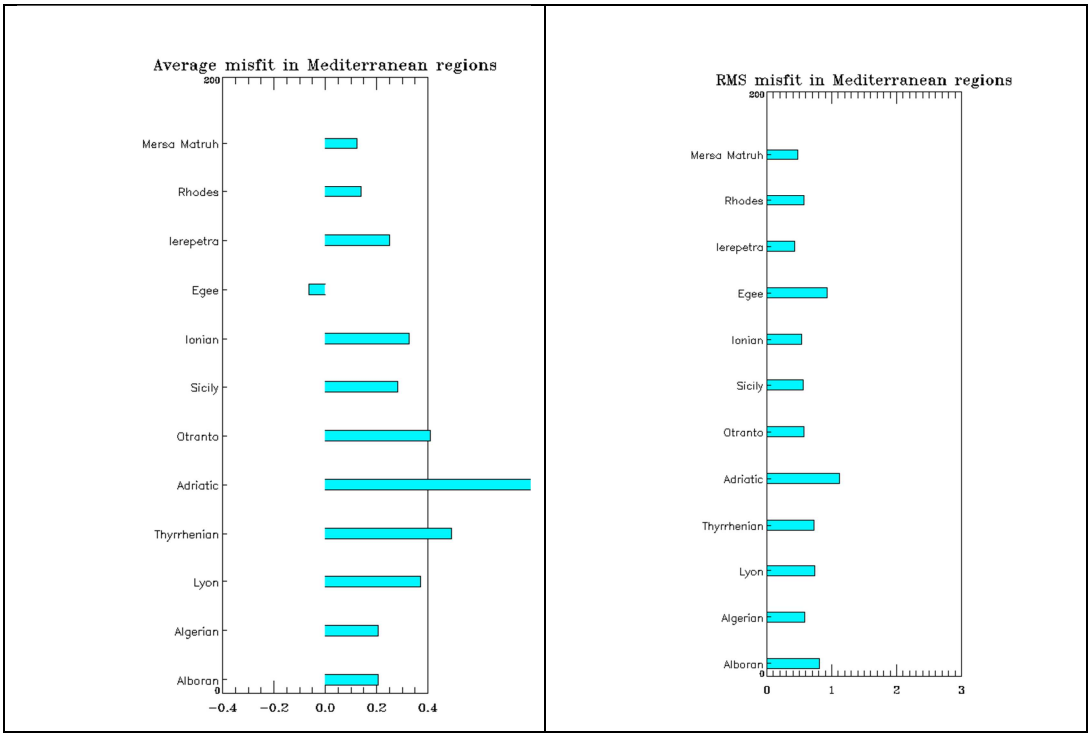

Figure 11: Comparison of SST data assimilation scores (left: average misfit in °C, right: RMS misfit in °C) in AMJ 2012 for each region for PSY2V4R2 (comparison with Reynolds ¼° AVHRR-AMSR). The geographical location of regions is displayed in annex B.

The Mediterranean regions display a cold bias of 0.2°C on average (Figure 11). The RMS error is generally lower than 1 °C. As in SLA, the performance of PSY2V4R2 is lower in the Adriatic Sea where a 1°C bias appears, explaining most of the RMS error.

V.1.2.2. Performance at global scale in PSY3 (1/4°) and PSY4 (1/12°)

PSY4V1R3 exhibits a cold bias at the global scale this AMJ season of about 0.1°C to 0.4°C, especially strong in coastal regions such as the Peru Coast of the California current. PSY3V3R1 is colder than the observations in most regions, except the coastal regions of the tropical Pacific and in the Antarctic. In general PSY3V3R1 performs better than PSY4V1R3 (Figure 12). Nevertheless PSY4V1R3 performs slightly better than PSY3V3R1 in the Antarctic, California Current and South Atlantic this winter (while it is better than PSY3V3R1 in the North Pacific in summer and autumn). The RMS error is of the same order of magnitude for both systems.

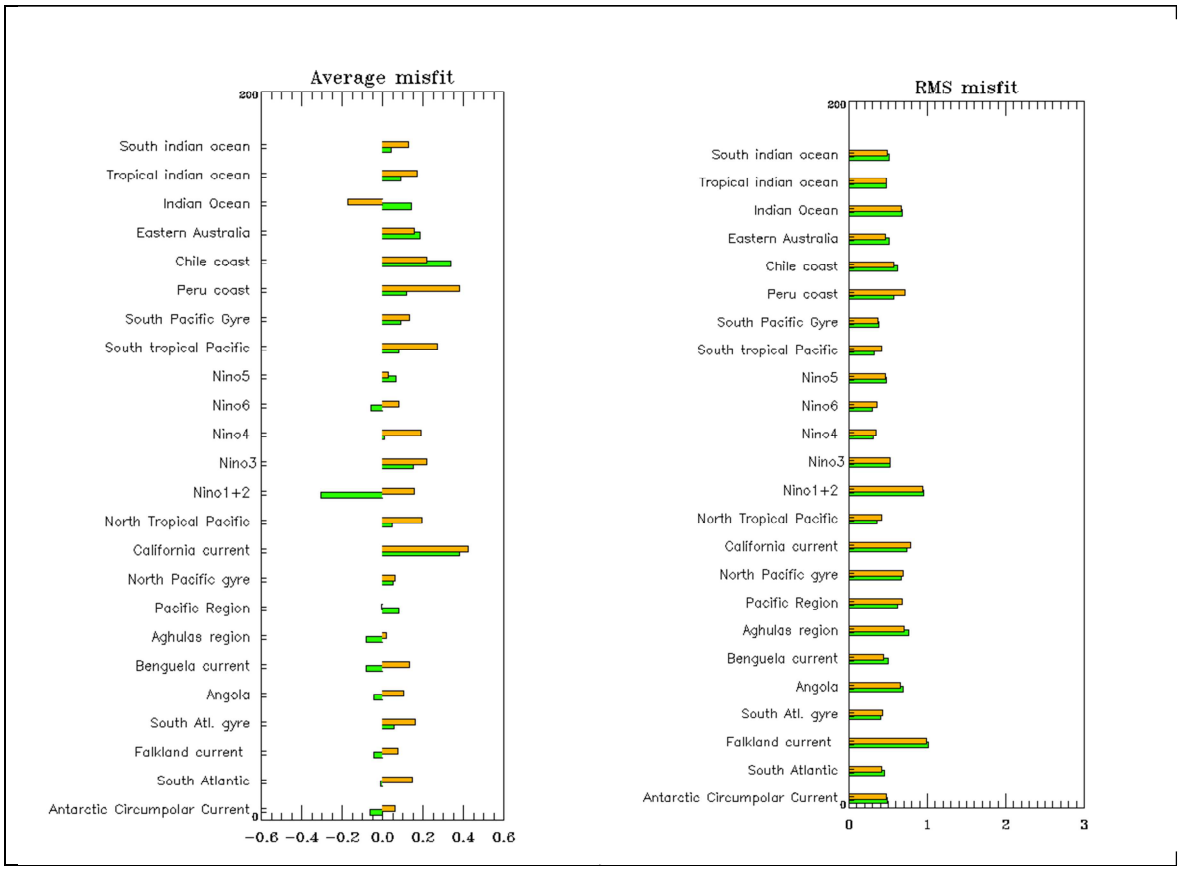

Figure 12: Comparison of RTG-SST data assimilation scores (left: average misfit in °C, right: RMS misfit in °C) in AMJ 2012 and between all available global Mercator Ocean systems in all basins but the Atlantic and Mediterranean: PSY3V3R1 (green) and PSY4V1R3 (orange). See annex B for geographical location of regions.

V.1.3. Temperature and salinity profiles

V.1.3.1. Methodology

All systems innovation (**observation – model first guess**) profiles are systematically intercompared in all regions given in annex B. In the following, intercomparison results are shown on the main regions of interest for Mercator Ocean users in AMJ 2012. Some more regions are shown when interesting differences take place, or when the regional statistics illustrate the large scale behaviour of the systems.

V.1.3.1.1. North Pacific gyre (global systems)

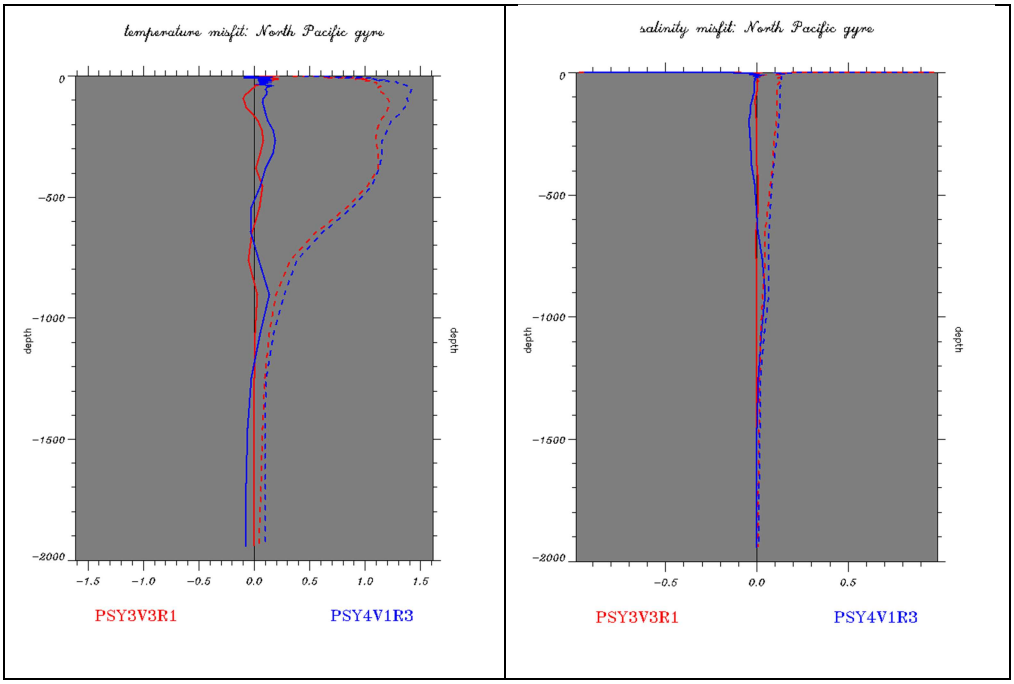

Figure 13: Profiles of AMJ 2012 innovations of temperature (°C, left panel) and salinity (psu, right panel), mean (solid line) and RMS (dotted line) for PSY3V3R1 in red and PSY4V1R3 in blue in North Pacific gyre region. The geographical location of regions is displayed in annex B.

As can be seen in Figure 13, the ¼° global PSY3V3R1 benefits from bias correction but it is still too warm and salty near 100 m (up to 0.25 °C and 0.01 psu). PSY4V1R3 is too cold between 0 and 500 m and near 900 m. It is too fresh from 0 m to 100m and then too salty 100 m and 600 m (0.05 psu) while it is fresher than observations between 600 m and 1200 m. This salinity bias of unprecedented amplitude appears in JFM 2012 (see *QuO Va Dis?* #8 for a special focus on this bias).

V.1.3.1.2. South Atlantic Gyre (global systems)

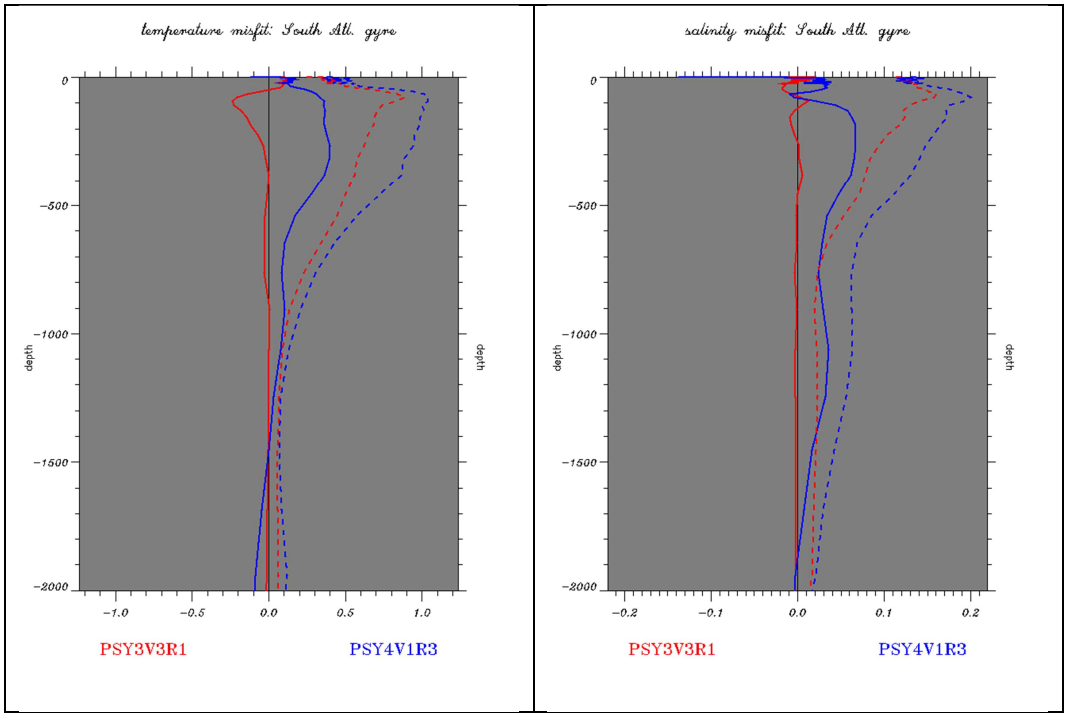

Figure 14: Profiles of AMJ 2012 innovations of temperature (°C, left panel) and salinity (psu, right panel), mean (solid line) and RMS (dotted line) for PSY3V3R1 in red and PSY4V1R3 in blue in South Atlantic gyre region. The geographical location of regions is displayed in annex B.

In this region a large cold bias (up to 0.4 °C) is present in PSY4V1R3 between 0 and 800 m, while PSY3V3R1 experiments a cold bias at the surface and a warm bias near 100m. A salty (up to 0.1 PSU at the surface) bias appears in PSY4V1R3. At depth, the bias is fresh on average and does not exceed 0.07 psu between 100 and 1500m. PSY3V3R1 has a smaller surface cold bias than PSY4V1R3 but becomes too warm (0.1°C) in the 100-300m layer. This region illustrates well that PSY3V3R1 is closer to subsurface in situ observations than PSY4V1R3 thanks to bias correction.

V.1.3.1.3. Indian Ocean (global systems)

In the Indian Ocean under 800 m, PSY3V3R1 is clearly closer to the observations than PSY4V1R3 in Figure 15. This is again due to the application of a bias correction in PSY3V3R1. PSY3V3R1 is nevertheless saltier (0.2 psu) and warmer (1°C) than the observations at the surface. PSY4V1R3 appears too cold and salty at the subsurface between 100 m and 500 m. Between 500 m and 800 m PSY4V1R3 is too warm and salty and under 800 m it is too cold and fresh.

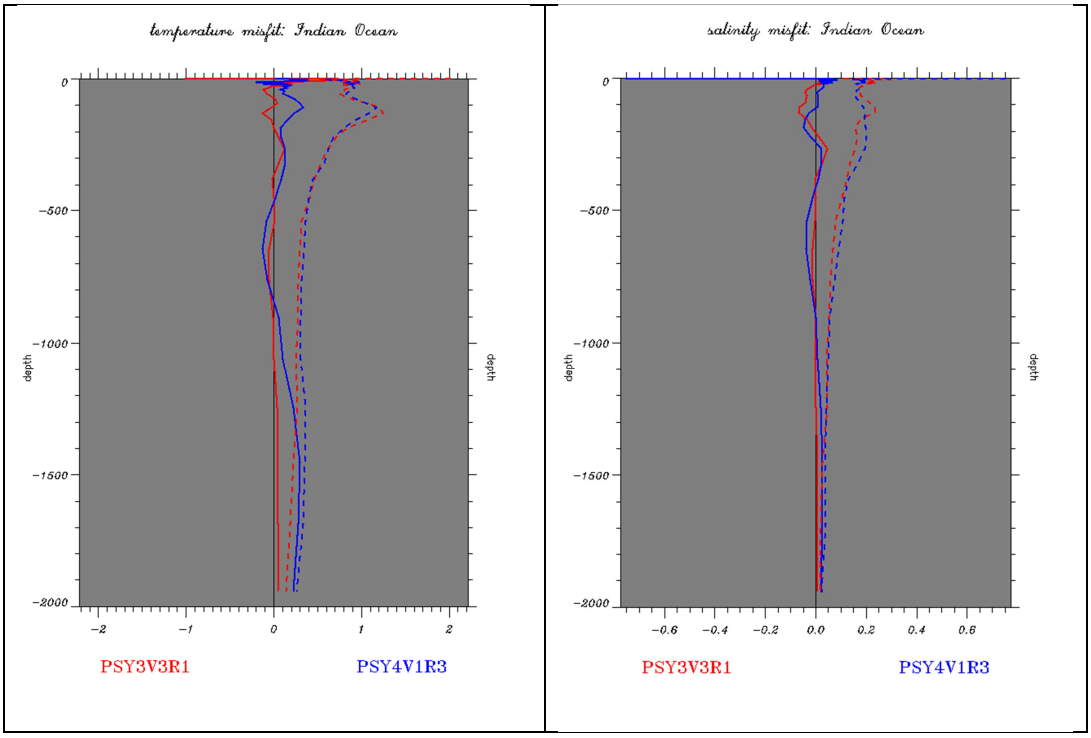

Figure 15: Profiles of AMJ 2012 innovations of temperature (°C, left panel) and salinity (psu, right panel), mean (solid line) and RMS (dotted line) for PSY3V3R1 (in red) and PSY4V1R3 (in blue) in the Indian Ocean region. The geographical location of regions is displayed in annex B.

V.1.3.2. Tropical and North Atlantic Ocean (all systems)

The regional high resolution system (PSY2V4R2) and the global 1/4° PSY3V3R1 have a better average performance than the global 1/12° PSY4V1R3 in the North Atlantic in AMJ 2012, again due to uncorrected biases in this system. It is the case for the temperature and salinity in the North Madeira region as illustrated in Figure 16. Strong biases are present in PSY4V1R3 between 1000m and 1500m, at the location of the Mediterranean outflow. The bias correction improves the results of PSY3V3R1 and PSY2V4R2 between 800 m and 2000 m with respect to PSY4V1R3. Mediterranean waters are too warm and salty near 800 m in PSY2V4R2.

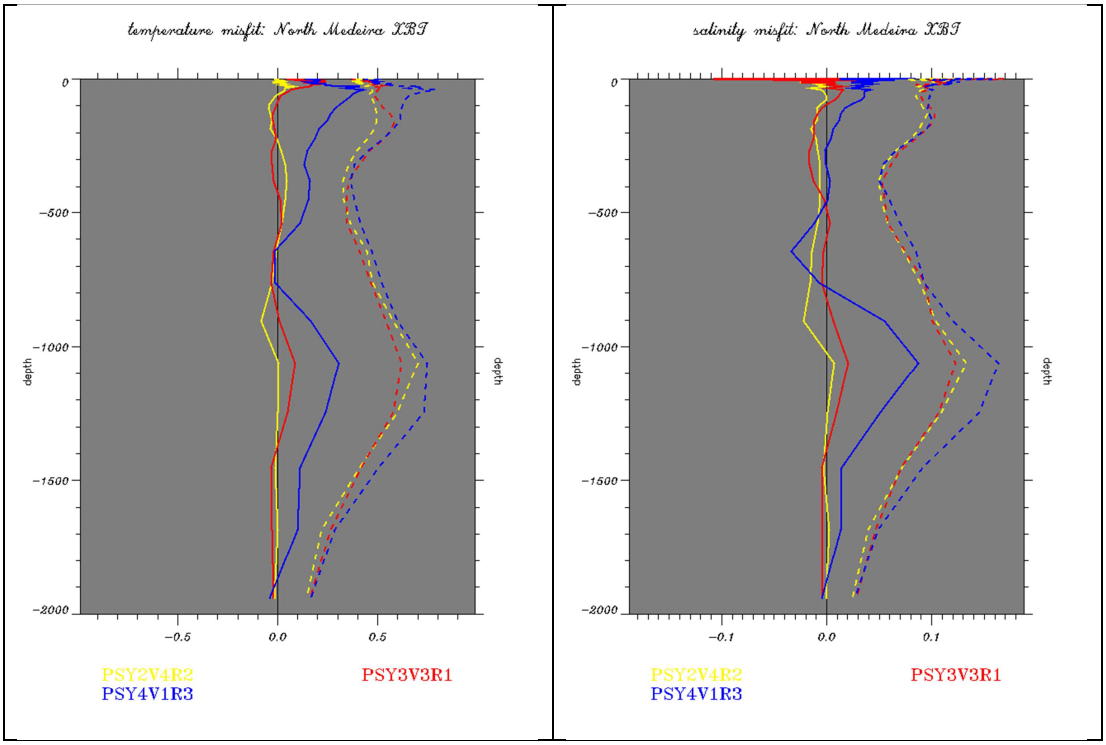

Figure 16: Profiles of AMJ 2012 innovations of temperature (°C, left panel) and salinity (psu, right panel), mean (solid line) and RMS (dotted line) for PSY4V1R3 in blue, PSY3V3R1 in red, and PSY2V4R2 in yellow in North Madeira region. The geographical location of regions is displayed in annex B.

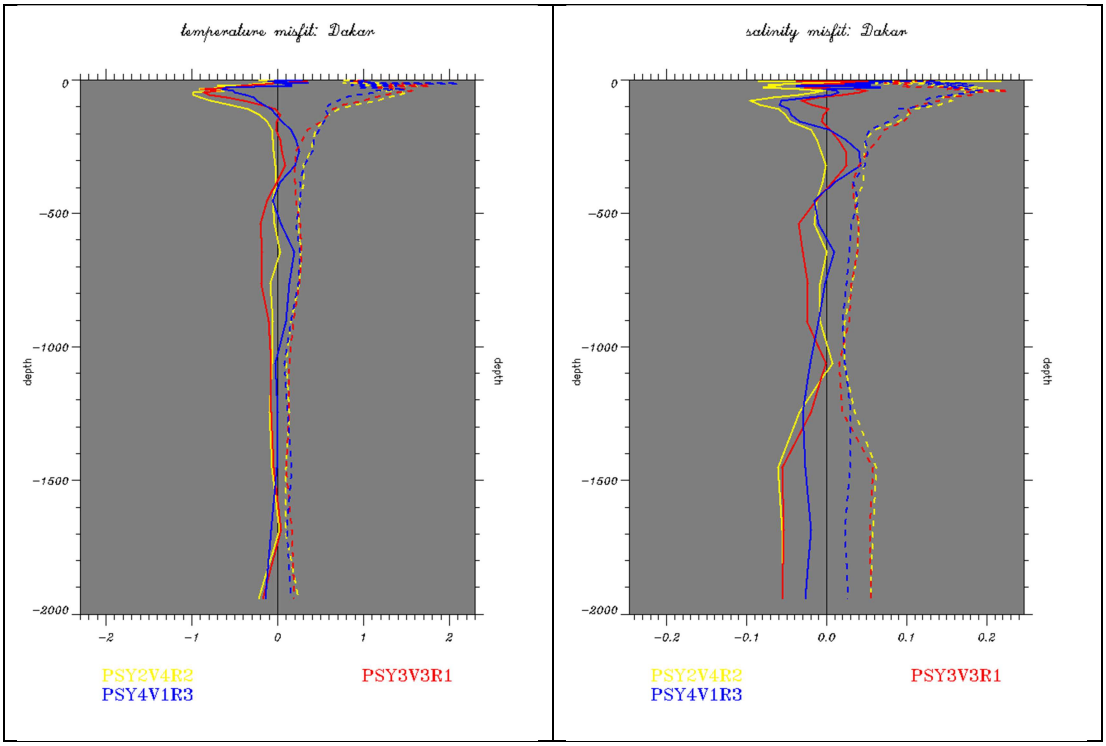

Figure 17: Profiles of AMJ 2012 innovations of temperature (°C, left panel) and salinity (psu, right panel), mean (solid line) and RMS (dotted line) for PSY4V1R3 in blue, PSY3V3R1 in red, and PSY2V4R2 in yellow in Dakar region. The geographical location of regions is displayed in annex B.

The upwelling is not well represented by any of the systems In the Dakar region (Figure 17): it is too generally weak resulting in a warm bias near 50 m. One can notice a salty bias at depth (0.05 psu, under 1200m) in both PSY2V4R2 and PSY3V3R1 in AMJ 2012, that is not present in PSY4V1R3 and that was not present in JFM 2012.

In the Gulf Stream region (Figure 18) all systems display similar levels of temperature and salinity RMS error. We note that the departures from observations are large in this region compared to other regions because of the high spatial and temporal variability of temperature and salinity due to eddy activity. Despite the bias correction, PSY3V3R1 and PSY2V4R2 are too cold and fresh between 200 m and 1200 m, which is the opposite from the previous JFM 2012 season. This probably indicates a major water masses change at the intraseasonal scale that the bias correction does not completely constrain. PSY4V1R3 which is usually too cold is consequently less biased than the other systems under 500m this season .It is still too warm from the surface to 200m and too cold and salty under 200m.

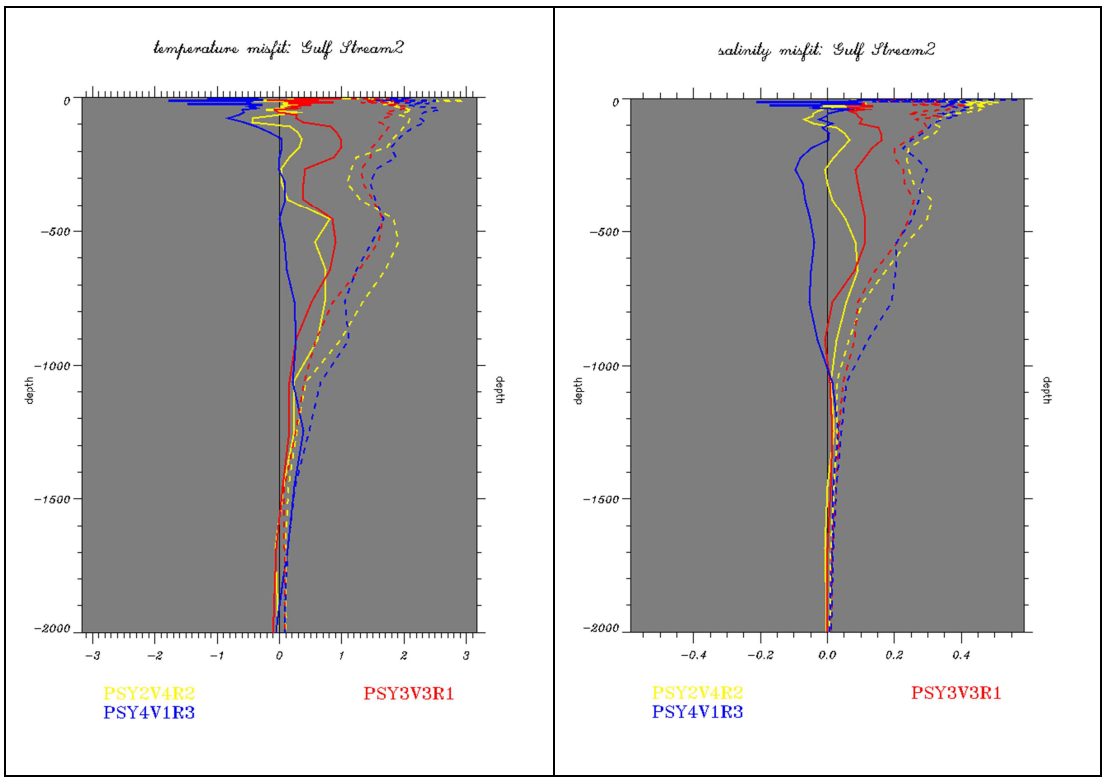

Figure 18: Profiles of AMJ 2012 innovations of temperature (°C, left panel) and salinity (psu, right panel), mean (solid line) and RMS (dotted line) for PSY4V1R3 in blue, PSY3V3R1 in red, and PSY2V4R2 in yellow in Gulf Stream 2 region. The geographical location of regions is displayed in annex B.

The Cape Verde region is characteristic of the subtropical gyre in the North Atlantic where all systems stay on average close to the temperature and salinity profiles as can be seen in Figure 19. The highest errors are located near the thermocline and halocline. A fresh bias (0.05 psu) is diagnosed in PSY2V4R2 at the surface. As in many regions, the global high resolution system with no bias correction PSY4V1R3 is too cold from the surface to 700m.

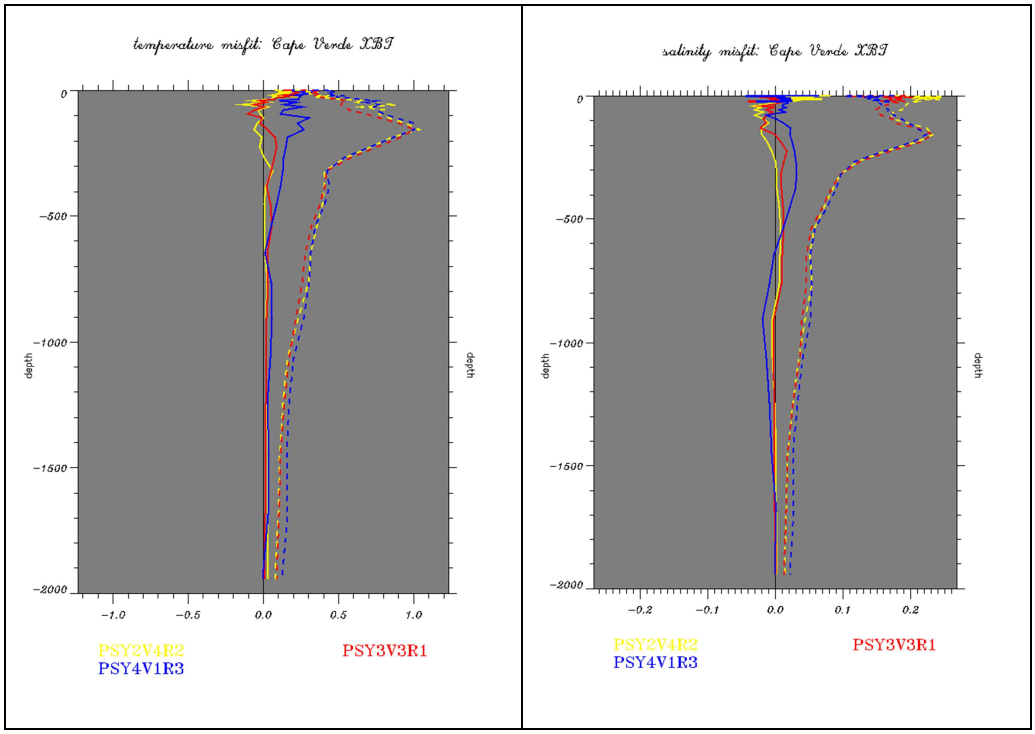

Figure 19: Profiles of AMJ 2012 innovations of temperature (°C, left panel) and salinity (psu, right panel), mean (solid line) and RMS (dotted line) for PSY4V1R3 in blue, PSY3V3R1 in red, and PSY2V4R2 in yellow in Cape Verde region. The geographical location of regions is displayed in annex B.

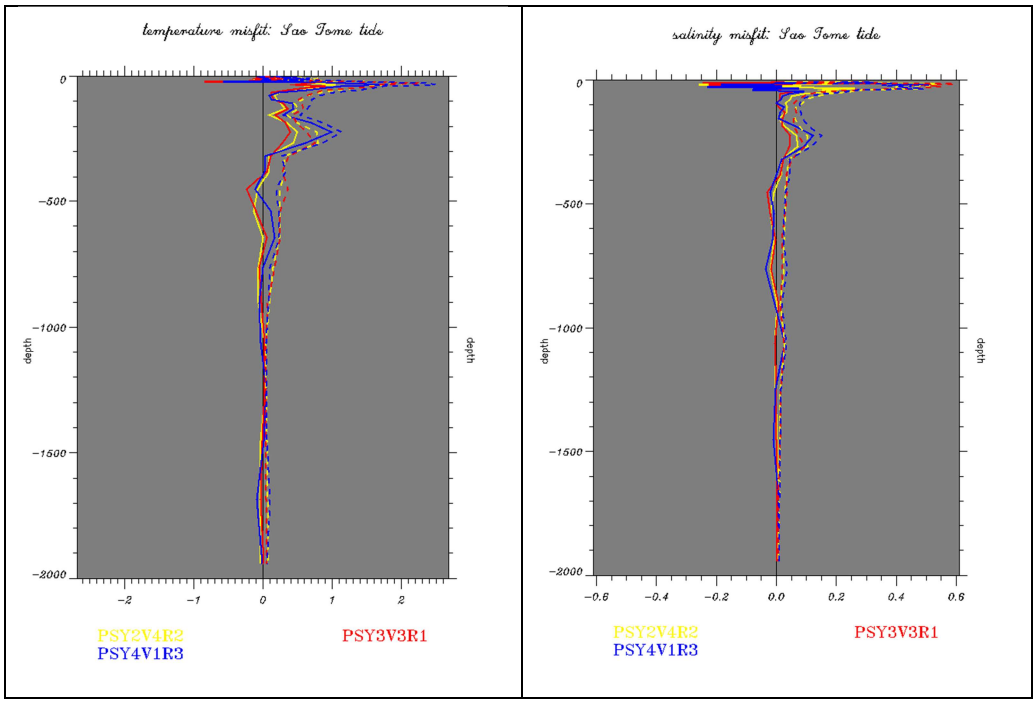

Figure 20: Profiles of AMJ 2012 innovations of temperature (°C, left panel) and salinity (psu, right panel), mean (solid line) and RMS (dotted line) for PSY4V1R3 in blue, PSY3V3R1 in red, and PSY2V4R2 in yellow in Sao Tome region. The geographical location of regions is displayed in annex B.

Around 20 profiles were sampled in the beginning of May in the small area of the Sao Tome tide region where usually not more than 4 profiles are assimilated per week. As can be seen in Figure 20 the systems have difficulties in reproducing the undercurrents in this region as a small number of profiles are available to constrain the water masses. The bias correction partly solves this problem in PSY2V4R2 and PSY3V3R1.

V.1.3.1. Mediterranean Sea (high resolution regional systems at 1/12°)

In the Mediterranean Sea the high resolution is mandatory to obtain good level of performance. Only PSY2V4R2 with bias correction is displayed as it has the best level of performance on this zone. We note in Figure 21 that the system displays a cold bias near the surface and then a warm bias with a peak at around 0.4 °C near 100 m in the Algerian region. This bias is generally higher (up to 0.5 °C) and present in most Mediterranean regions in summer and autumn. In most regions a fresh bias can be detected between 0 and 200 m. It reaches 0.3 psu in the Algerian region. The bias is consistent with a general underestimation of stratification in the systems, and with errors in the positioning of the separation between the Atlantic Inflow and the Levantine intermediate waters. Biases with similar feature but with smaller amplitudes can be observed in the Gulf of Lion (Figure 22).

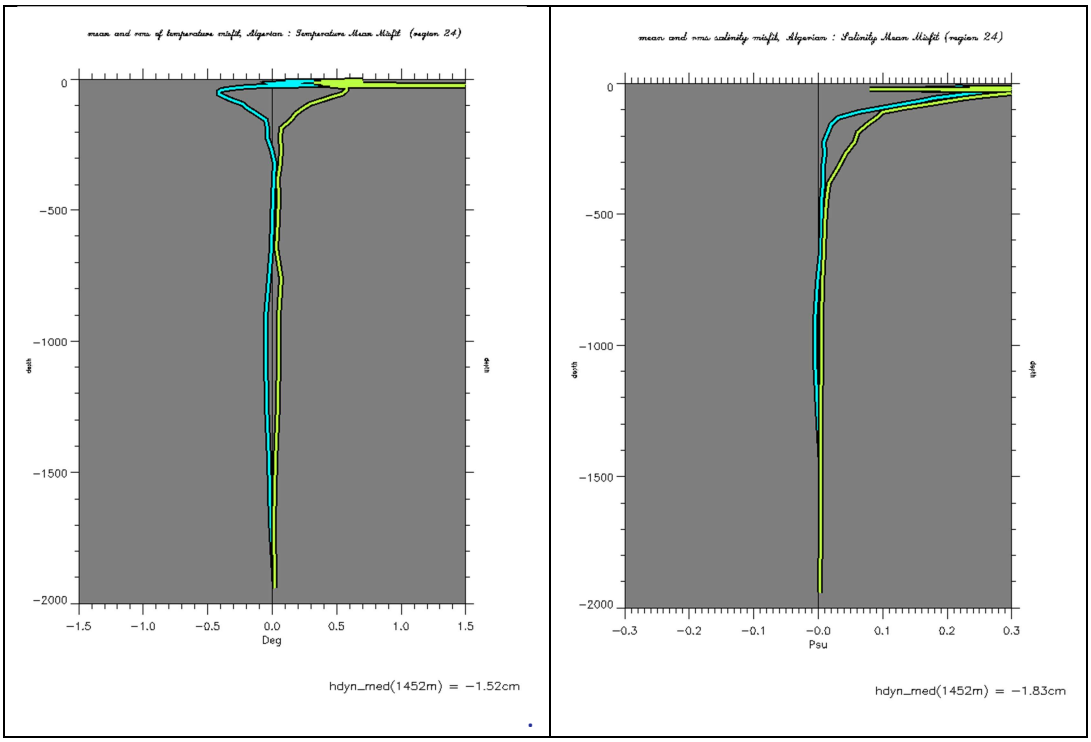

Figure 21: Profiles of AMJ 2012 mean (cyan) and RMS (yellow) innovations of temperature (°C, left panel) and salinity (psu, right panel) in the Algerian region. The geographical location of regions is displayed in annex B.

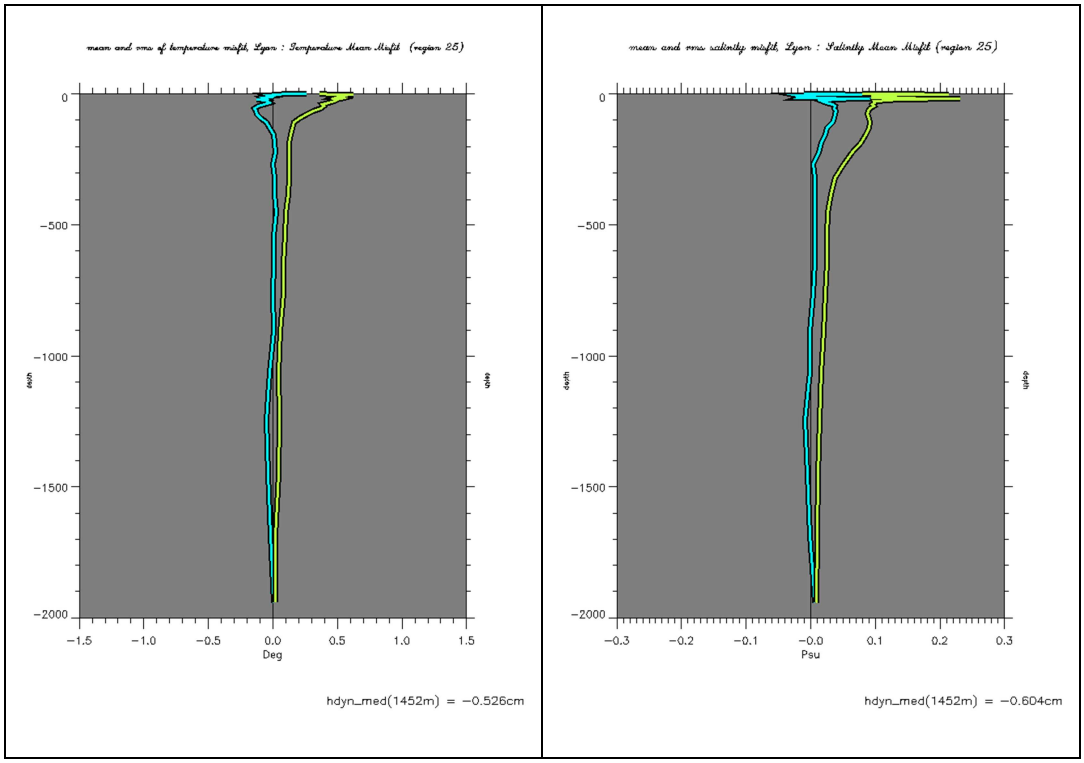

Figure 22: Profiles of AMJ 2012 mean (cyan) and RMS (yellow) innovations of temperature (°C, left panel) and salinity (psu, right panel) in the Gulf of Lion region. The geographical location of regions is displayed in annex B.

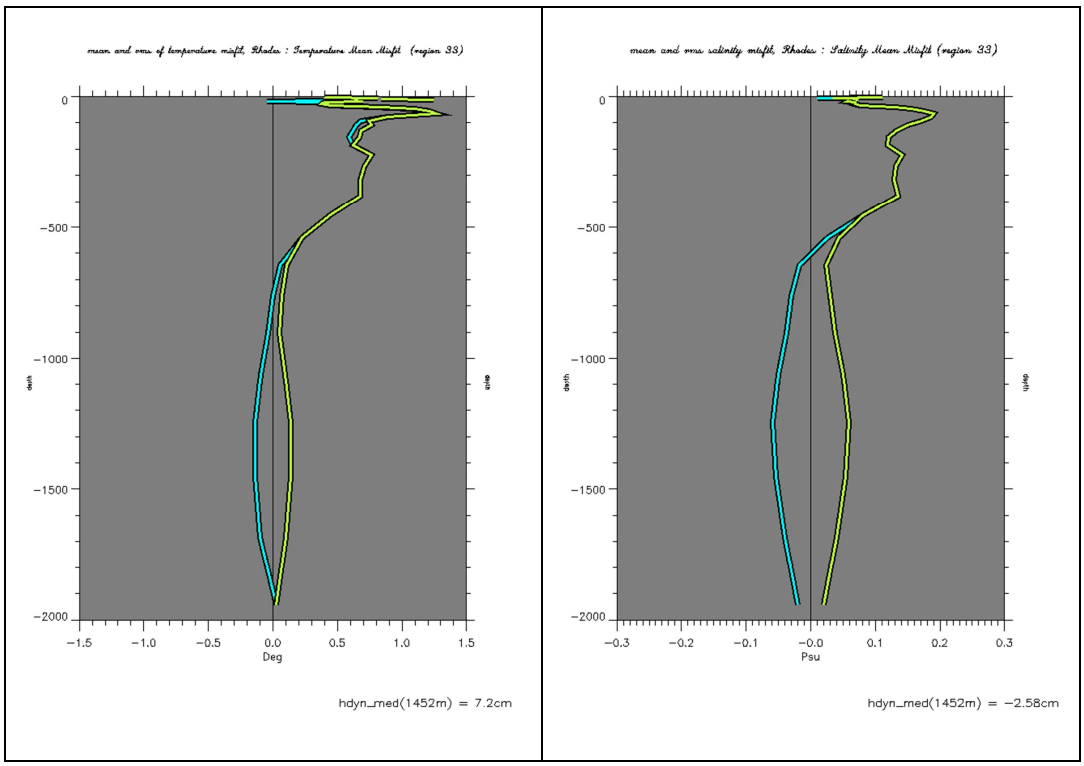

Figure 23: Profiles of AMJ 2012 mean (cyan) and RMS (yellow) innovations of temperature (°C, left panel) and salinity (psu, rightpanel) in the Rhodes region. The geographical location of regions is displayed in annex B.

In the Rhodes region (Eastern Mediterranean basin) a strong cold (1°C) and fresh (0.2 psu) bias appears on the 0-600m layer, while a warm and salty bias of smaller amplitude can be diagnosed between 600 and 2000 m.

Summary: While most of the deep biases disappear in the systems including bias correction, seasonal biases remain. One of the hypotheses is that the SST assimilation is not as efficient as it used to be. The Incremental Analysis Update together with the bulk formulation rejects part of the increment. There is too much mixing in the surface layer inducing a cold (and salty) bias in surface and warm (and fresh) bias in subsurface. The bias is intensifying with the summer stratification and the winter mixing episodes reduce the bias. The bias correction is not as efficient on reducing seasonal biases as it is on reducing long term systematic biases. A correction of air-sea fluxes depending on the SST increment is considered for future versions of the system. The use of Reynolds ¼° L4 SST product (AVHRR AMSR-E) for data assimilation reduces part of the surface bias in the North Atlantic and changes the signal in the Mediterranean. The use of Reynolds ¼° AVHRR analyses will be extended to the other Mercator Ocean systems in 2012. The PSY2V4R2 system is different from the other systems:

- Update of the MDT with GOCE and bias correction
- Assimilation of Reynolds ¼° AVHRR-AMSRE SST observations instead of ½° RTG-SST
- Increase of observation error for the assimilation of SLA near the coast and on the shelves, and for the assimilation of SST near the coast
- Modification of the correlation/influence radii for the analysis specifically near the European coast.
- Restart from October 2009 from WOA05 climatology

In PSY2V4R2:

- The products are less constrained by altimetry near the coast and on the shelves but are generally closer to in situ observations and climatologies in these regions
- The quality is slightly degraded in the Eastern Mediterranean and in the Caribbean region

In PSY4V1R3:
A strong salinity bias (PSY4V1R3 is too salty near 100 m) is present in the North Pacific (Alaska Gyre). It strengthens in AMJ 2012 and alters the global statistics.

V.2.Accuracy of the daily average products with respect to observations

V.2.1. T/S profiles observations

V.2.1.1. Global statistics for AMJ 2012

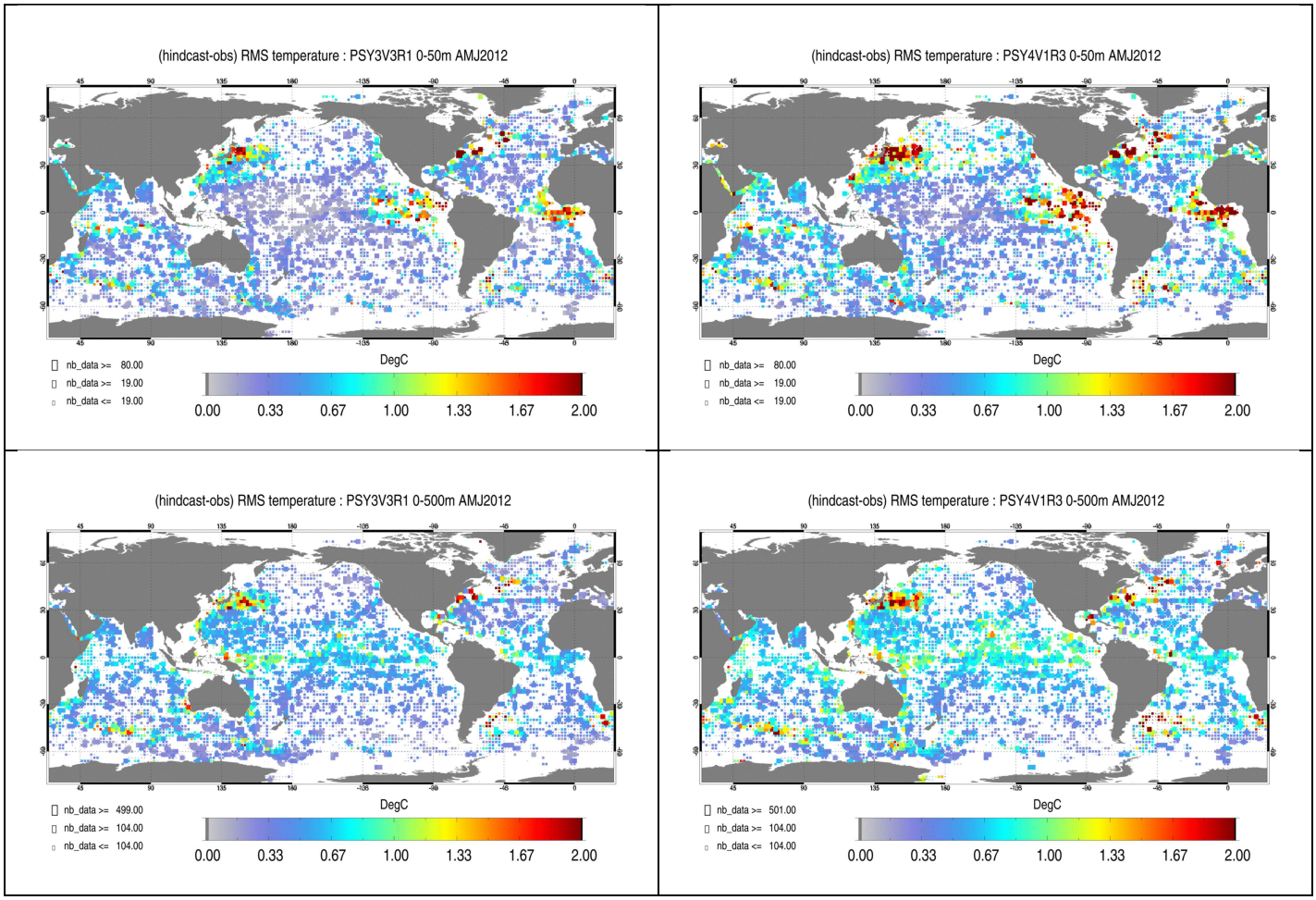

Figure 24: RMS temperature (°C) difference (model-observation) in AMJ 2012 between all available T/S observations from the Coriolis database and the daily average hindcast PSY3V3R1 products on the left and hindcast PSY4V1R3 on the right column colocalised with the observations. Averages are performed in the 0-50m layer (upper panel) and in the 0-500m layer (lower panel). The size of the pixel is proportional to the number of observations used to compute the RMS in 2°x2° boxes.

As can be seen in Figure 24, in both PSY3V3R1 and PSY4V1R3 temperature errors in the 0-500m layer stand between 0.5 and 1°C in most regions of the globe. Regions of high mesoscale activity (Kuroshio, Gulf Stream, Agulhas current) and regions of upwelling in the tropical Atlantic and Tropical Pacific display higher errors (up to 3°C). PSY4V1R3 has higher variability and no bias correction and thus departures from the observations are higher than in PSY3V3R1 on average in these regions. PSY3V3R1 seems to perform better than PSY4V1R3 in the tropical Pacific but both systems have a strong temperature (cold) biases in the Eastern part of the Pacific basin at the surface (in the 0-50m layer) and in the western part of

the Pacific basin in the 0-500m layer (warm pool). This is mainly due to the transition towards el Niño conditions. Again, larger errors naturally occur in regions of strong variability. This is consistent with the RMS errors of SST in the nino3 region that can be seen in Figure 12.

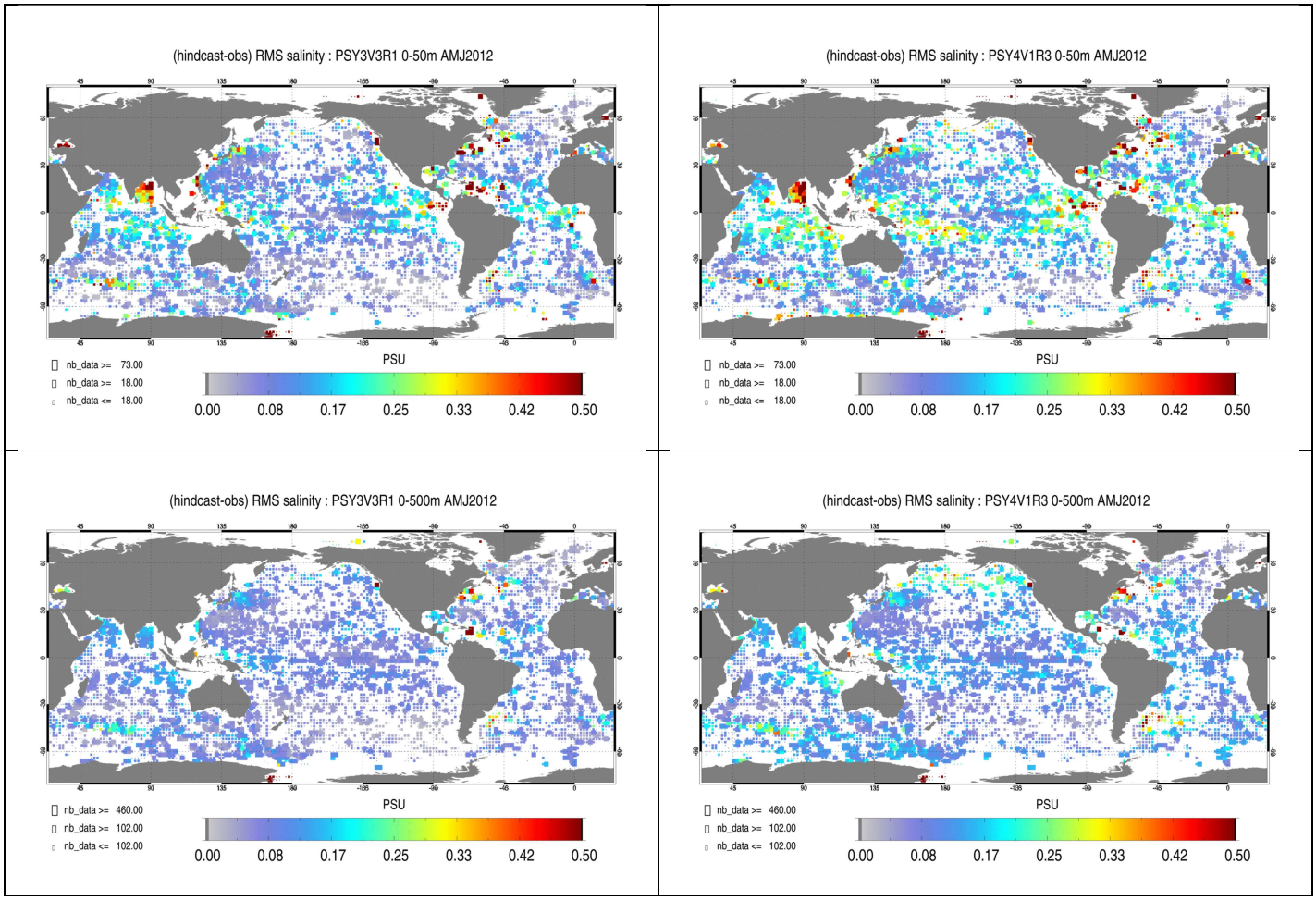

Figure 25: RMS salinity (psu) difference (model-observation) in AMJ 2012 between all available T/S observations from the Coriolis database and the daily average hindcast PSY3V3R1 products on the left and hindcast PSY4V1R3 on the right column, colocalised with the observations. Averages are performed in the 0-50m layer (upper panel) and in the 0-500m layer (lower panel). The size of the pixel is proportional to the number of observations used to compute the RMS in 2°x2° boxes.

The salinity RMS errors (Figure 25) are usually less than 0.2 psu but can reach higher values in regions of high runoff (Amazon, Sea Ice limit) or precipitations (ITCZ, SPCZ, Gulf of Bengal), and in regions of high mesoscale variability. The salinity error is generally less in PSY3V3R1 than in PSY4V1R3 for instance here in the North Pacific gyre (where a salty bias develops as already mentioned), the Indian Ocean, the South Atlantic Ocean or the Western Pacific Ocean. Precipitations are overestimated in the tropical band, leading to a fresh bias in this region.

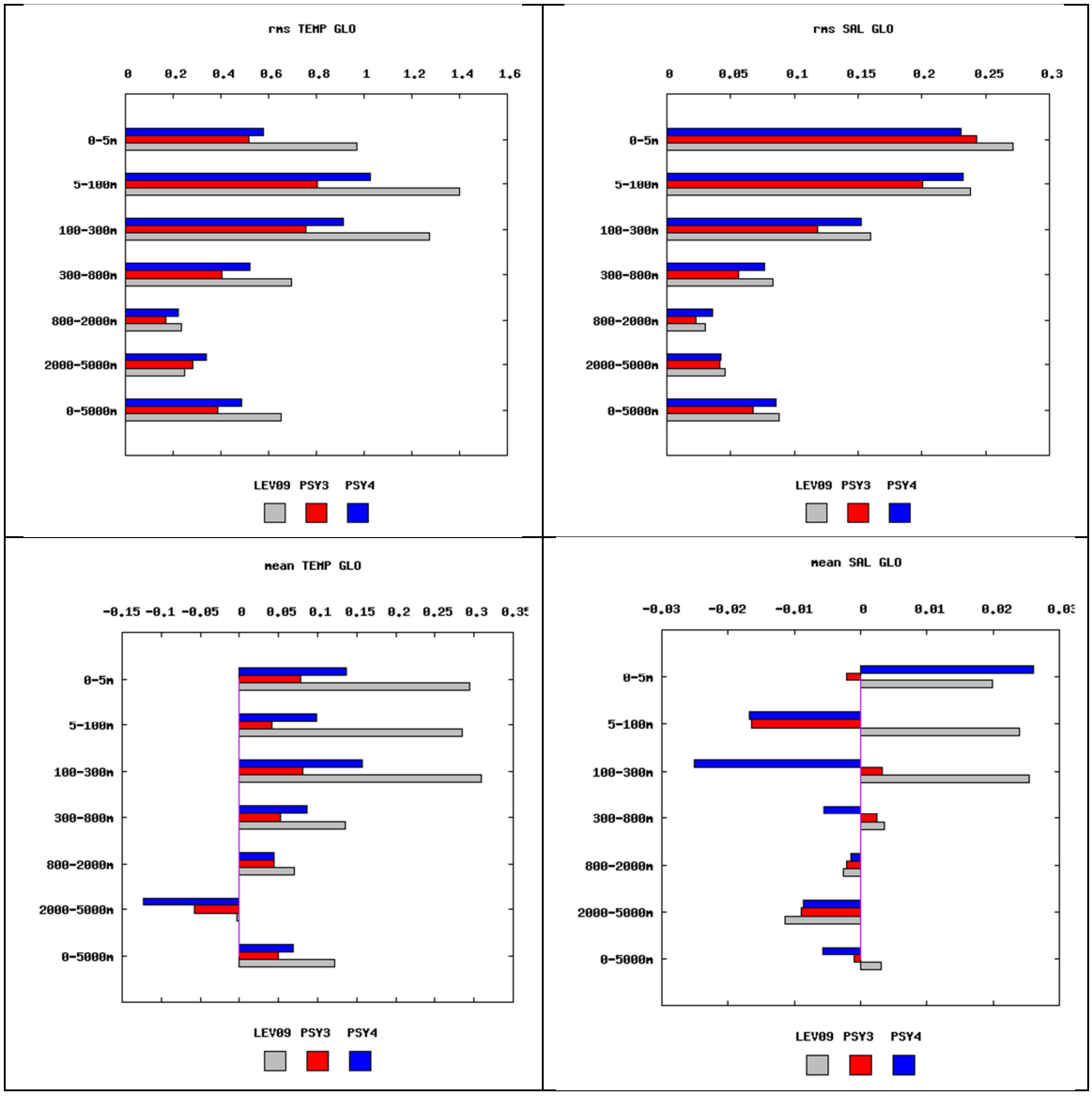

Figure 26 : Global statistics for temperature (°C, left column) salinity (psu, right column) and averaged in 6 consecutive layers from 0 to 5000m. RMS difference (upper panel) and mean difference (observation-model, lower panel) between all available T/S observations from the Coriolis database and the daily average hindcast PSY3V3R1 products (green) , hindcast PSY4V1R3 (red) and WOA09 climatology (blue) colocalised with the observations. NB: average on model levels is performed as an intermediate step which reduces the artefacts of inhomogeneous density of observations on the vertical.

For the global region in Figure 26, the intermediate resolution model (PSY3V3R1) is more accurate than the high resolution model (PSY4V1R3) in terms of RMS and mean difference for both temperature and salinity mainly thanks to the bias correction which is applied in PSY3V3R1 and not yet in PSY4V1R3. The effects of this correction are on the whole water column for temperature and salinity. Both global systems are too cold on the whole water column, PSY3V3R1 being significantly closer to the observations than PSY4V1R3. A warm bias seems to appear under 2000m but cannot be confirmed because only few observations are available at these depths. PSY4V1R3 is globally too salty in the 5-800 m layer contrary to PSY3V3R1 which becomes slightly fresh from 100 m down to 800 m depth. At the surface PSY3V3R1 exhibits a salty bias while PSY4V1R3 is too fresh on average. In PSY3V3R1 the salty surface bias is very small as the departures from the observations are centred around zero

(not shown). This explains why the RMS difference is finally slightly higher in PSY3V3R1 at the surface than in PSY4V1R3. In PSY4V1R3 the fresh bias mostly comes from the tropical belt (not shown).The two systems are more accurate than the WOA09 climatology (Levitus 2009) over the whole water column in temperature. In salinity, PSY3V3R1 is performing better than PSY4V1R3.

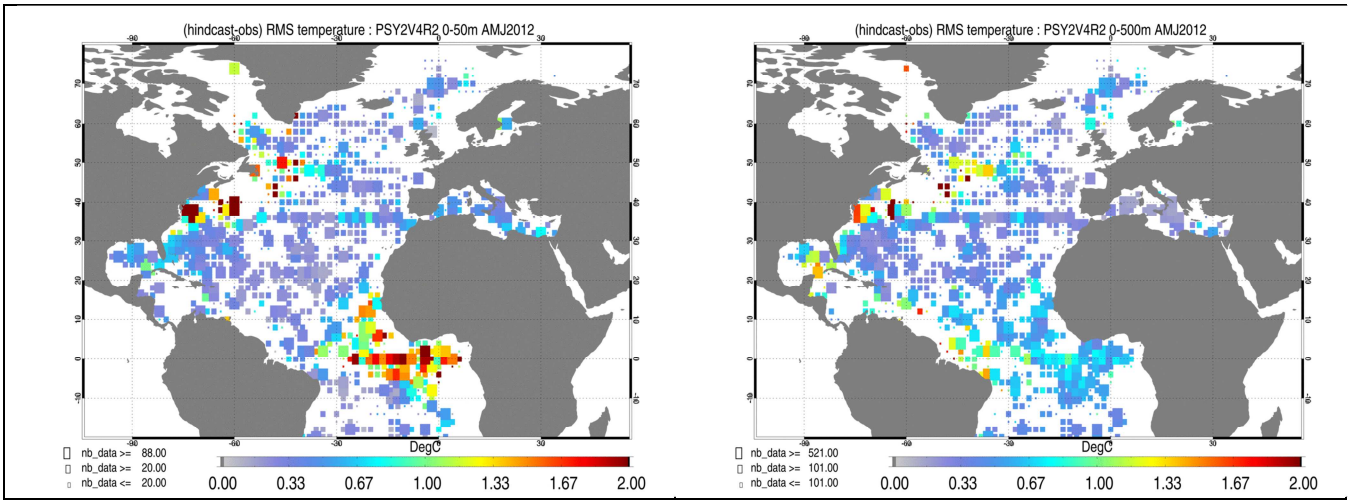

Figure 27: Upper panel: RMS difference (model-observation) of temperature (°C) in AMJ 2012 between all available T/S observations from the Coriolis database and the daily average PSY2V4R2 hindcast products colocalised with the observations in the 0-50m layer (left column) and 0-500m layer (right column).

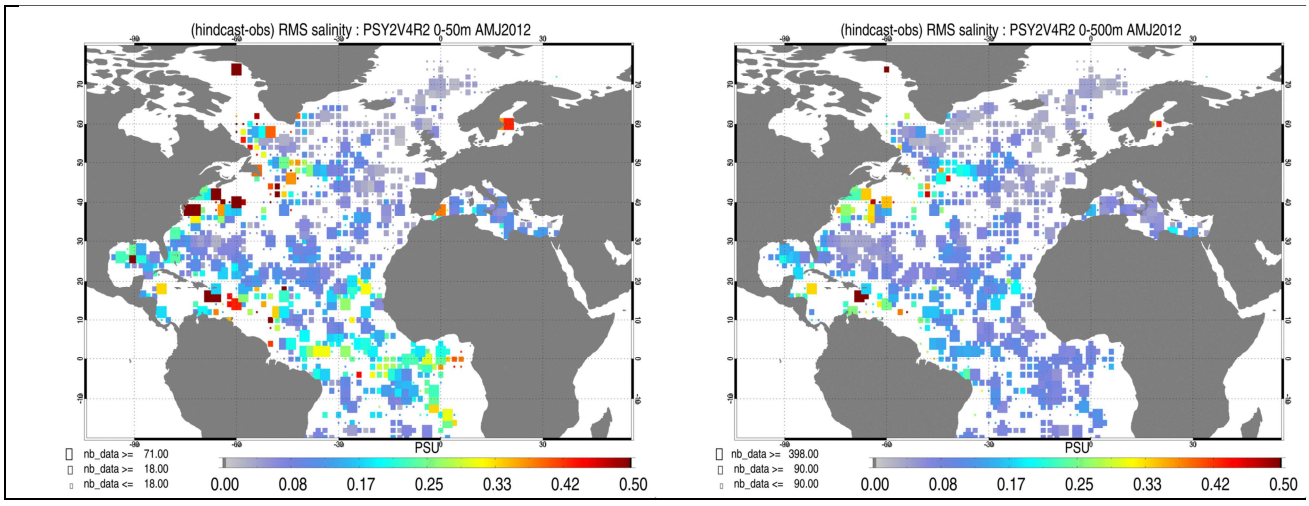

Figure 28: Upper panel: RMS difference (model-observation) of salinity (psu) in the 0-50m layer in AMJ 2012 between all available T/S observations from the Coriolis database and the daily average PSY2V4R2 hindcast products colocalised with the observations observations in the 0-50m layer (left column) and 0-500m layer (right column).

The general performance of PSY2V4R2 (departures from observations in the 0-500m layer) is less than 0.3°C and 0.05 psu in many regions of the Atlantic and Mediterranean (Figure 27 and Figure 28). The strongest departures from temperature and salinity observations are always observed in the Gulf Stream and the tropical Atlantic. Near surface salinity biases appear in the Algerian Sea, the Gulf of Guinea, the Caribbean Sea, the Labrador Sea, the Baltic Sea and the Gulf of Mexico. In the eastern tropical Atlantic biases concentrate in the 0-

50m layer (cold and fresh bias), while in the Western tropical Atlantic the whole 0-500m layer is biased (cold and fresh bias, not shown).

V.2.1.2. Water masses diagnostics

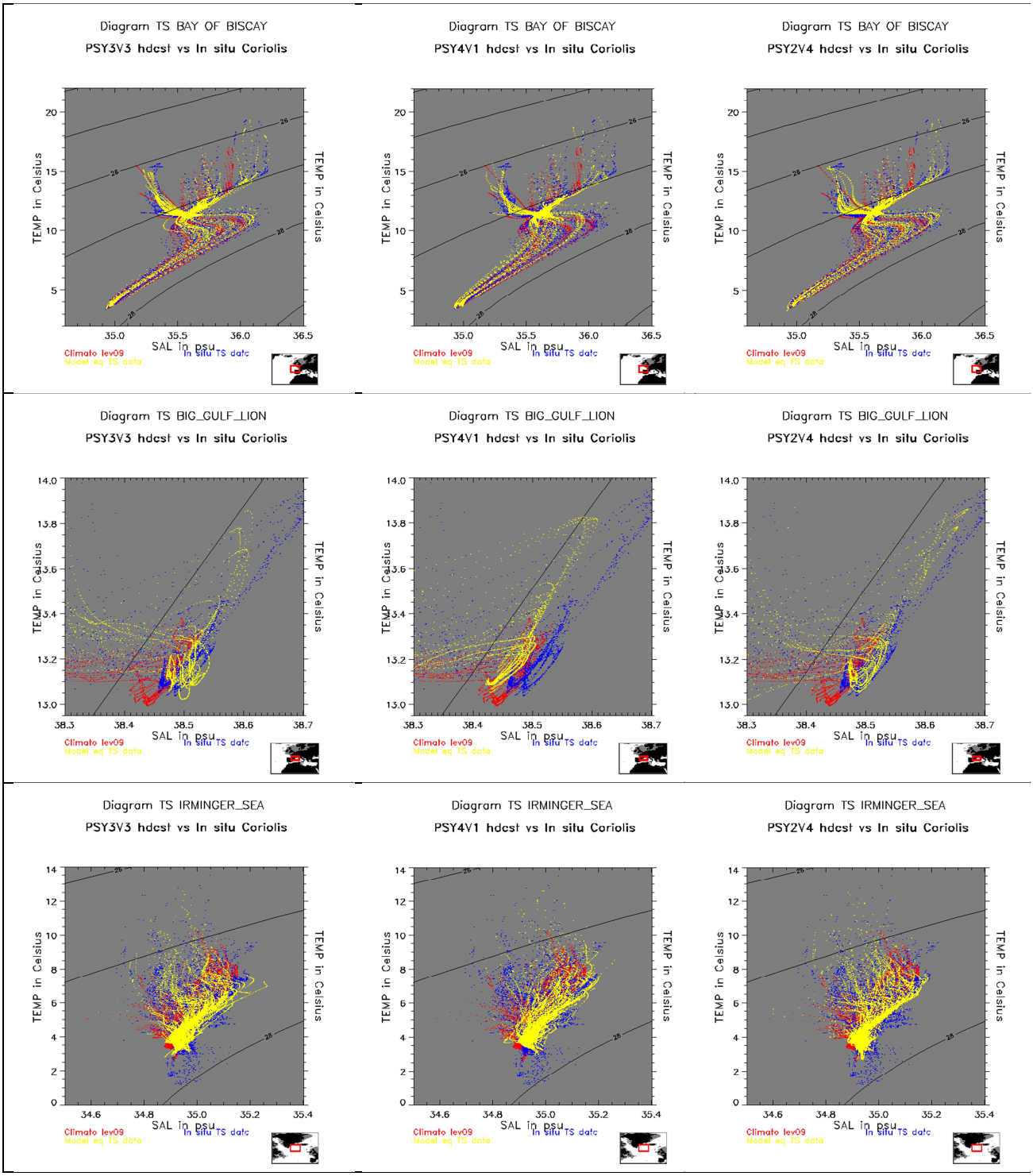

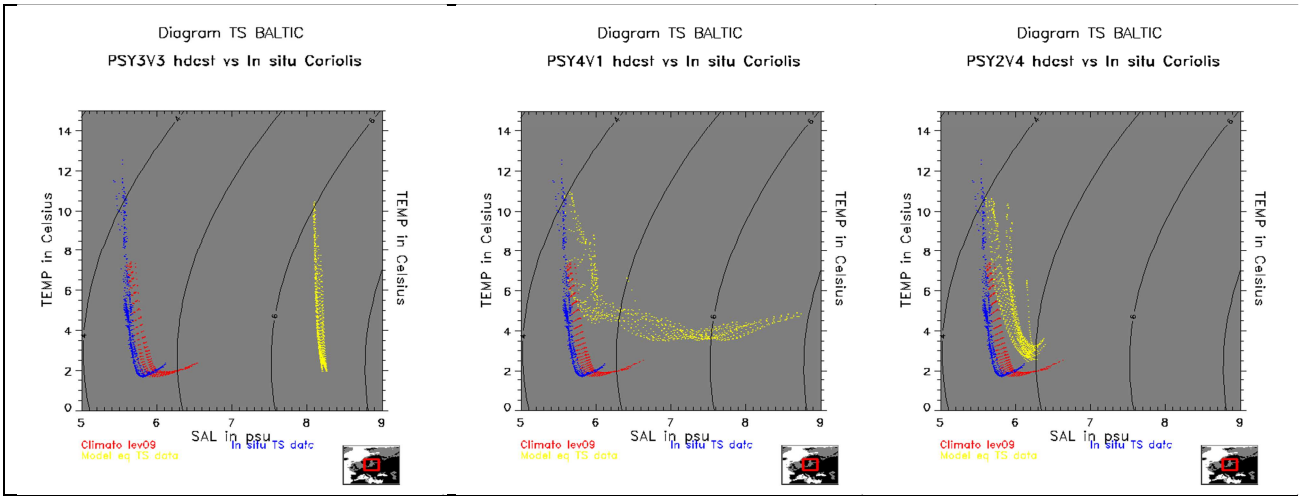

Figure 29: Water masses (Theta, S) diagrams in the Bay of Biscay (upper panel), Gulf of Lion (second panel) and Irminger Sea (third panel) and Baltic Sea (upper panel), comparison between PSY3V3R1 (left column) and PSY4V1R3 (middle column) and PSY2V4R2 (right column) in AMJ 2012. PSY2, PSY3 and PSY4: yellow dots; Levitus WOA09 climatology: red dots; in situ observations: blue dots.

We use here the daily products (analyses) collocated with the T/S profiles to draw "T, S" diagrams.

In the Bay of Biscay (Figure 29) we have the main influence of the Eastern North Atlantic Central Water, Mediterranean and Labrador Sea Water.

- Between 11°C and 20°C, 35.5 and 36.5 psu, warm and relatively salty Eastern North Atlantic Central Water gets mixed with the shelf water masses. PSY3V3R1 and PSY2V4R2 with bias correction both capture the spread of the freshest waters (35.5 psu, 11 °C)
- The "bias corrected" systems PSY3V3R1 and PSY2V4R2 better represent the Mediterranean Water characterized by high salinities (Salinities near 36psu) and relatively high temperatures (Temperatures near 10°C).
- Between 4°C and 7°C, 35.0 and 35.5 psu the fresher waters of the Labrador Sea are slightly better represented in PSY2V4R2 than in PSY3V3R1 and PSY4V1R3..

In the Gulf of Lion:

- The Levantine Intermediate Water (salinity maximum near 38.6 psu and 13.6°C) is too fresh in all systems this AMJ season. PSY4V1R3 intermediate waters the freshest of all systems. This AMJ 2012 season, PSY2V4R2 gives the most realistic water masses characteristics in this region

In the Irminger Sea:

- The North Atlantic Water (T > 7°C and S > 35.1 psu) is well represented by the three systems.
- The Irminger Sea Water (≈ 4°C and 35 psu) is too salty and warm in the three systems but PSY2V4R2 and PSY3V3R1 seems to be better than the global 1/12° PSY4V1R3.
- Waters colder than 3°C and ≈ 34.9 psu (Iceland Scotland Overflow waters) are not represented by any of the systems.

In the Baltic Sea:

- In the Baltic Sea, both global systems are very far from the observations, on the whole water column for PSY3V3R1, and especially at depth for PSY4V1R3. This region

is far better represented in PSY2V4R2, which prescribed errors for SLA and SST are higher in this region, and which benefits from a more recent version of the MDT.

In the western tropical Atlantic and in the Gulf of Guinea the water masses are well represented by all systems. PSY2V4R2 does not represent well the subsurface salinity maximum between the isopycn 24 and 26 (South Atlantic Subtropical waters) that both global systems capture.

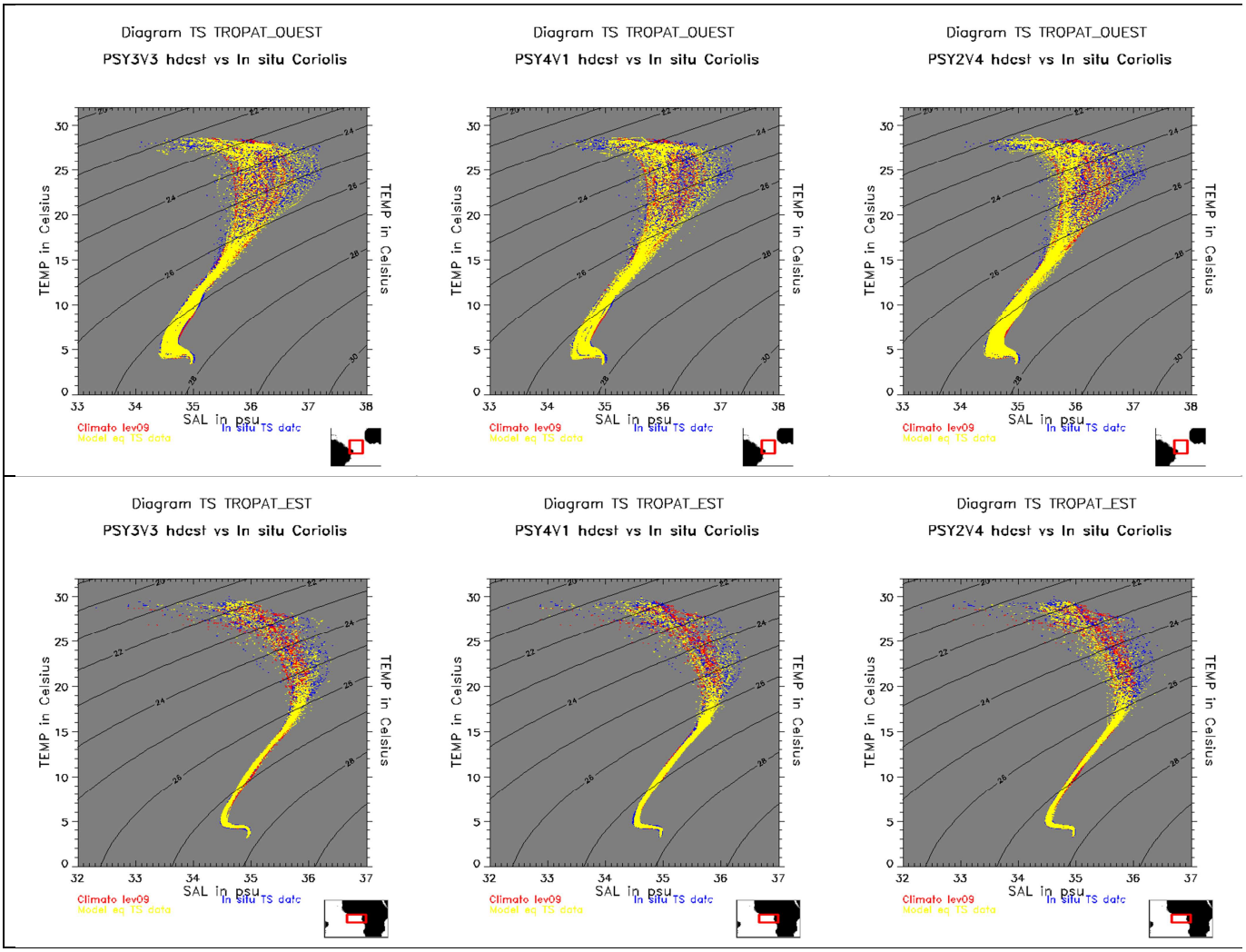

Figure 30 : Water masses (T, S) diagrams in the Western Tropical Atlantic (upper panel) and in the Eastern Tropical Atlantic (lower panel): for PSY3V3R1 (left); PSY4V1R3 (middle); and PSY2V4R2 (right) in AMJ 2012. PSY2, PSY3 and PSY4: yellow dots; Levitus WOA09 climatology; red dots, in situ observations: blue dots.

In the Agulhas current and Kuroshio Current (Figure 31) PSY3V3R1 and PSY4V1R3 give a realistic description of water masses. In both regions, a fresh bias appears in PSY4V1R3 around the isopycn '27' at around 5°C while it is not present in the PSY3V3R1 system. In general, the water masses characteristics display a wider spread in the high resolution 1/12° than in the ¼°, which is more consistent with T and S observations. This is especially true at the surface in the highly energetic regions of the Agulhas and of the Gulf Stream.

In the Gulf Stream region, models are too salty from the '27' to the '28' isopycn, where they miss the cold and fresh waters of the Labrador current. In the Gulf of Cadiz the signature of the Mediterranean outflow is better reproduced by PSY3V3R1 than by PSY4V1R3, as in the bay of Biscay.

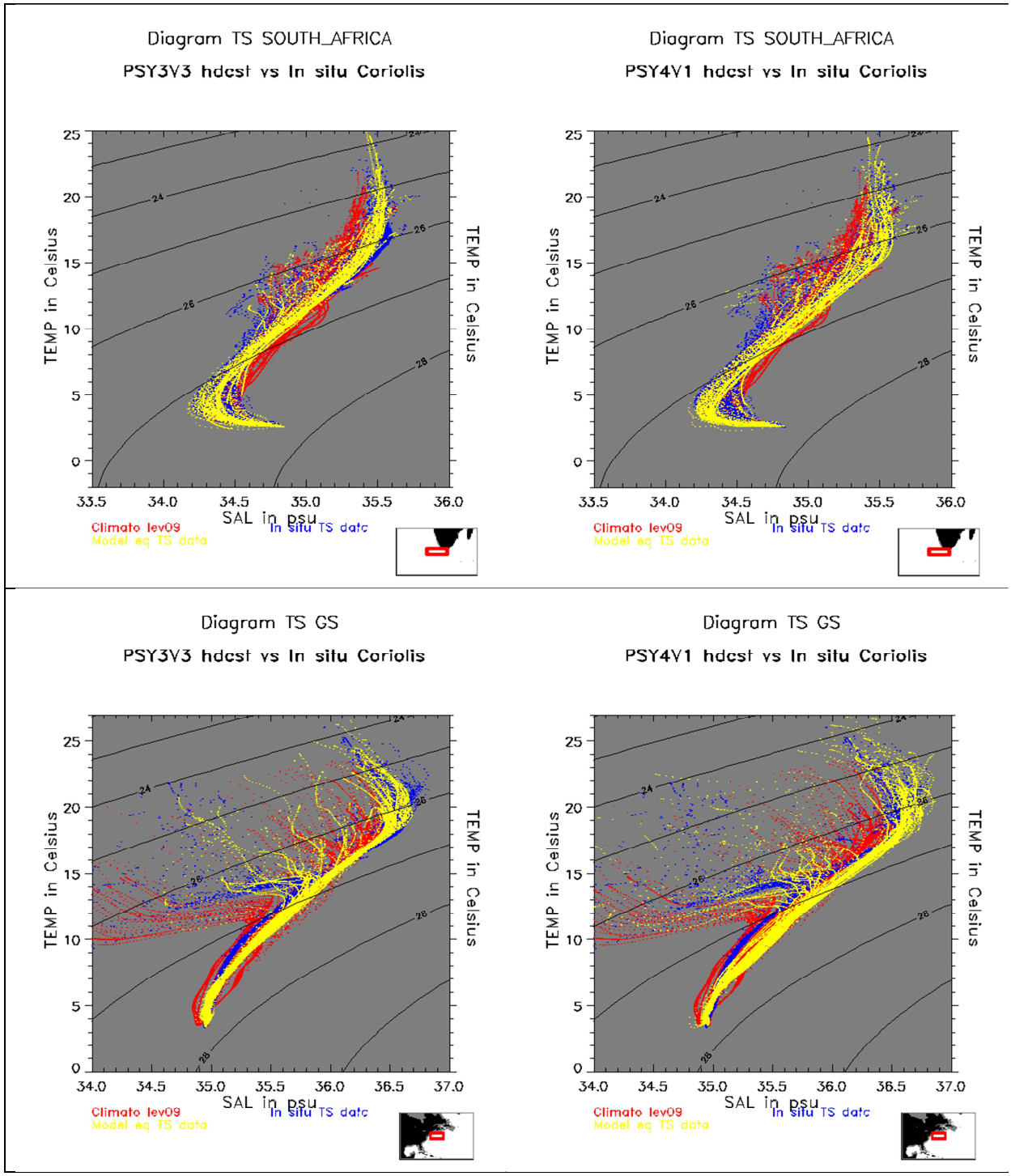

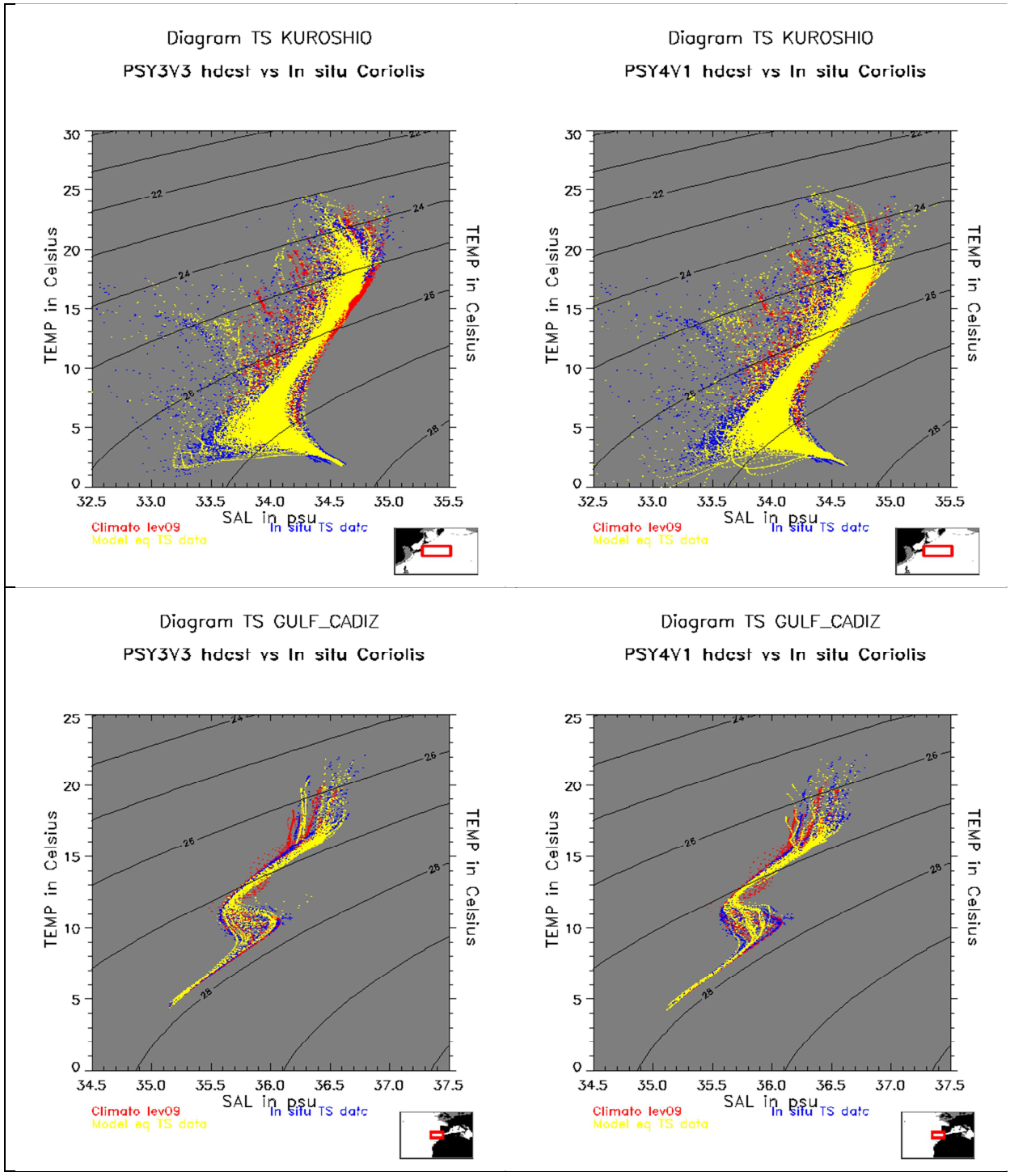

Figure 31: Water masses (T, S) diagrams in South Africa, Kuroshio, Gulf Stream region and Gulf of Cadiz (respectively from top to bottom): for PSY3V3R1 (left); PSY4V1R3 (right) in AMJ 2012. PSY3 and PSY4: yellow dots; Levitus WOA09 climatology: red dots; in situ observations: blue dots.

V.2.2. SST Comparisons

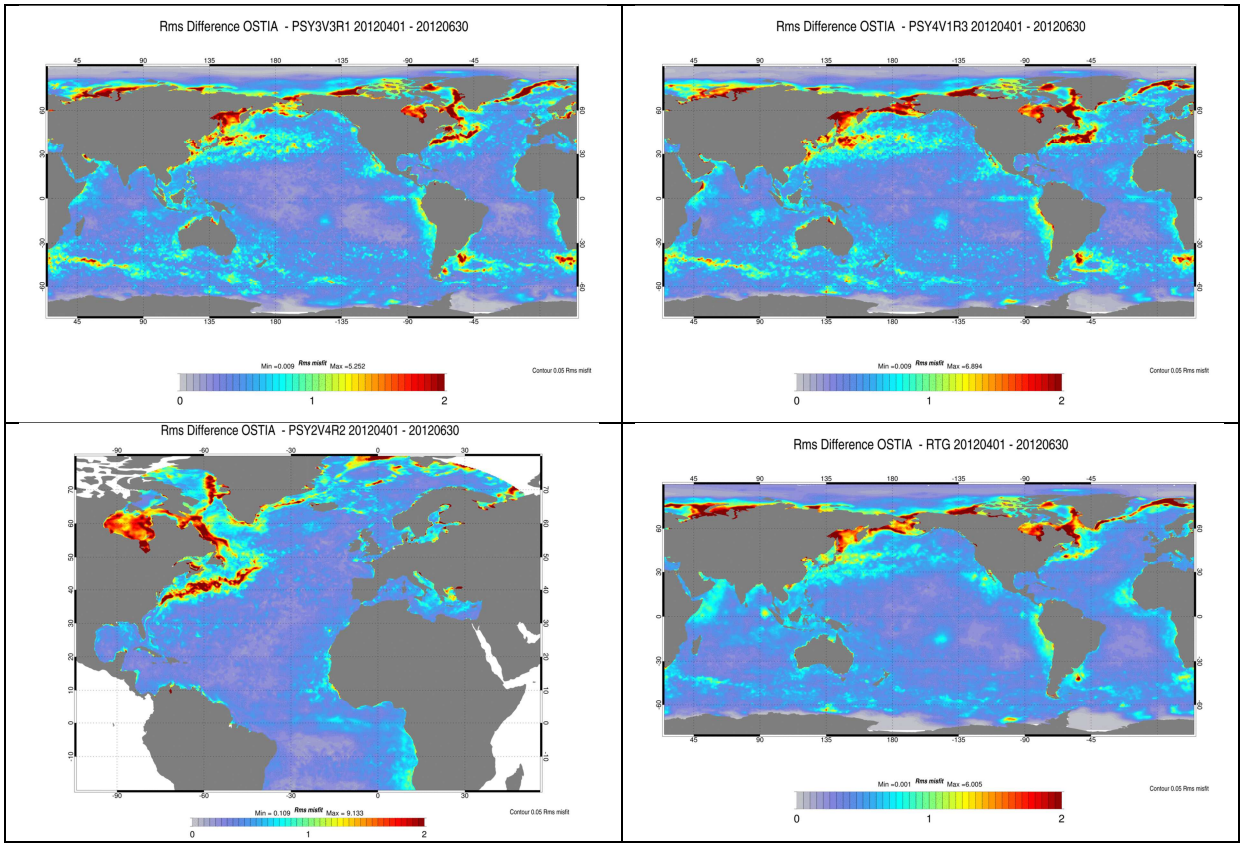

Figure 32 : RMS temperature (°C) differences between OSTIA daily analyses and PSY3V3R1 daily analyses (upper left); between OSTIA and PSY4V1R3 (upper right), between OSTIA and PSY2V4R2 (lower left), and between OSTIA and RTG daily analyses (lower right). The Mercator Océan analyses are colocalised with the satellite observations analyses.

Quarterly average SST differences with OSTIA analyses show that in the subtropical gyres the SST is very close to OSTIA, with difference values staying below the observation error of 0.5 °C on average. High RMS difference values are encountered in high spatio-temporal variability regions such as the Gulf Stream or the Kuroshio. The stronger is the intrinsic variability of the model (the higher the resolution), the stronger is the RMS difference with OSTIA. The strong regional biases that are diagnosed in summer in the PSY3V3R1 global system in the North Pacific (see *QuO Va Dis?*#6) start to appear this spring season, with cold biases of around 1°C in the Northern Hemisphere (Figure 33) Strong differences can be detected near the sea ice limit in the Arctic in all the systems particularly in the Labrador Sea and in the Barents Sea for the global systems. There are also differences in the Bering Sea where ice cover remained unusually extensive. Part of this disagreement with the OSTIA analysis can be attributed to the assimilation of RTG SST in PSY3V3R1 and PSY4V1R3, while Reynolds ¼° AVHRR only is assimilated in PSY2V4R2. These products display better performance than RTG SST especially in the high latitudes[2]

[2] Guinehut, S.: Validation of different SST products using Argo dataset, CLS, Toulouse, Report CLS-DOS-NT-10-264, 42 pp., 2010.

The difference between PSY3 and OSTIA in the South Pacific near 20°S and 140°W is due to a warm SST core in this region that is present in OSTIA and not in the other products (either RTG or AVHRR, Figure 33).

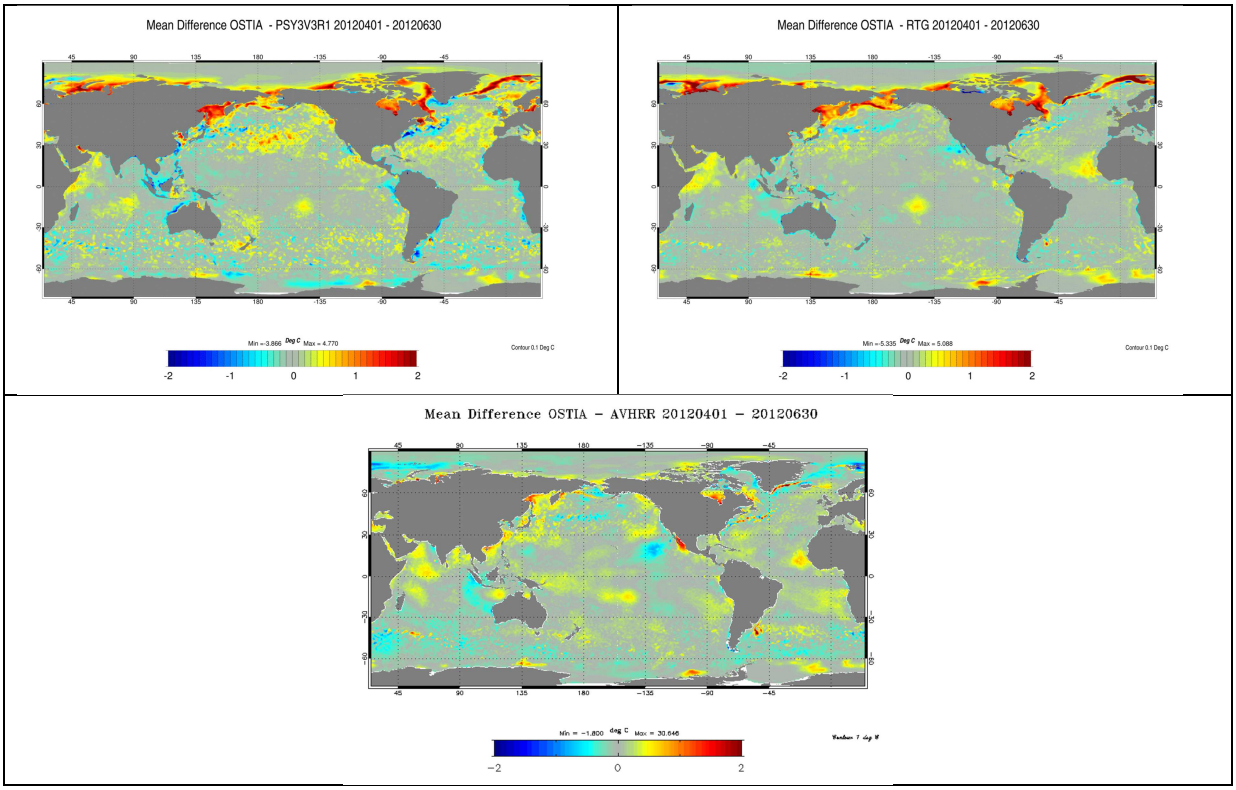

Figure 33: Mean SST (°C) daily differences between OSTIA daily analyses and PSY3V3R1 daily analyses (upper left), between OSTIA and RTG daily analyses (upper right) and between OSTIA and Reynolds ¼° AVHRR daily analyses (lower left).

V.2.3. Drifting buoys velocity measurements

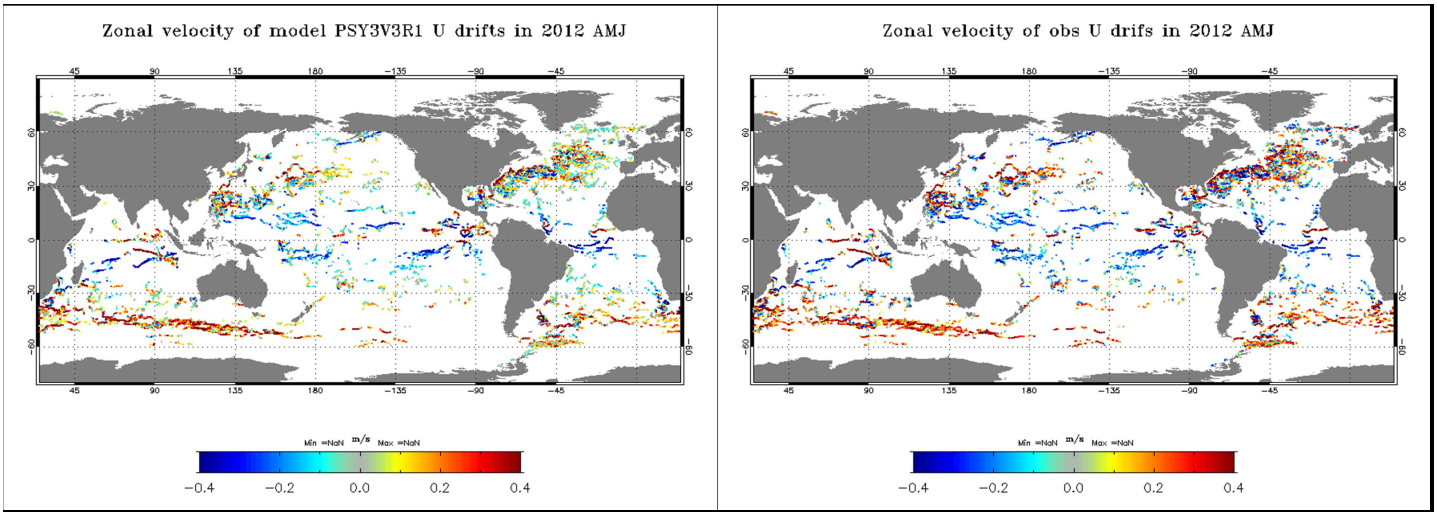

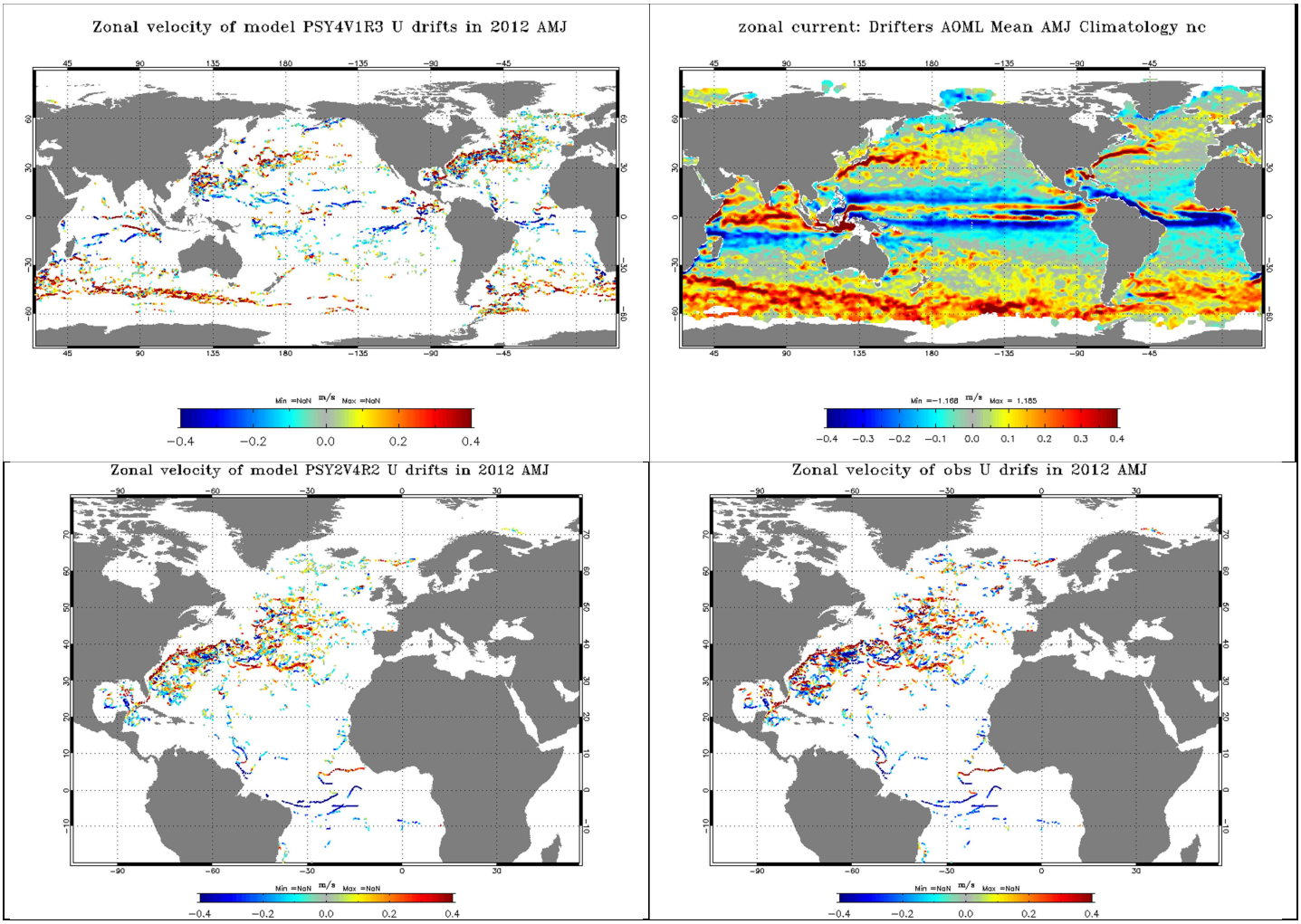

Figure 34: Comparison between modelled zonal current (left panel) and zonal current from drifters (right panel) in m/s. In the left column: velocities collocated with drifter positions in AMJ 2012 for PSY3V3R1 (upper panel), PSY4V1R3 (middle panel) and PSY2V4R2 (bottom panel). In the right column, zonal current from drifters in AMJ 2012 (upper panel) at global scale, AOML drifter climatology for AMJ with new drogue correction from Lumpkin & al, in preparation (middle) and zonal current in AMJ 2012 from drifters (lower panel) at regional scale.

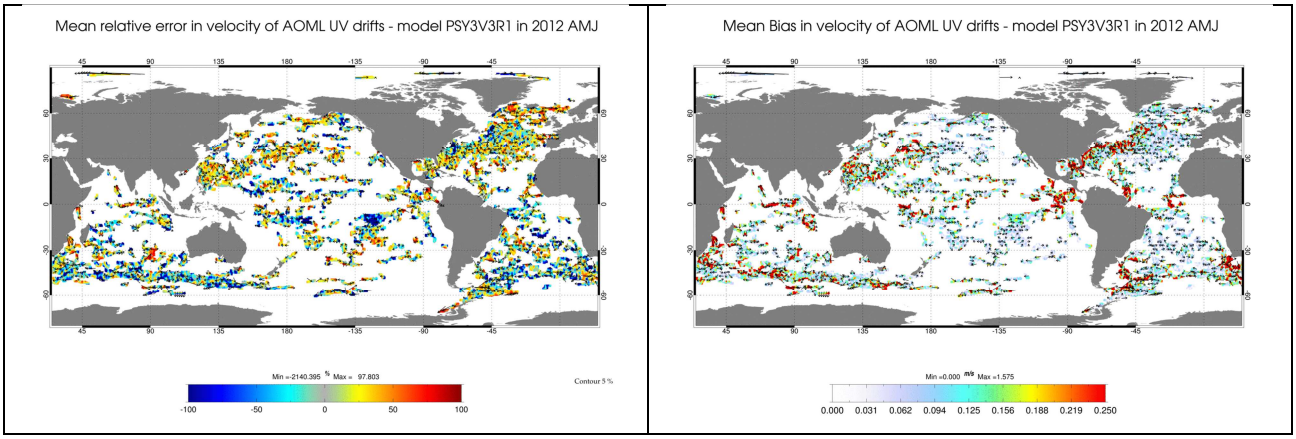

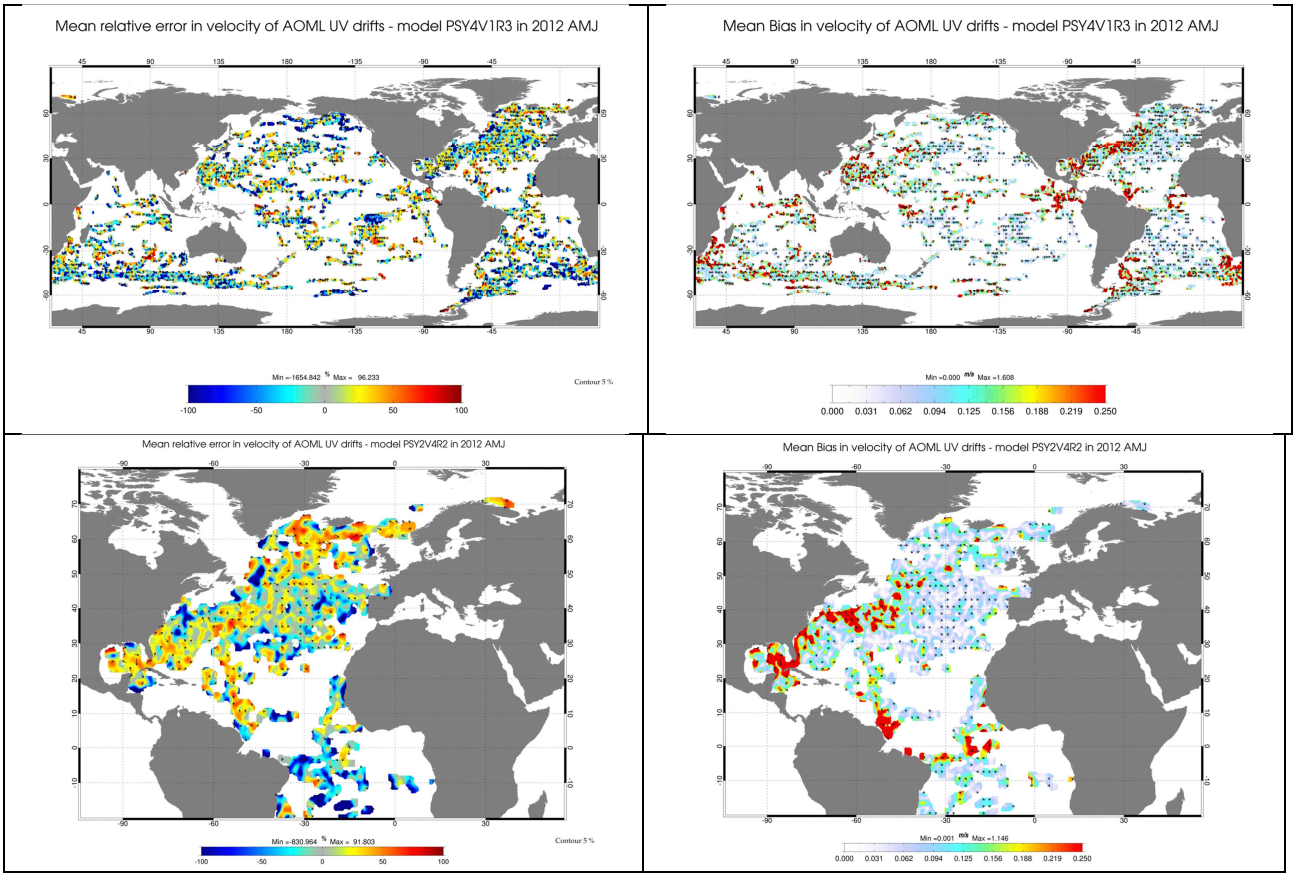

Figure 35 : In AMJ 2012, comparison of the mean relative velocity error between in situ AOML drifters and model data on the left side and mean zonal velocity bias between in situ AOML drifters with Mercator Océan correction (see text) and model data on the right side. Upper panel: PSY3V3R1, middle panel: PSY4V1R3, bottom panel : PSY2V4R2. NB: zoom at 500% to see the arrows

Since *QuO Va Dis?* #5 we have been taking into account the fact that velocities estimated by the drifters happen to be biased towards high velocities.
As in *QuO Va Dis?* #5 we compute comparisons with slippage and windage corrections (cf *QuO Va Dis?* #5 and Annex C) . Once this "Mercator Océan" correction is applied to the drifter observations, the zonal velocity of the model (Figure 35) at 15 m depth and the meridional velocity (not shown) seem to be more consistent with the observations for the AMJ 2012 period.

The main differences between the systems appear in the North Atlantic and North Pacific Oceans where PSY3V3R1 underestimate on average the eastward currents, which is less pronounced in the high resolution systems PSY4V1R3 and PSY2V4R2. This season especially in the northern hemisphere, and in the Equatorial Indian ocean, PSY4V1R3 is closer to observed velocities than PSY3V3R1.

On average over longer periods, the usual behaviour compared to drifters velocities is that PSY4V1R3 and PSY3V3R1 underestimate the surface velocity in the mid latitudes. All systems overestimate the Equatorial currents and southern part of the North Brazil Current (NBC).
For all systems the largest direction errors are local (not shown) and generally correspond to ill positioned strong current structures in high variability regions (Gulf Stream, Kurioshio,

North Brazil Current, Zapiola eddy, Agulhas current, Florida current, East African Coast current, Equatorial Pacific Countercurrent).

V.2.4. Sea ice concentration

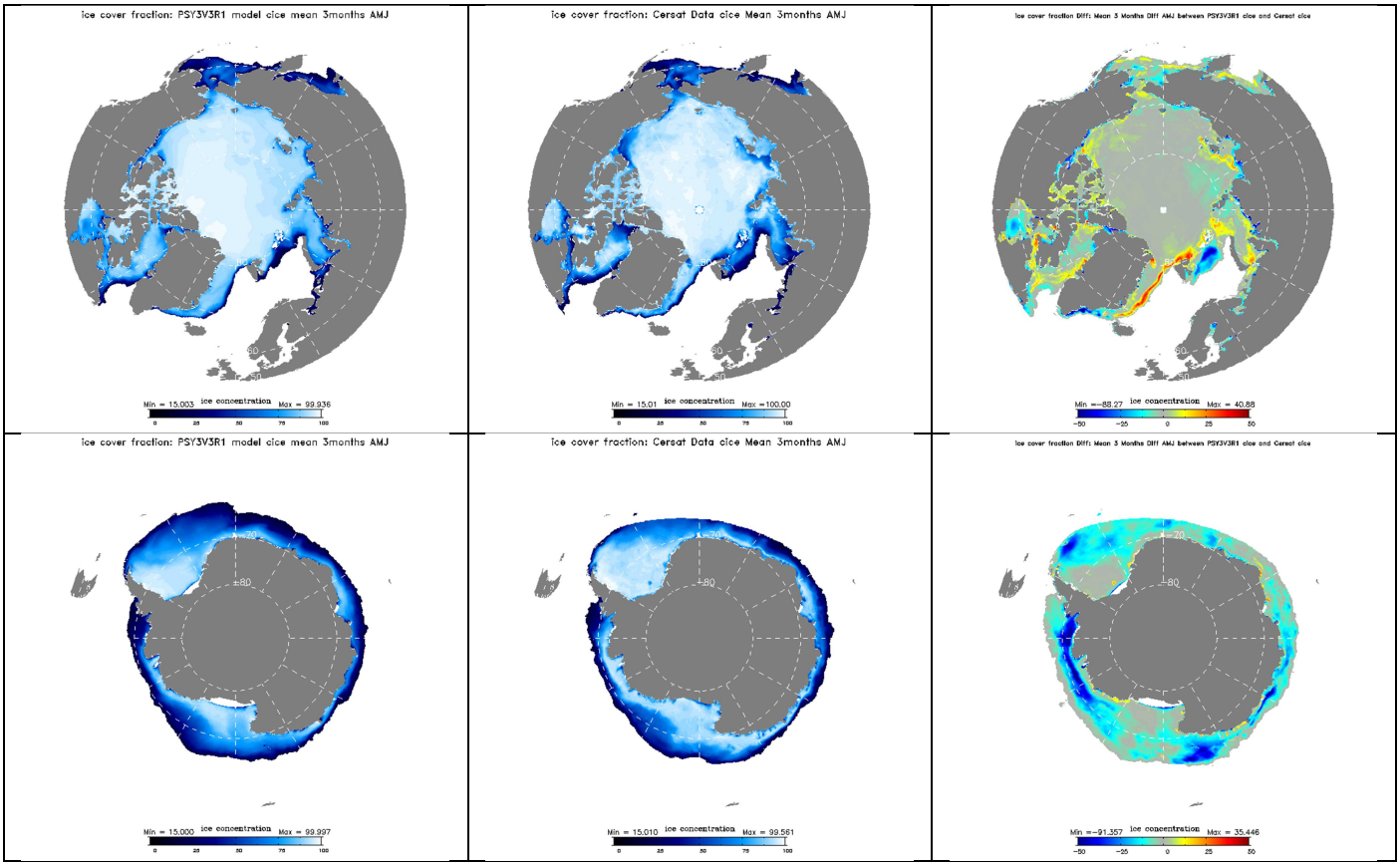

Figure 36: Comparison of the sea ice cover fraction mean for AMJ 2012 for PSY3V3R1 in the Arctic (upper panel) and in the Antarctic (lower panel), for each panel the model is on the left, the mean of Cersat dataset in the middle and the difference on the right.

In AMJ 2012 the PSY3V3R1 Arctic sea ice fraction is in agreement with the observations on average. The relatively small discrepancies inside the sea ice pack will not be considered as significant as the sea ice concentration observations over 95% are not reliable. Strong discrepancies with observed concentration remain in the marginal seas mainly in the North Atlantic Ocean side of the Arctic, especially in the Fram strait and the Barents Sea this AMJ 2012 season (Figure 36).

Model studies show that the overestimation in the Canadian Archipelago is first due to badly resolved sea ice circulation (should be improved with higher horizontal resolution). The overestimation in the eastern part of the Labrador Sea is due to a weak extent of the West Greenland Current; similar behaviour in the East Greenland Current.

The calibration on years 2007 to 2009 has shown that the PSY3V3R1 system tends to melt too much ice during the summer, while the winter sea ice covers are much more realistic in PSY3V3R1 than in previous versions of PSY3. See Figure 59 for monthly averages time series over the last 12 months. On the contrary PSY4V1R3 sea ice cover is unrealistic

(overestimation throughout the year) due to the use of a previous version of LIM2 and daily atmospheric forcings.

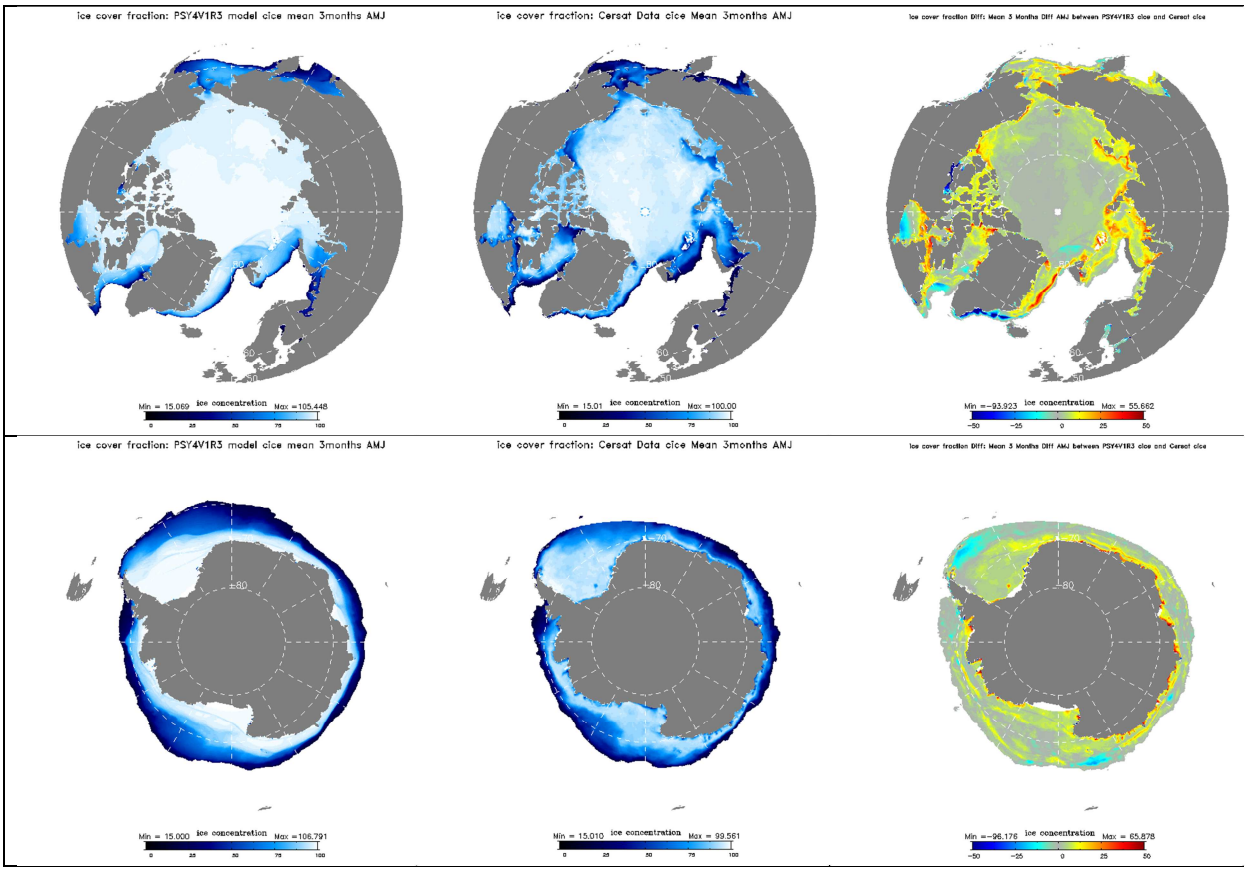

Figure 37: Comparison of the sea ice cover fraction mean for AMJ 2012 for PSY4V1R3 in the Arctic (upper panel) and in the Antarctic (lower panel), for each panel the model is on the left, the mean of Cersat dataset in the middle and the difference on the right.

As expected in the Antarctic during the beginning of the austral summer the sea ice concentration is underestimated in the model PSY3V3R1 and overestimated in PSY4V1R3, especially at the south of the Ross Sea, in the Weddel Sea, Bellinghausen and Admundsen Seas and along the Eastern coast.

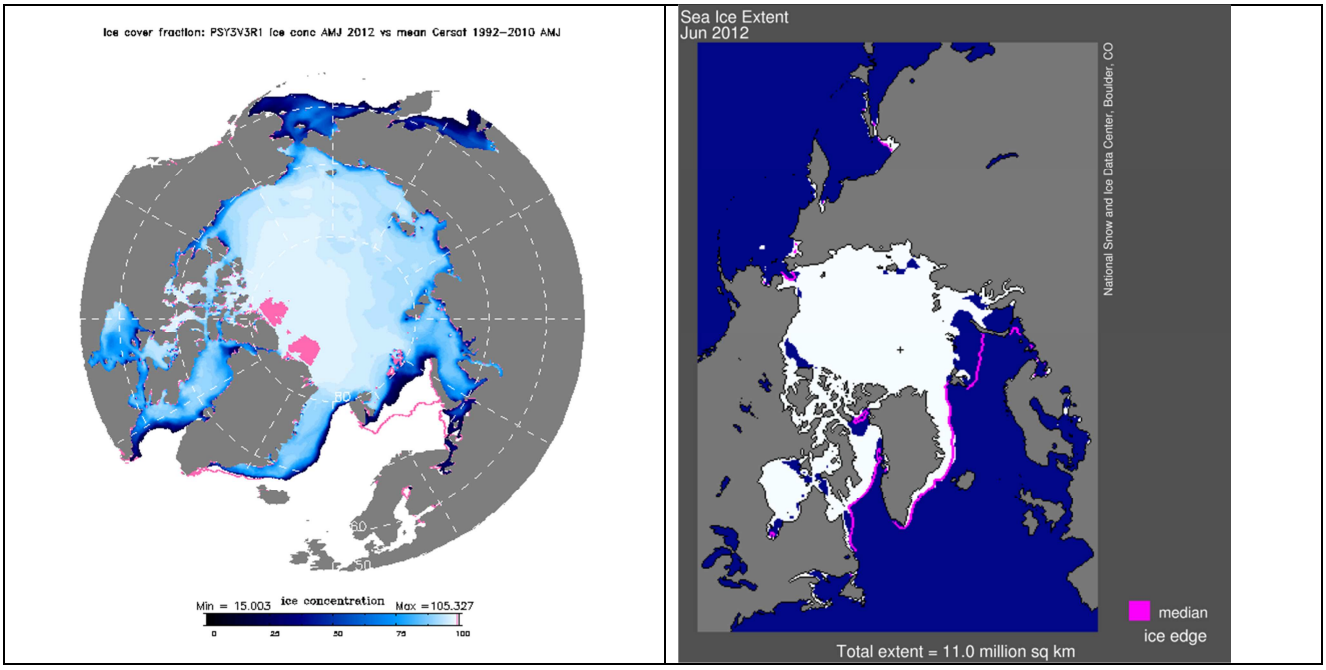

Figure 38: AMJ 2012 Arctic sea ice extent in PSY3V3R1 with overimposed climatological AMJ 1992-2010 sea ice fraction (magenta line, > 15% ice concentration) (left) and NSIDC map of the sea ice extent in the Arctic for June 2012 in comparison with a 1979-2000 median extend (right).

Figure 38 illustrates the fact that sea ice cover in AMJ 2012 is less than the past years climatology, especially in the Barents Sea, even with a slight underestimation in PSY3V3R1 in this region in AMJ 2012. In the Antarctic the model bias prevents us from commenting the climate signal (not shown).

V.2.5. Closer to the coast with the IBI36V2 system: multiple comparisons

V.2.5.1. Comparisons with SST from CMS

Figure 39 displays bias, RMS error and correlation calculated from comparisons with SST measured by satellite in AMJ 2012 (Météo-France CMS high resolution SST at 1/10°). The model displays a cold bias in the North Sea shelf, and a warm bias in the Bay of Biscay and in the abyssal plain west of the Iberian coast. We note that less than 30 observations per month are available in most pixels of this last region, while twice as much observations are available in the Mediterranean Sea or in the North Sea. Warm biases persist along the Moroccan and Iberian coasts where upwelling occurs. In the English Channel and Celtic Sea, the biases are linked to tidal mixing. In the Mediterranean Sea, biases are associated to the Alboran gyre and the Algerian current. Away from the shelf, the RMS error is small (less than 0.5°C), except between 45 and 50°N; but this area has the smallest number of observations. The biases are higher this spring AMJ 2012 season (especially along Iberian coasts) with respect to the previous winter season; while the variability is better reproduced (higher correlation in the abyssal plain).

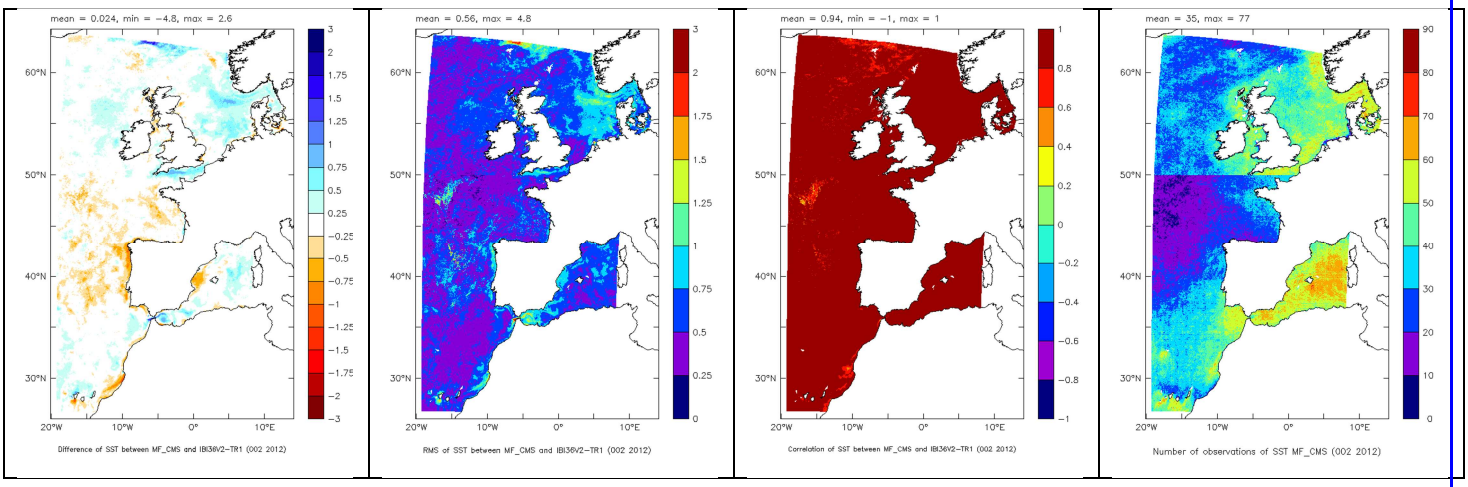

Figure 39 : Comparisons (model – observation) between IBI36V2 and analysed SST from MF_CMS for the AMJ 2012 period. From the left to the right: mean bias, RMS error, correlation, number of observations

V.2.5.2. Comparisons with in situ data from EN3/ENSEMBLE for AMJ 2012

Averaged temperature profiles (Figure 40) show that the strongest mean bias and RMS error are observed between 20 and 80 m depth, in the thermocline, and also near 1200m, at the average depth of the Mediterranean outflow. The model is close to the observations on the whole water column. Below the thermocline, the mean bias is almost zero, and the strongest RMS is found at the Mediterranean Sea Water level. In the Bay of Biscay, the Mediterranean waters are significantly too warm. As shown by the mean temperature profiles, PSY2V4R2 is closer to the temperature observations than IBI36V2 on the whole water column, even if IBI is initialized with, and forced at the boundaries by PSY2V4R2. Super-obervations (as for Figure 24 and Figure 26) will be computed in the next *QuO Va Dis?* issue in order to reduce differences that may come from the data sampling. It is also the case when we compare RMS errors (not shown). However, IBI36V2 tend to display at least as good results as PSY2V4R2 in the surface layer (0-50m). The same comments apply on salinity (Figure 41).

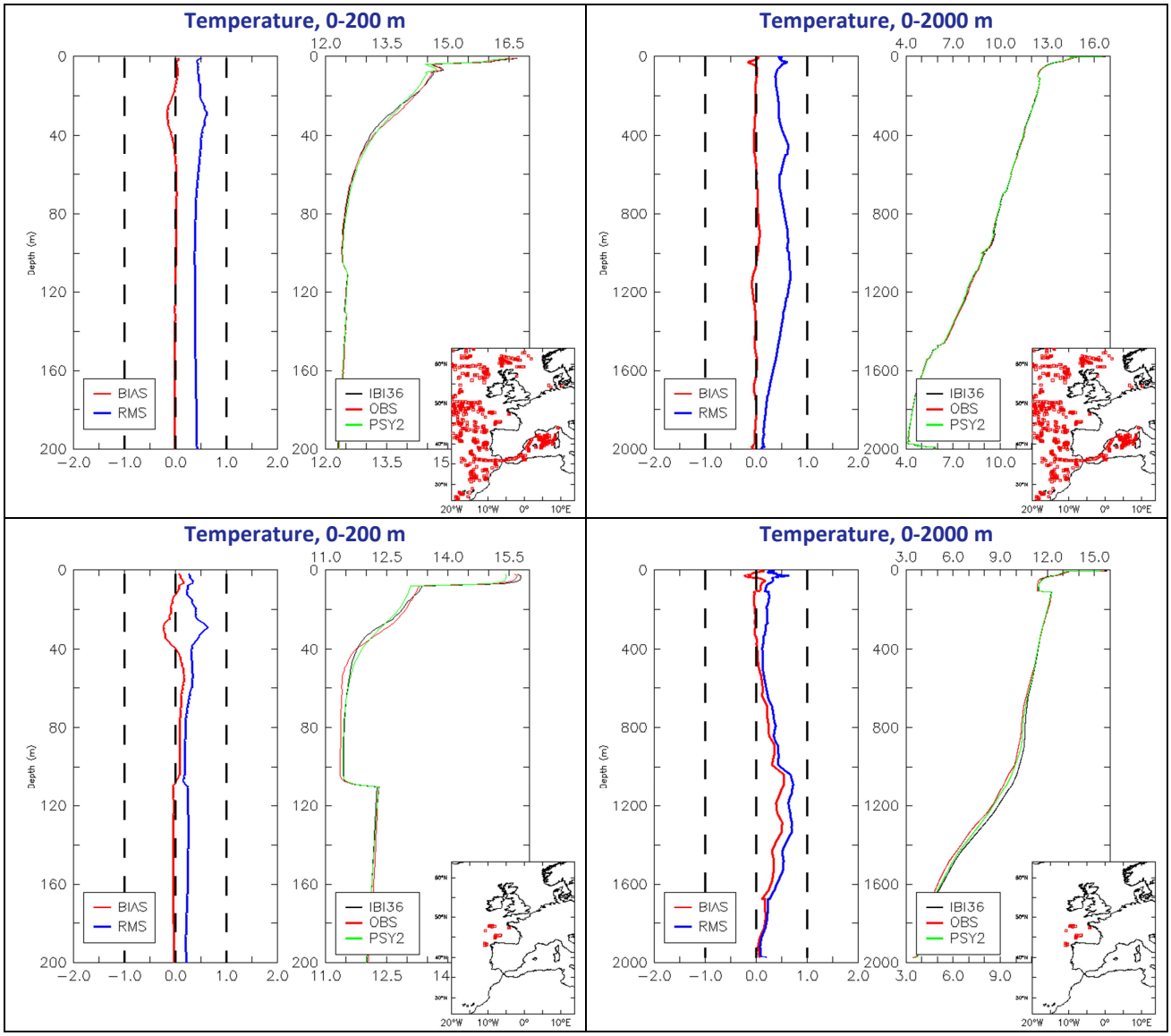

Figure 40 : For IBI36V2: On the left:mean "model - observation" temperature(°C) bias (red curve) and RMS error (blue curve) in AMJ 2012, On the right: mean profile of the model (black curve) and of the observations (red curve) in AMJ 2012. In the lower right corner: position of the profiles. Top panel: the whole domain; bottom panel: the Bay of Biscay region.

The maximum salinity bias and RMS error (Figure 41) occur near the surface. The model is too fresh near the surface. Below 100 m depth, the bias is almost zero. The RMS error is strong at the Mediterranean Sea Water level (as for temperature). In the Bay of Biscay the Mediterranean waters are too salty.

Note: averaged profiles are discontinuous because the number of observations varies with depth.

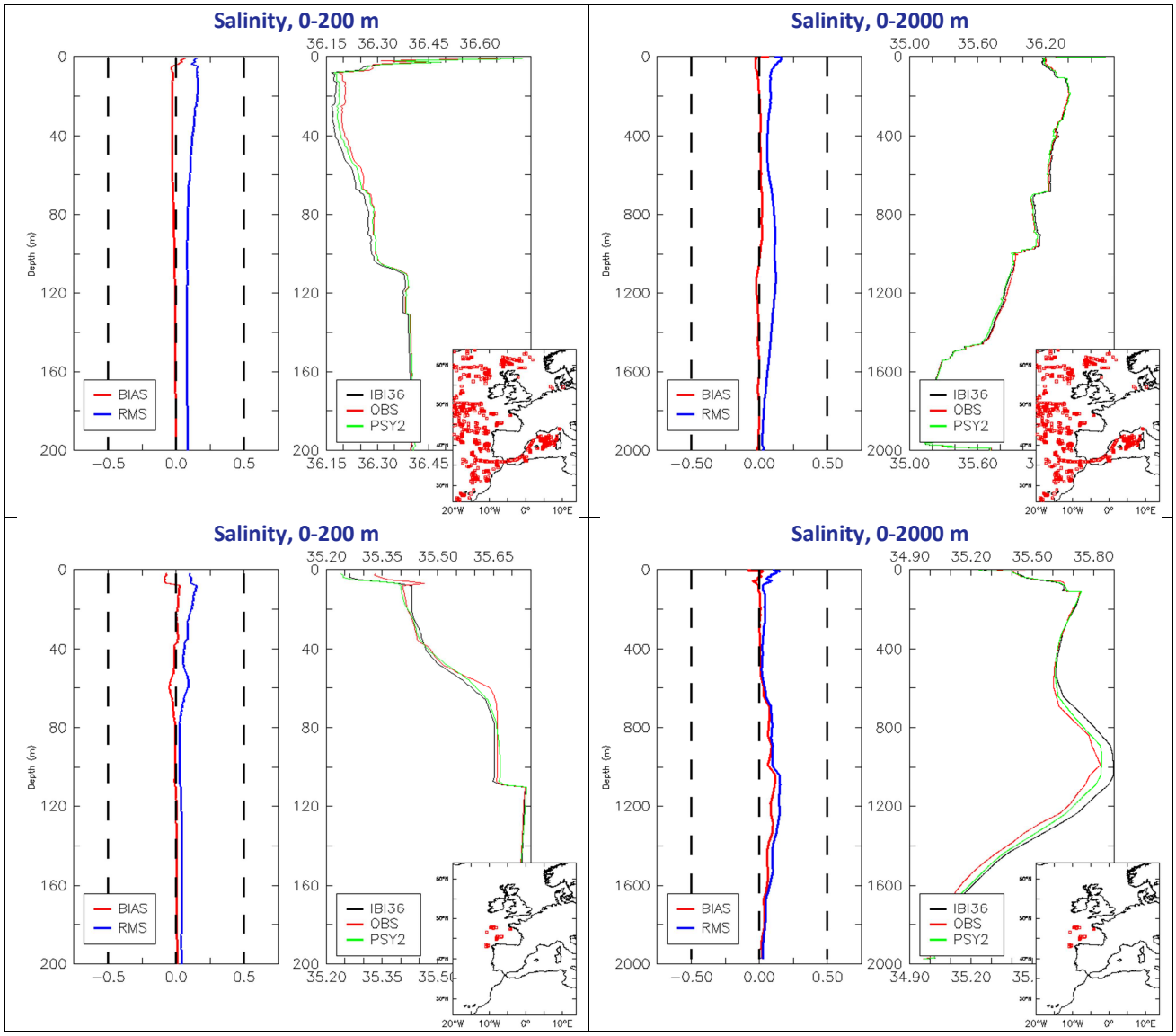

Figure 41: For IBI36V2: On the left: mean "model - observation" salinity (psu) bias (red curve) and RMS error (blue curve) in AMJ 2012, On the right: mean profile of the model (black curve) and of the observations (red curve) in AMJ 2012. In the lower right corner: position of the profiles. Top panel: the whole domain; bottom panel: the Bay of Biscay region.

V.2.5.3. MLD Comparisons with in situ data

Figure 42 shows that the distribution of modeled mixed layer depths among the available profiles is close to the observed distribution. Values of the mixed layer depth between 10 m and 30 m occur too often in the model compared with the observations, especially in the Bay of Biscay.

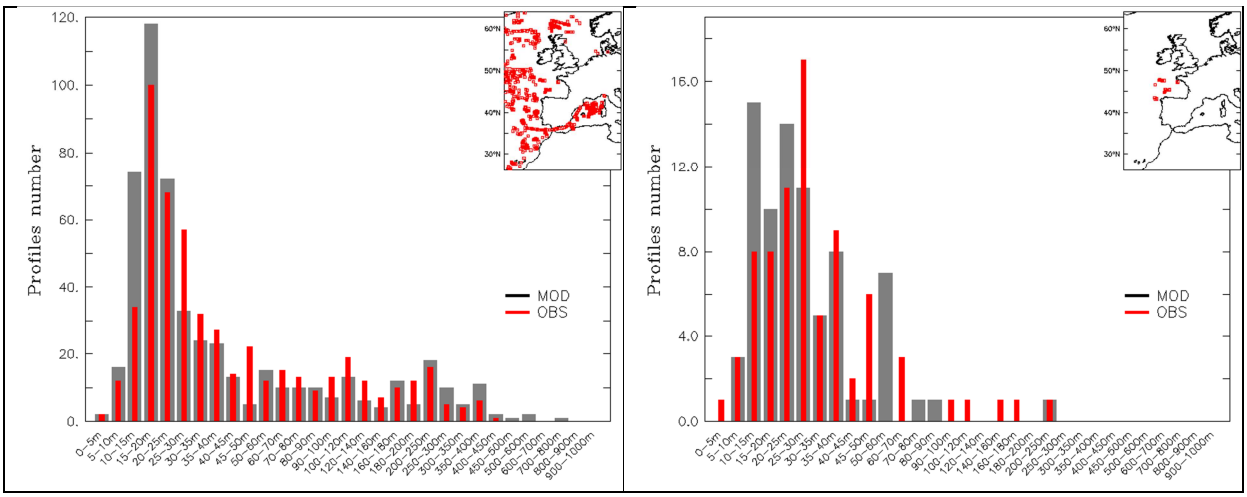

Figure 42 : For IBI36V2: Mixed Layer Depth distribution in AMJ 2012 calculated from profiles with the temperature criteria (difference of 0.2°C with the surface); the model is in grey, the observations in red. Left panel: whole domain; right panel: Bay of Biscay.

V.2.5.4. Comparisons with moorings and tide gauges

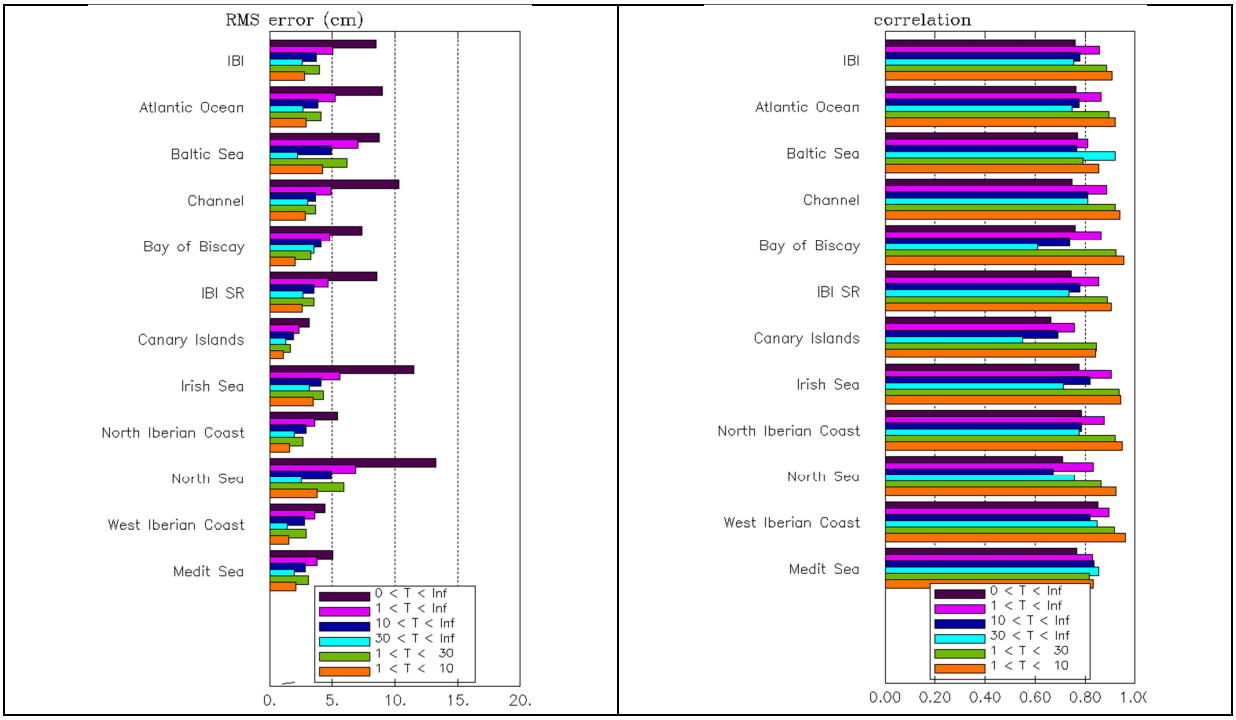

Figure 43 : For IBI36V2: RMS error (cm) and correlation for the non-tidal Sea Surface Elevation at tide gauges in AMJ 2012, for different regions and frequencies.

The RMS error of the residual elevation of sea surface (Figure 43) computed with an harmonic decomposition method (Foreman 1977) and a Loess low-pass filtering, is comprised between 2 and 15 cm. It is close to 5 cm in the Canary Islands and in the Mediterranean Sea. The RMS decreases for some frequency bands, and the smallest values occur in the 1-10-day band. The correlation is significant at all frequencies, and reach high values for periods lower than 10 days (at high frequencies).

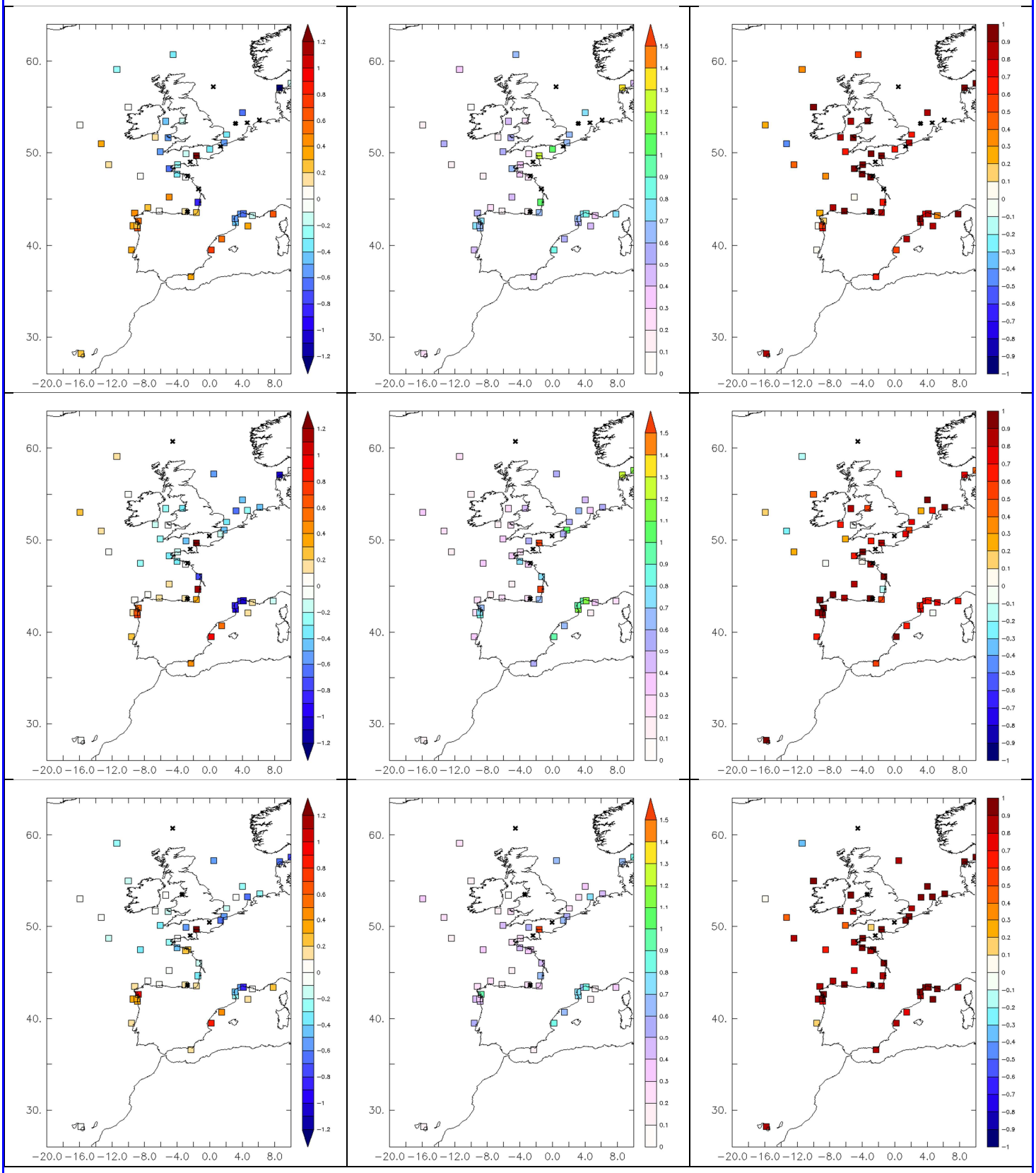

Figure 44 : For IBI36V2: Bias (Model–Observation), RMS error (°C) and correlation of the Sea Surface Temperature between IBI model and moorings measurements in January (upper panel), February (middle panel) and March 2012 (lower panel).

In Figure 44 we can see that the SST correlations between the coastal moorings and the IBI model are very high for the three months in nearly the whole domain. Bad correlations appear in the abyssal plain. The model is generally too cold in the northern part of the domain and too warm in its southern part, consistently with the L3 SST biases of Figure 39.

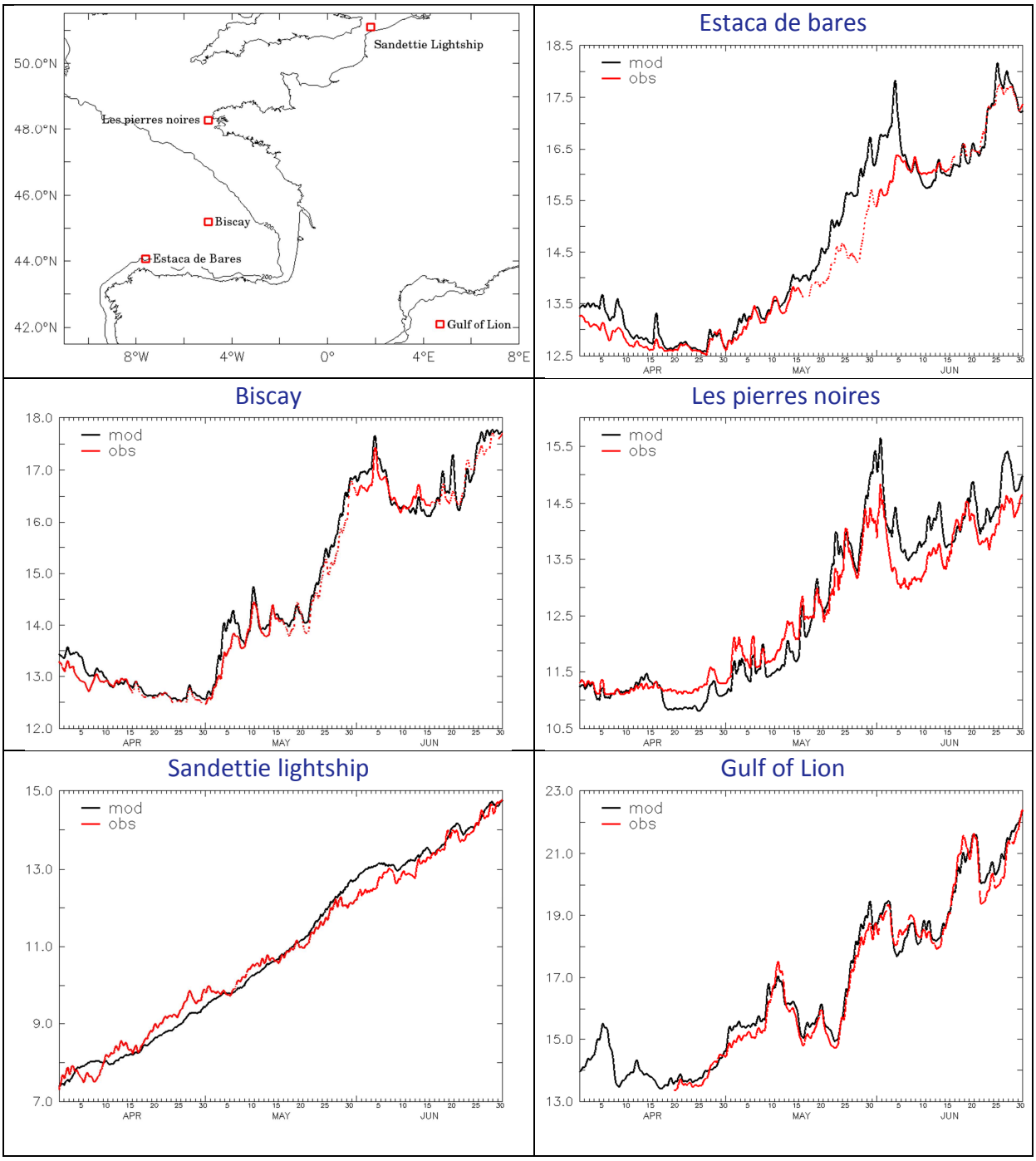

Figure 45:Surface temperature (°C) time series at a selection of moorings which locations are shown on the upper left panel.

V.2.6. Biogeochemistry validation: ocean colour maps

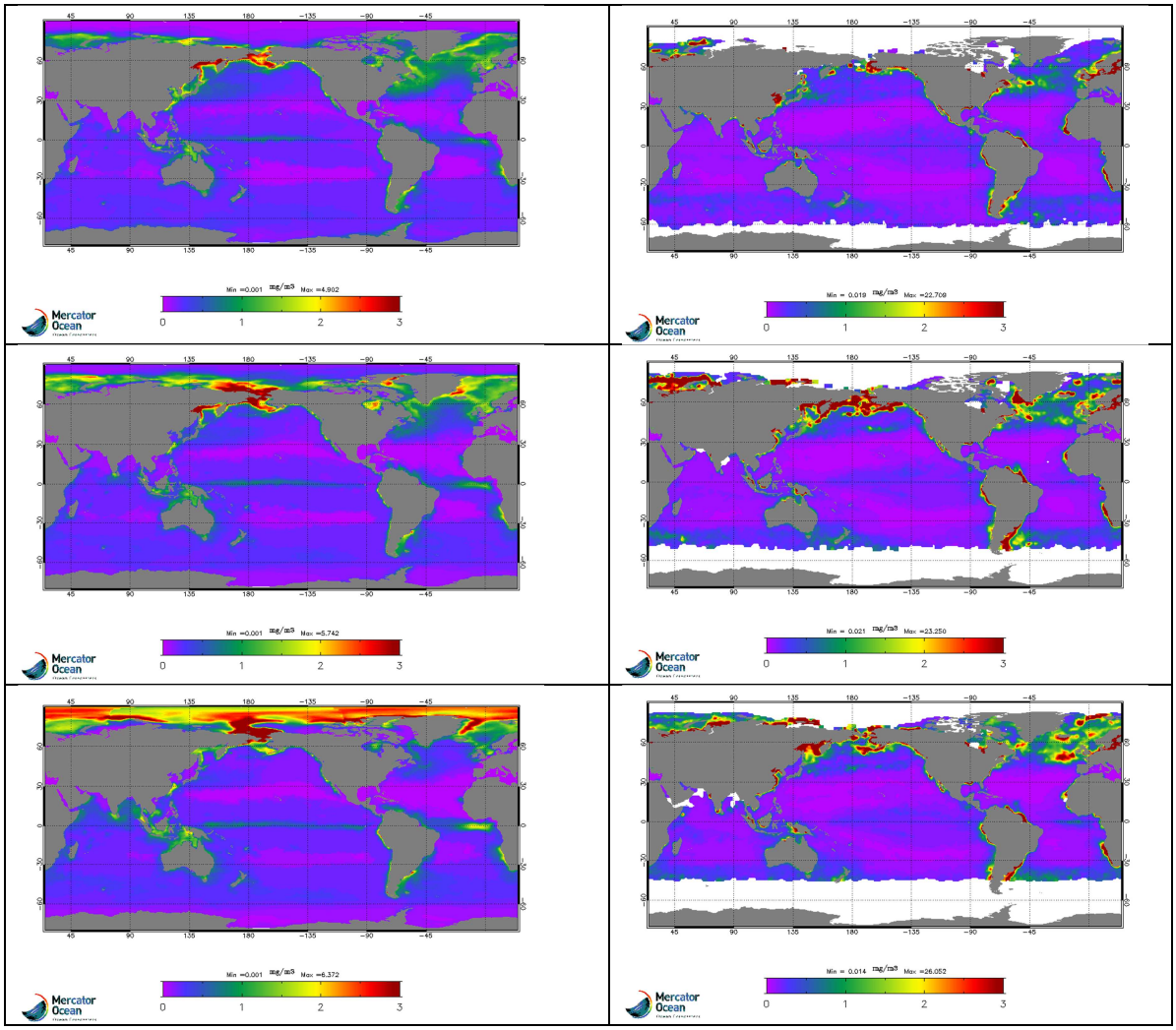

Figure 46 : Chlorophyll-a concentration (mg/m^3) for the Mercator system BIOMER (left panels) and Chlorophyll-a concentration from Globcolor (right panels). The upper panel is for April, the medium panel is for May and the bottom panel is for June 2012.

As can be seen on Figure 46 the surface chlorophyll-a concentration is overestimated by BIOMER on average over the globe. The production is especially overestimated in the Pacific and Atlantic equatorial upwellings. On the contrary near the coast BIOMER displays significantly lower chlorophyll concentrations than Globcolor ocean color maps. A bloom takes place in April in the North Atlantic in BIOMER and does not persist over May and June, while it is growing stronger in the observations. All these discrepancies (south of 50°N) appear in the RMS differences for the mean AMJ season (Figure 47).

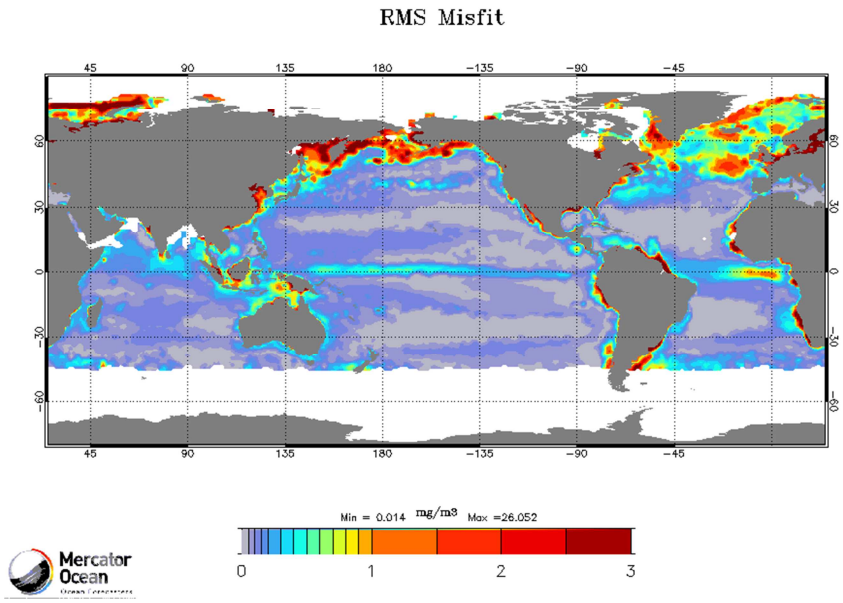

Figure 47:RMS difference between BIOMER and Globcolour Chl-a concentrations (mg/m^3) in AMJ 2012.

VI Forecast error statistics

VI.1. General considerations

The daily forecasts (with updated atmospheric forcings) are validated in collaboration with SHOM/CFUD. This collaboration has been leading us to observe the actual degradation of the forecast quality depending on the forecast range. When the forecast range increases the quality of the ocean forecast decreases as the initialization errors propagate and the quality of the atmospheric forcing decreases. Additionally the atmospheric forcing frequency also changes (see Figure 48). The 5-day forecast quality is optimal; starting from the 6th day a drop in quality can be observed which is linked with the use of 6-hourly atmospheric fields instead of 3-hourly; and starting from the 10th day the quality is strongly degraded due to the use of persisting atmospheric forcings (but not constant from the 10th to the 14th day as they are relaxed towards a 10-day running mean).

Figure 48: Schematic of the change in atmospheric forcings applied along the 14-day ocean forecast.

VI.2. Forecast accuracy: comparisons with observations when and where available

VI.2.1. North Atlantic region

As can be seen in Figure 49 the PSY2V4R2 products have a better accuracy than the climatology on average in the North Atlantic region in AMJ 2012, except the salinity forecast between 0 and 100 m. The analysis is systematically more accurate than the 3-day and 6-day forecast for both temperature and salinity. The RMS error thus increases with the forecast range (shown for NAT region Figure 49 and MED region Figure 51). The biases in temperature and salinity are generally small (of the order of 0.1 °C and 0.02 psu) compared to the climatology's biases (of the order of 0.4 °C and 0.05 psu). The 3-day forecast and the analysis display similar biases near the surface this AMJ 2012 season.

On average in the North Atlantic, the PSY2V4R2 system is fresher and colder than the observations at the surface, and warmer and saltier in the 300-2000 m layer. This signal is due to a relatively small number of observations where large differences are observed, as can be seen on Figure 50 on average in the layer 0-500m. Finally, the main message would be that the systems biases are far smaller than the climatology biases. In the 2000-5000 m layer, the statistics are performed on a very small sample of observations, and thus are not representative of the region or layer.

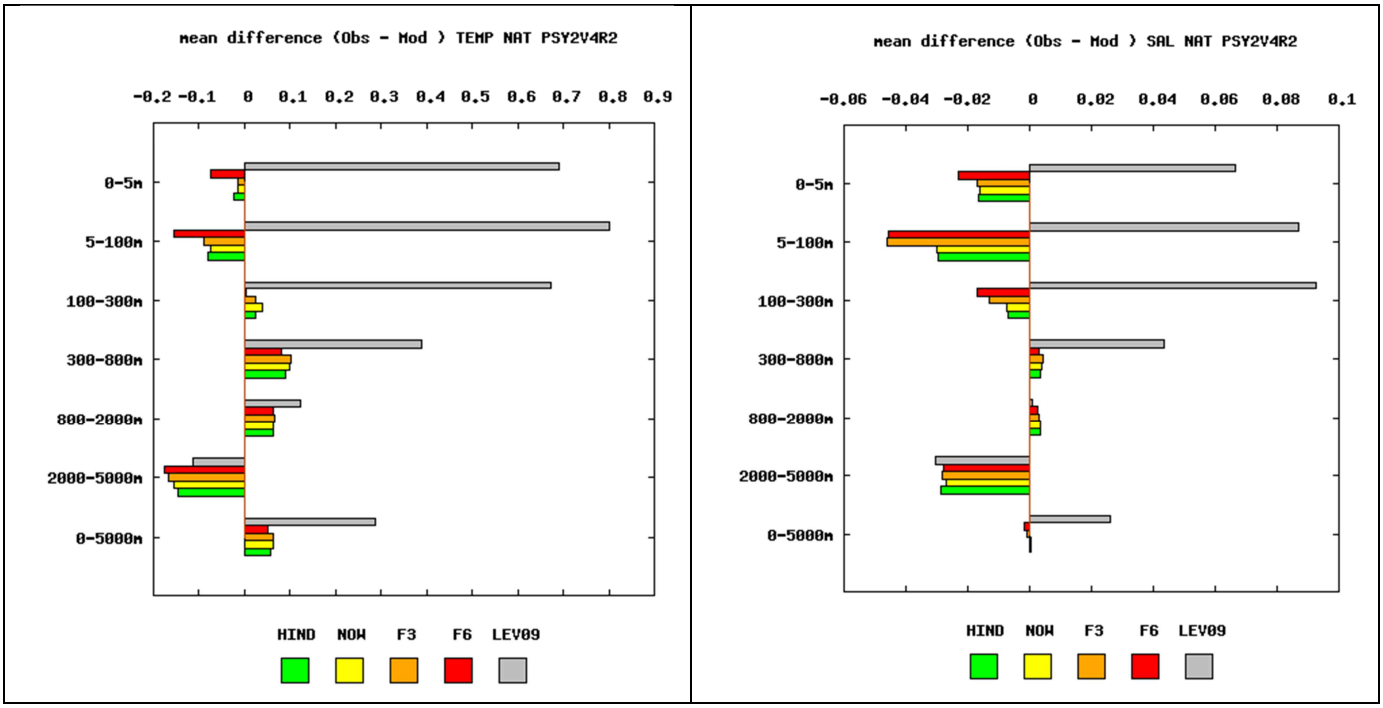

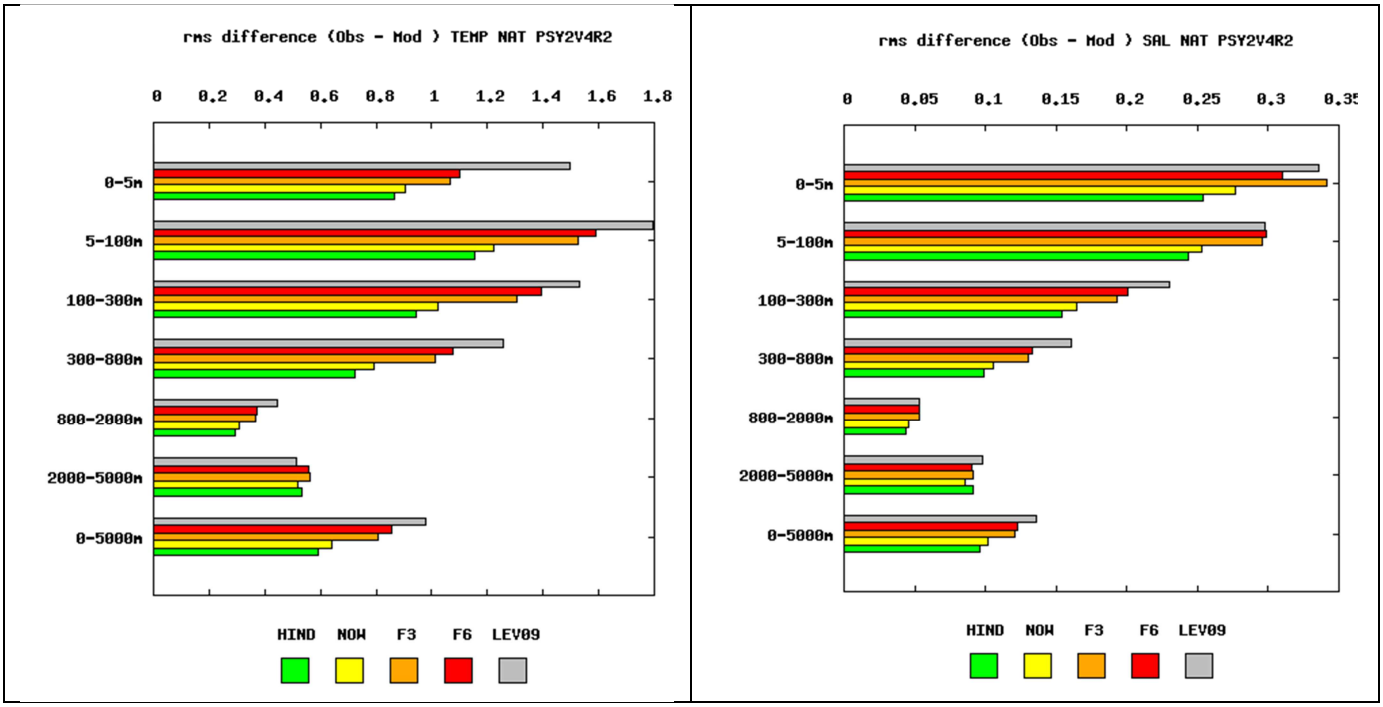

Figure 49: Accuracy intercomparison in the North Atlantic region for PSY2V4R2 in temperature (left panel) and salinity (right panel) between hindcast, nowcast, 3-day and 6-day forecast and WO09 climatology. Accuracy is measured by a mean difference (upper panel) and by a rms difference (lower panel) of temperature and salinity with respect to all available observations from the CORIOLIS database averaged in 6 consecutive layers from 0 to 5000m. All statistics are performed for the AMJ 2012 period. NB: average on model levels is performed as an intermediate step which reduces the artefacts of inhomogeneous density of observations on the vertical.

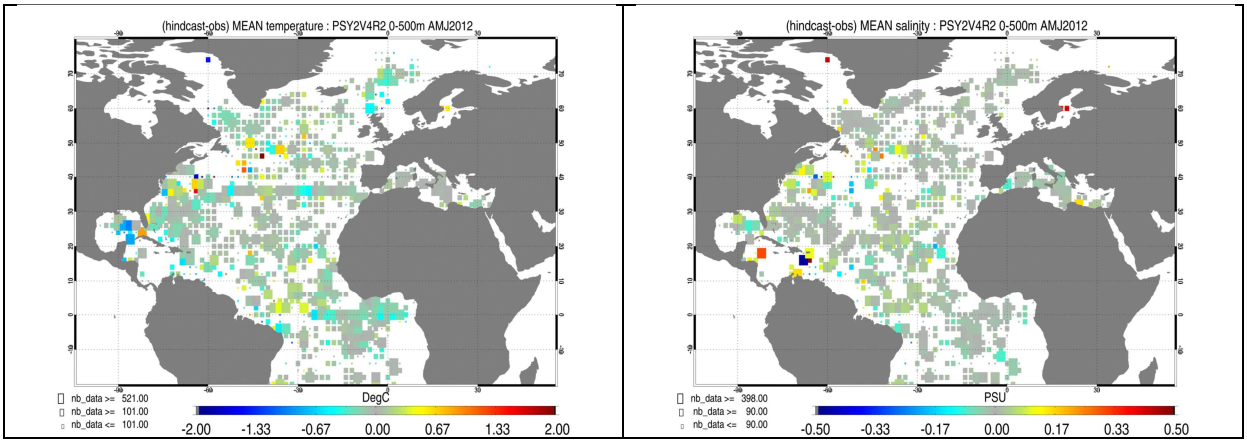

Figure 50: maps of the mean difference of temperature (left panel) and salinity (right panel) between thePSY2V4R2 hindcast and in situ observations, averaged between 0 and 500 m, in the AMJ 2012 season.

VI.2.2. Mediterranean Sea

In the Mediterranean Sea in AMJ 2012 (Figure 51) the PSY2V4R2 products are more accurate (lower RMS) than the climatology on average except at the surface. However the products

are still less biased than the climatology. At the surface the system is too cold *on average* (0-5 m) and fresh (0-100 m). It is too warm between 5 and 300 m.

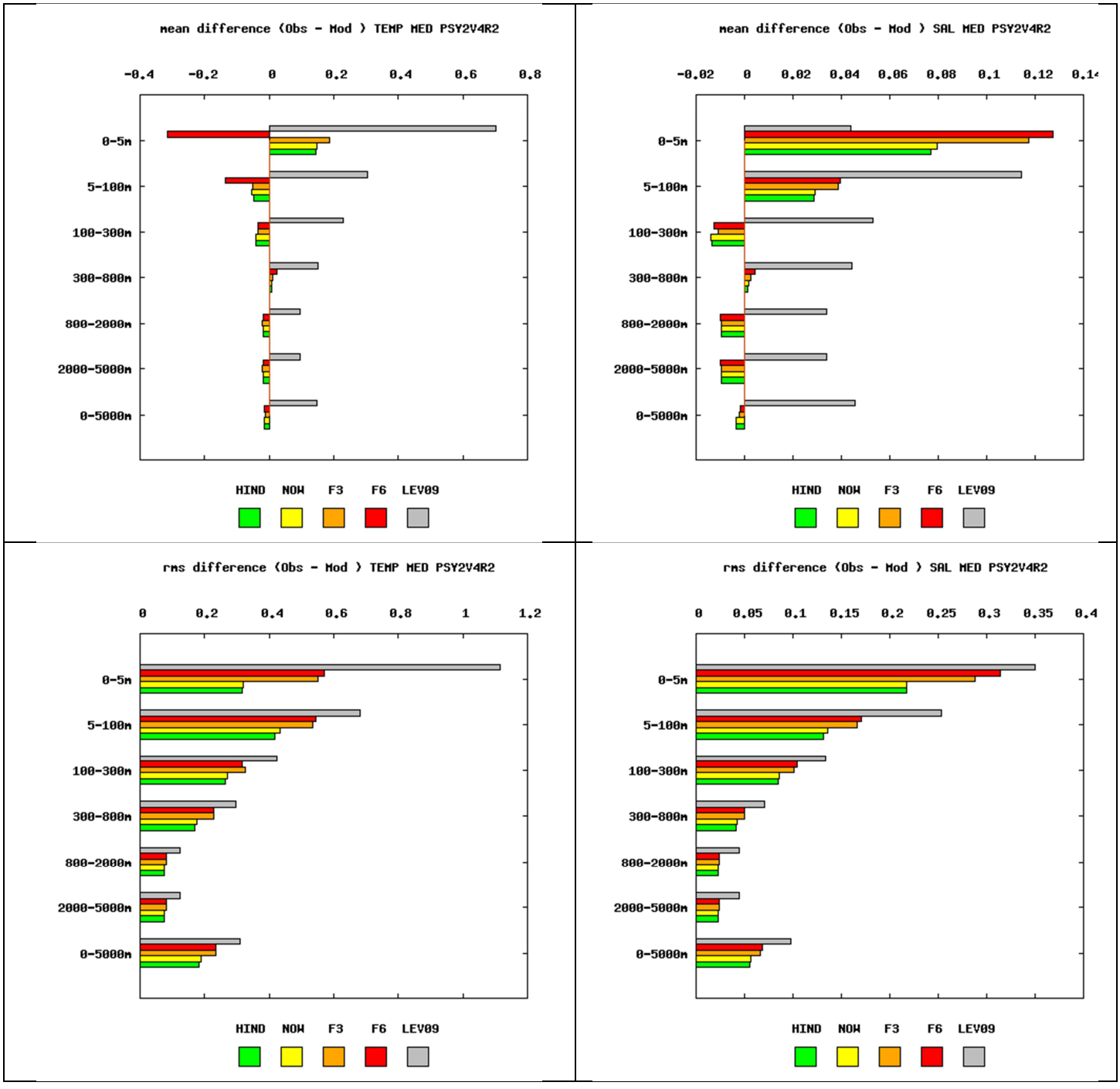

Figure 51: Accuracy intercomparison in the Mediterranean Sea region for PSY2V4R2 in temperature (°C, left column) and salinity (psu, right column) between hindcast, nowcast, 3-day and 6-day forecast and WO09 climatology. Accuracy is measured by a rms difference (lower panel) and by a mean difference (upper panel) with respect to all available observations from the CORIOLIS database averaged in 6 consecutive layers from 0 to 5000m. All statistics are performed for the AMJ 2012 period. NB: average on model levels is performed as an intermediate step which reduces the artefacts of inhomogeneous density of observations on the vertical.

VI.2.3. Tropical Oceans, Indian, Global: what system do we choose in AMJ 2012?

The best performing system in AMJ 2012 in terms of water masses is PSY3V3R1 (and PSY2V4R2 in the Tropical Atlantic) as can be seen in Figure 52. This is not surprising when we take into account that PSY4V1R3 has no bias correction for the moment. Nevertheless, the high resolution global PSY4V1R3 beats the climatology and is very promising in many regions, for instance in the Atlantic, the Indian ocean or the North Pacific. PSY4V1R3 surface currents may also be preferred to PSY3V3R1's currents, as mentioned in V.2.3.
We also note that at all depth in all regions the PSY3V3R1 RMS error increases with forecast range, as could be expected, and that the 6-day forecast still beats the climatology. Some exceptions are noted under 2000 m in the tropical Atlantic and Indian oceans, probably corresponding to sampling problems (very few observations are available at these depths).

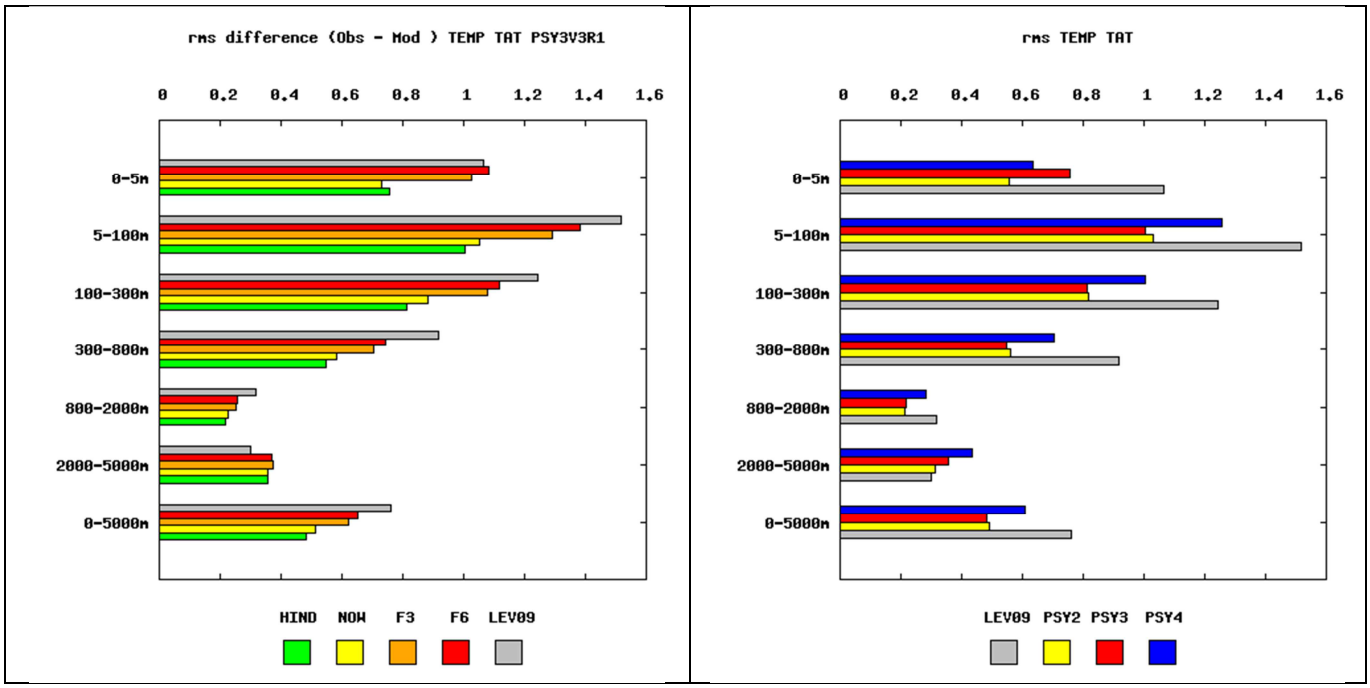

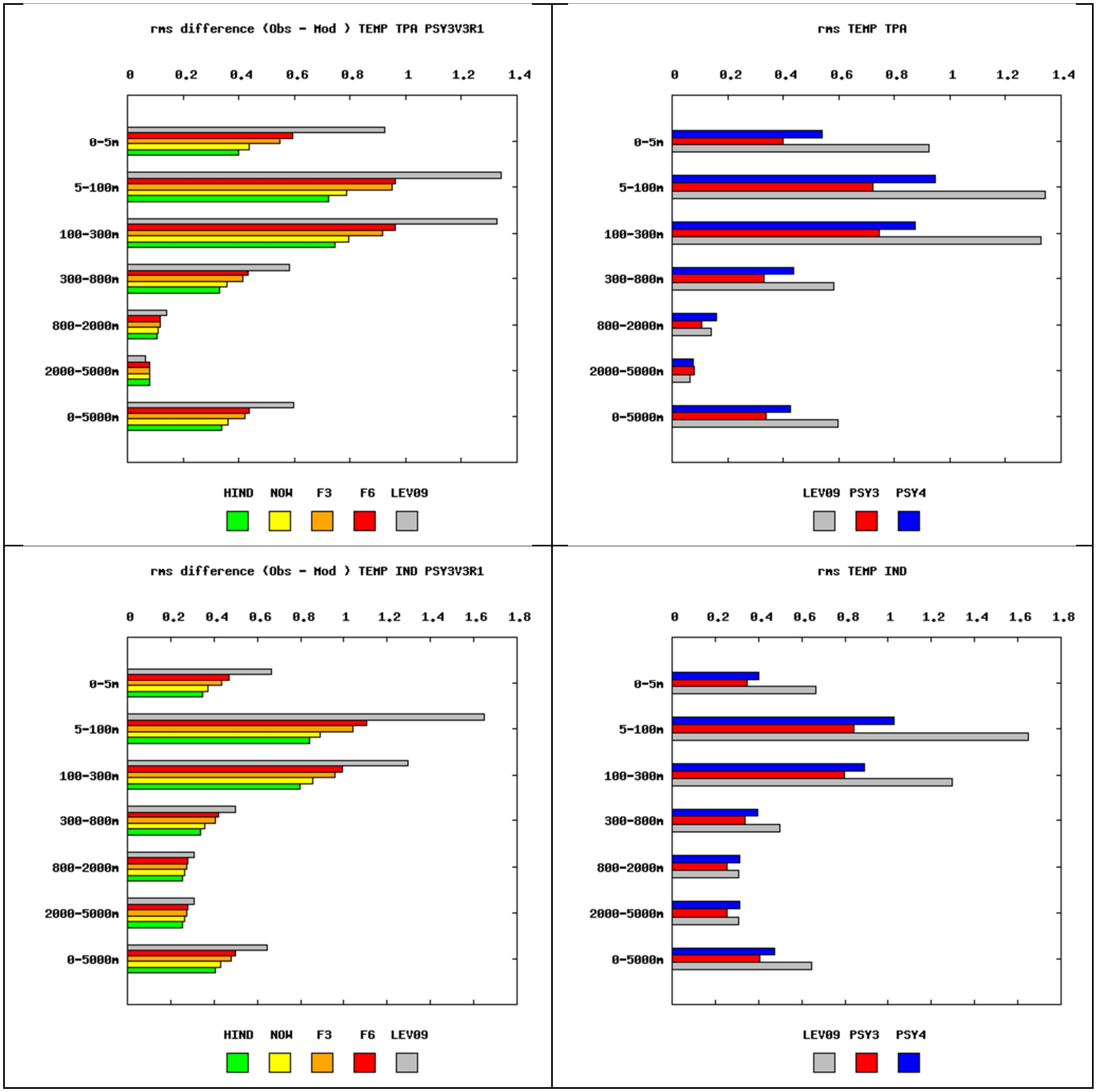
rms difference (Obs - Mod) TEMP TPA PSY3V3R1
0 0.2 0.4 0.6 0.8 1 1.2 1.4
0-5m
5-100m
100-300m
300-800m
800-2000m
2000-5000m
0-5000m
HIND NOW F3 F6 LEV09
rms TEMP TPA
0 0.2 0.4 0.6 0.8 1 1.2 1.4
0-5m
5-100m
100-300m
300-800m
800-2000m
2000-5000m
0-5000m
LEV09 PSY3 PSY4
rms difference (Obs - Mod) TEMP IND PSY3V3R1
0 0.2 0.4 0.6 0.8 1 1.2 1.4 1.6 1.8
0-5m
5-100m
100-300m
300-800m
800-2000m
2000-5000m
0-5000m
HIND NOW F3 F6 LEV09
rms TEMP IND
0 0.2 0.4 0.6 0.8 1 1.2 1.4 1.6 1.8
0-5m
5-100m
100-300m
300-800m
800-2000m
2000-5000m
0-5000m
LEV09 PSY3 PSY4

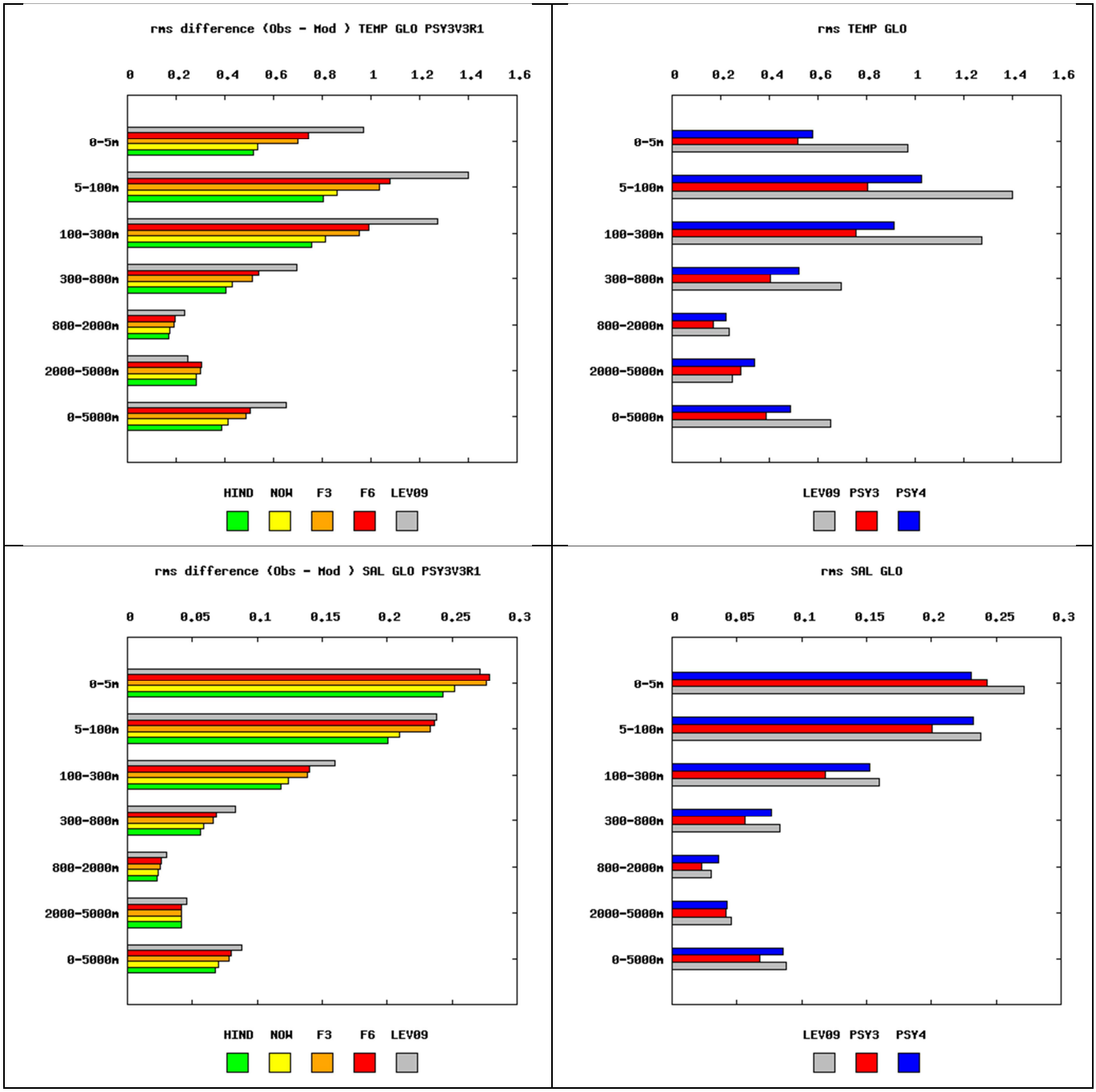

Figure 52: same as Figure 49 but for RMS statistics and for temperature (°C), PSY3V3R1 and PSY4V1R3 systems and the Tropical Atlantic (TAT), the Tropical Pacific (TPA) and the Indian Ocean (IND). The global statistics (GLO) are also shown for temperature and salinity (psu). The right column compares the analysis of the global ¼° PSY3 with the analysis of the global 1/12° PSY4 available at the end of December 2011.

VI.3. Forecast verification: comparison with analysis everywhere

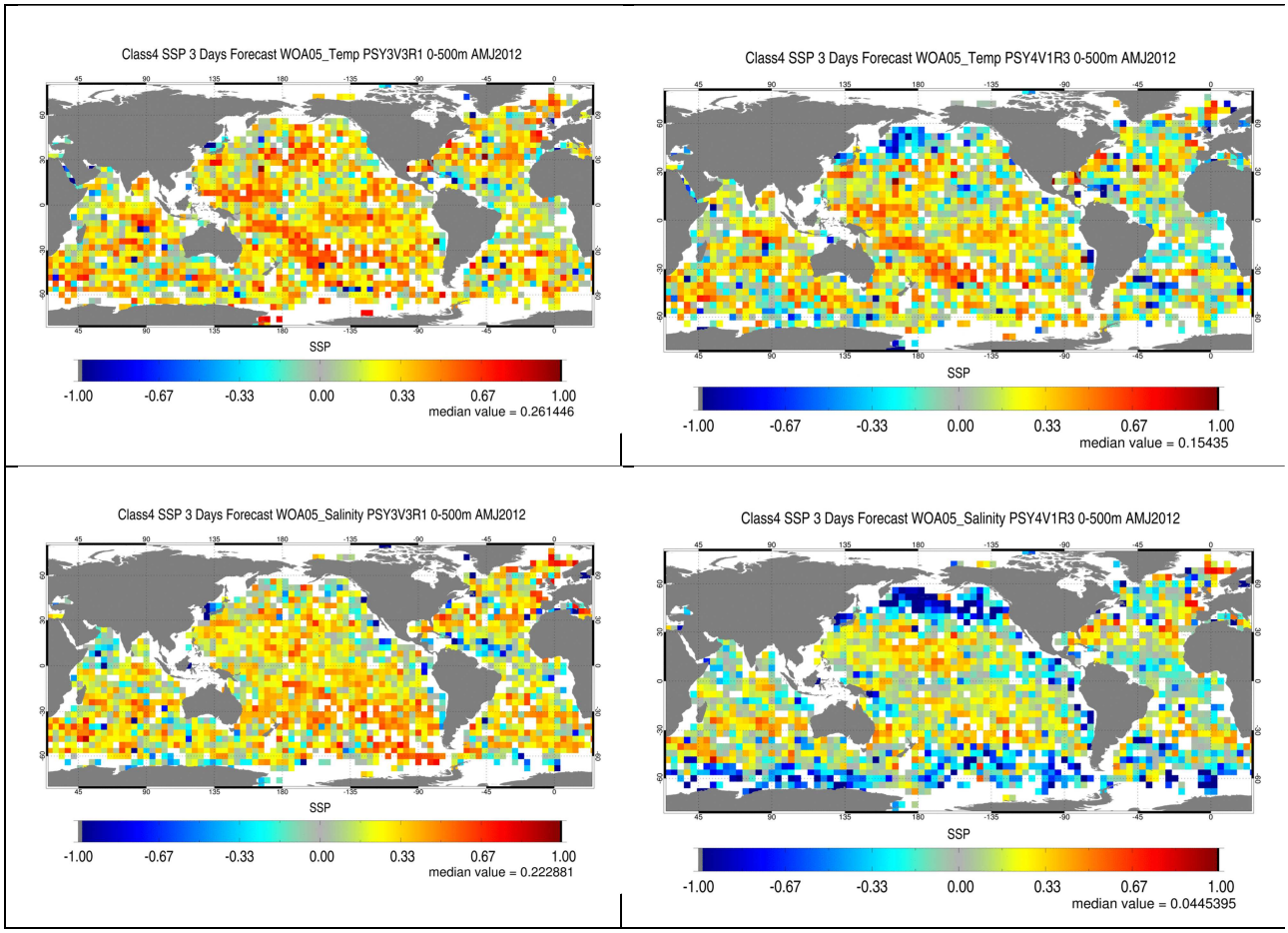

Figure 53 : Temperature (left) and salinity (right) skill scores in 4°x4° bins and in the 0-500m layer in AMJ 2012, illustrating the ability of the 3-days forecast to be closer to in situ observations than a reference state (climatology or persistence of the analysis, see Equation 1). Yellow to red values indicate that the forecast is more accurate than the reference. Here the reference value is the WOA05 climatology. Upper panel: PSY3V3R1; middle panel: PSY4V1R3; lower panel: PSY2V4R2.

The Murphy Skill Score (see Equation 1) is described by Wilks, *Statistical Methods in the Atmospheric Sciences*, Academic Press, 2006. This score is close to 0 if the forecast is equivalent to the reference. It is positive and aims towards 1 if the forecast is more accurate than the reference.

$$SS = 1 - \frac{\sum_{k=1}^{n}\left[\frac{1}{M}\sum_{m=1}^{M}\left(Forecast_m - Obs_m\right)^2\right]}{\sum_{k=1}^{n}\left[\frac{1}{M}\sum_{m=1}^{M}\left(Ref_m - Obs_m\right)^2\right]}$$

Equation 1

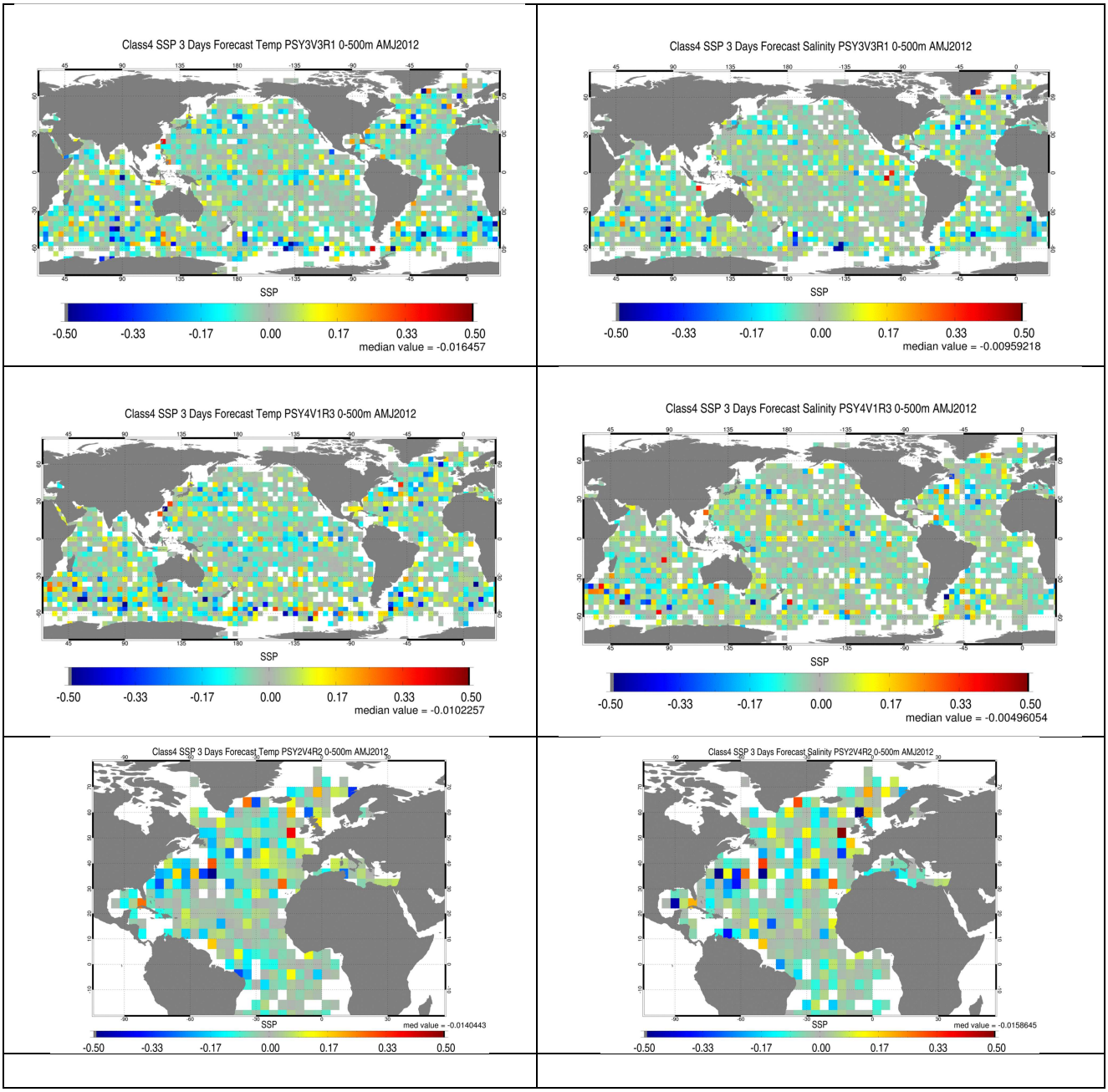

Figure 54: As Figure 53 but the reference is the persistence of the analysis. Temperature (upper panel) and salinity (lower panel) skill scores are displayed, on the left for PSY3V3R1 and on the right for PSY4V1R3.

The Skill Score displayed on Figure 53 show the added value of PSY3V3R1 forecast with respect to the climatology. All Mercator Ocean systems have a very good level of performance with respect to the climatology (see previous section). When the reference is the persistence of the last analysis (Figure 53), the result is noisier and the systems 3-day forecast seems to have skill in some regions in particular: North East Atlantic, central pacific, Indian basin and Tropical Atlantic. In some regions of high variability (for instance in the Antarctic, Gulf Stream, Agulhas Current, Zapiola) the persistence of the previous analysis is locally more accurate than the forecast. As expected PSY4V1R3 displays less forecast skill than the other systems with respect to the climatology, at least in terms of water masses

(forecast skills with respect to other types of observations have to be computed in the future). This is especially the case in the Antarctic near the sea ice limit, in the Bering Sea, in the Zapiola anticyclone and in the Caribbean Sea.

The PSY3V3R1 "forecast errors" illustrated by the sea surface temperature and salinity RMS difference between the forecast and the hindcast for all given dates of April-May-June 2012 are displayed in Figure 55. The values on most of the global domain do not exceed 1°C and 0.2 PSU. In regions of high variability like the western boundary currents, the Circumpolar current, Zapiola eddy, Agulhas current, Gulf Stream, Japan Sea and Kuroshio region the errors reach around 3°C or 0.5 PSU. For salinity, the error can exceed 1 PSU in regions of high runoff (Gulf of Guinea, Bay of Bengal, Amazon, Sea Ice limit) or precipitations (ITCZ, SPCZ).

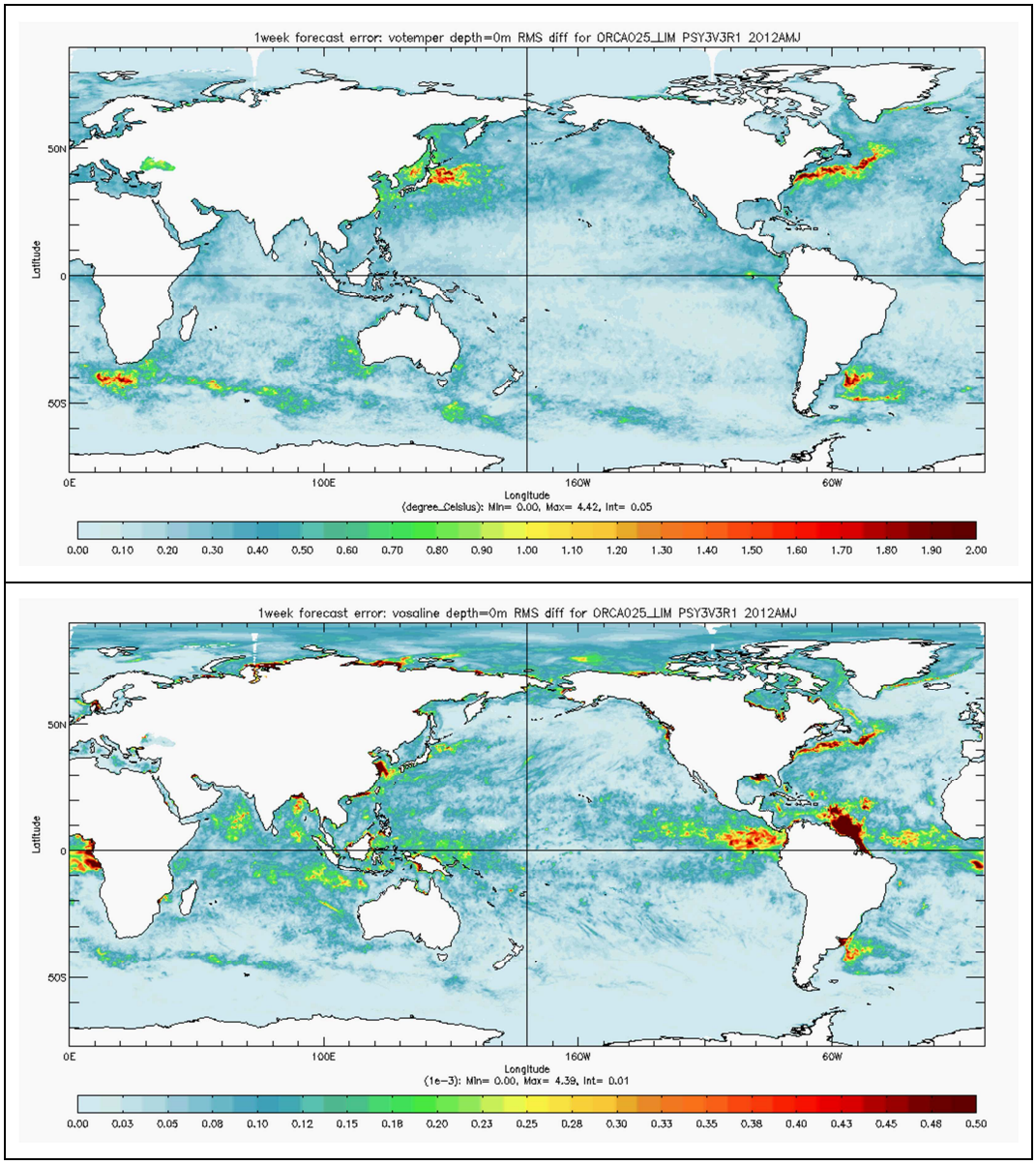

Figure 55: comparison of the sea surface temperature (°C, upper panel) and salinity (PSU, lower panel) forecast – hindcast RMS differences for the 1 week range for the PSY3V3R1 system for the AMJ 2012 period.

VII Monitoring of ocean and sea ice physics

VII.1. Global mean SST and SSS

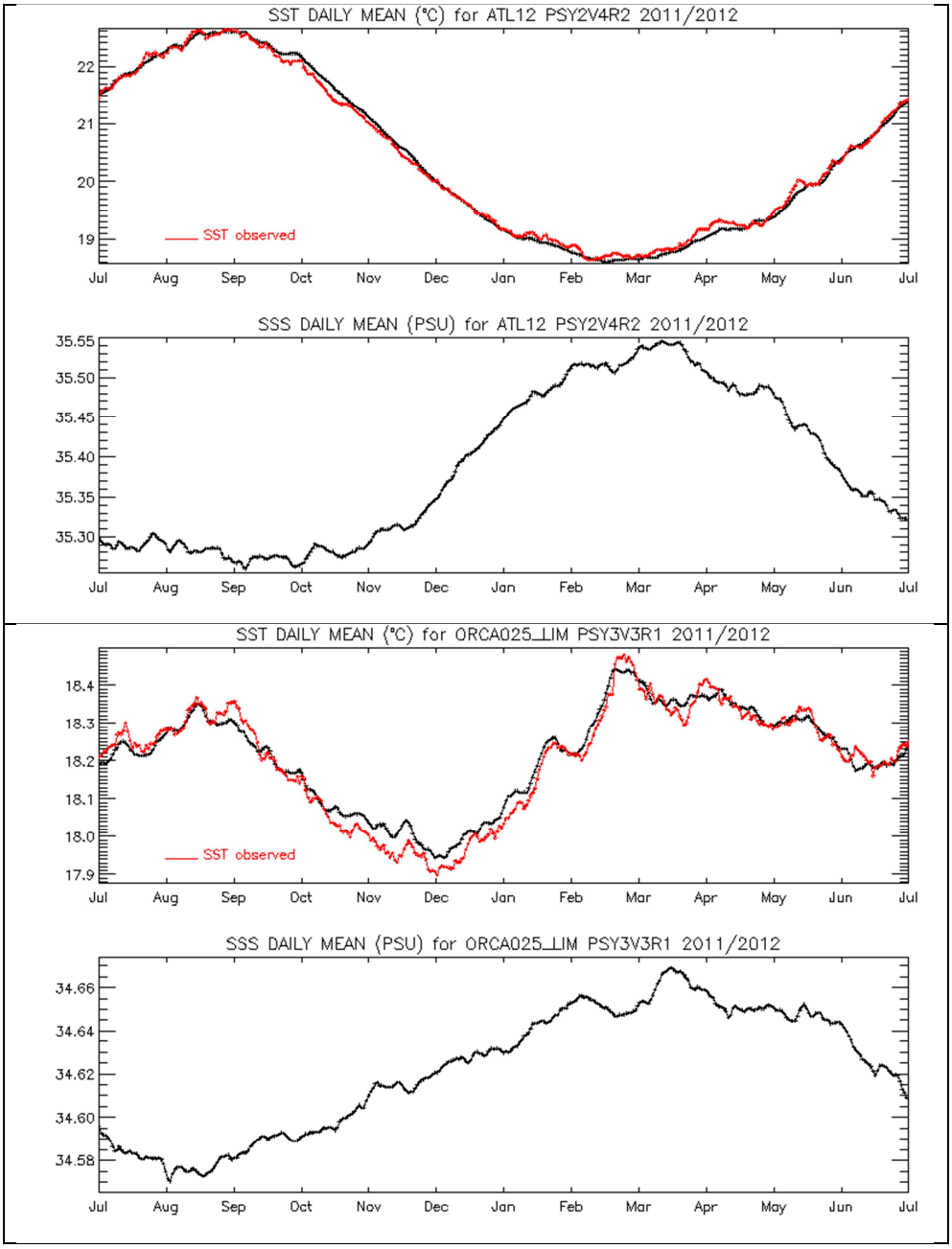

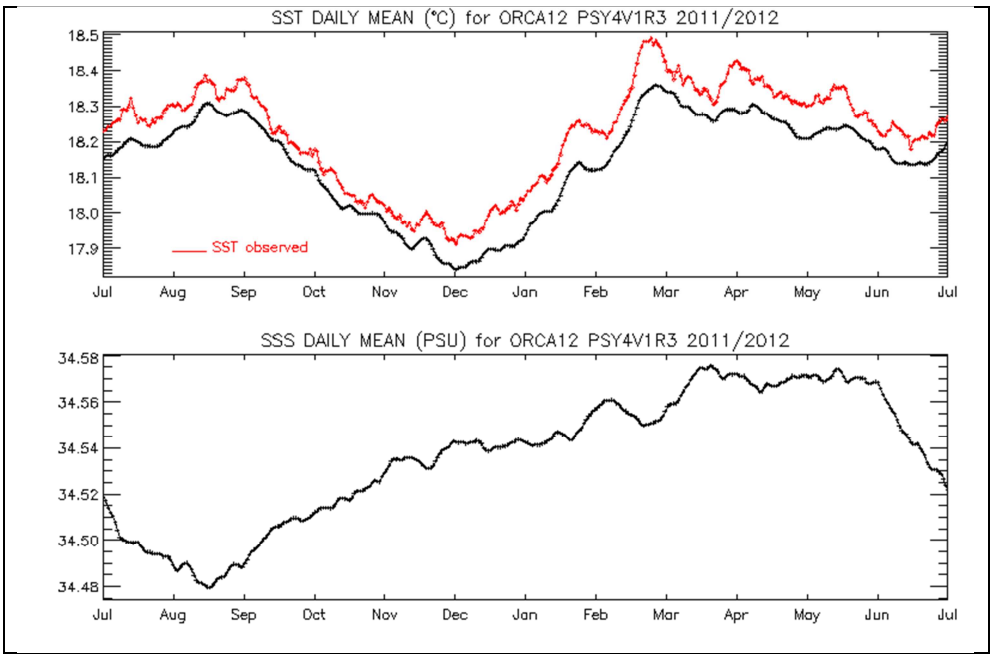

Figure 56: daily SST (°C) and salinity (psu) spatial mean for a one year period ending in AMJ 2012, for Mercator Ocean systems (in black) and RTG-SST observations (in red). Upper: PSY2V4R2, middle: PSY3V3R1, lower: PSY4V1R3.

The spatial means of SST and SSS are computed for each day of the year, for PSY2V4R2, PSY3V3R1 and PSY4V1R3 systems. The mean SST is compared to the mean of RTG-SST on the same domain (Figure 56), except for PSY2V4R2 where it is compared with Reynolds AVHRR SST.

The main feature is a the good agreement of PSY2V4R2 and Reynolds SST, and of PSY3V3R1 and RTG-SST on global average, especially this AMJ 2012 season. On the contrary the global mean of PSY4V1R3 SST is biased of about 0.1°C all year long, consistently with data assimilation scores of section V.1.2. This bias is mainly located in the tropics which are too cold on average. Paradoxically, local departures from RTG-SST are much stronger in PSY3V3R1 (more than 2°C at the peak of the seasonal bias) than in PSY4V1R3 (not shown).

VII.2. Surface EKE

Regions of high mesoscale activity are diagnosed in Figure 57: Kuroshio, Gulf Stream, Niño 3 region in the central Equatorial pacific, Zapiola eddy, Agulhas current. The mesoscale activity is reduced in the equatorial regions with respect to the previous JFM season, especially in the Indian and Pacific basins. PSY3V3R1 at ¼° and PSY4V1R3 at 1/12° are in very good agreement. EKE is generally higher in the high resolution PSY4V1R3 system, for instance in the subtropical gyres.

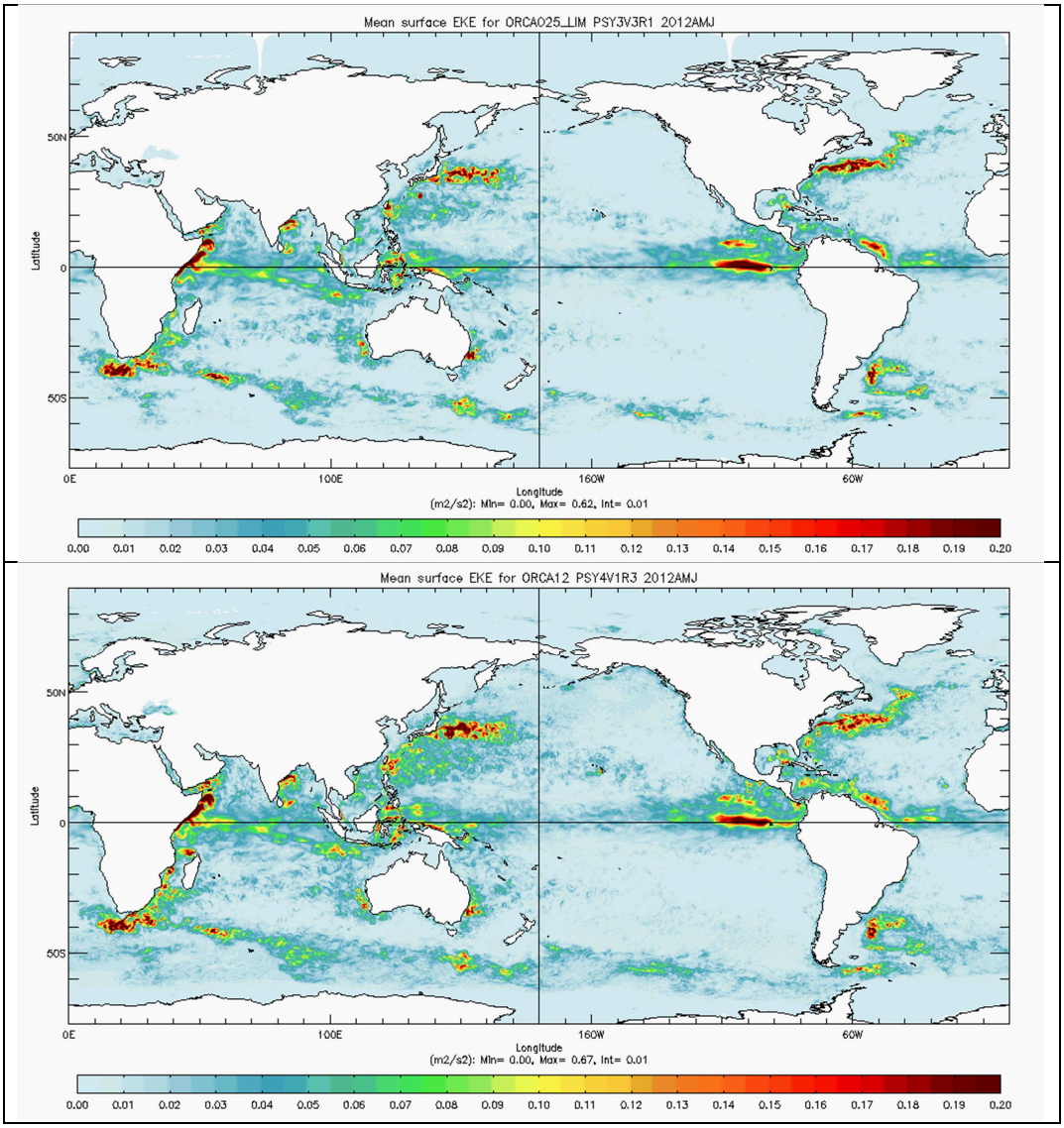

Figure 57: surface eddy kinetic energy EKE (m^2/s^2) for PSY3V3R1 (upper panel) and PSY4V1R3 (lower panel) for AMJ 2012.

VII.3. Mediterranean outflow

In PSY3V3R1 the Mediterranean outflow is too shallow with respect to the climatology in the Gulf of Cadiz. Anyway, consistently with Figure 31, the outflow is better reproduced by PSY3V3R1 than by PSY4V1R3. The Mediterranean outflow of PSY2V4R2 (with high resolution and bias correction) is the most realistic of all systems.

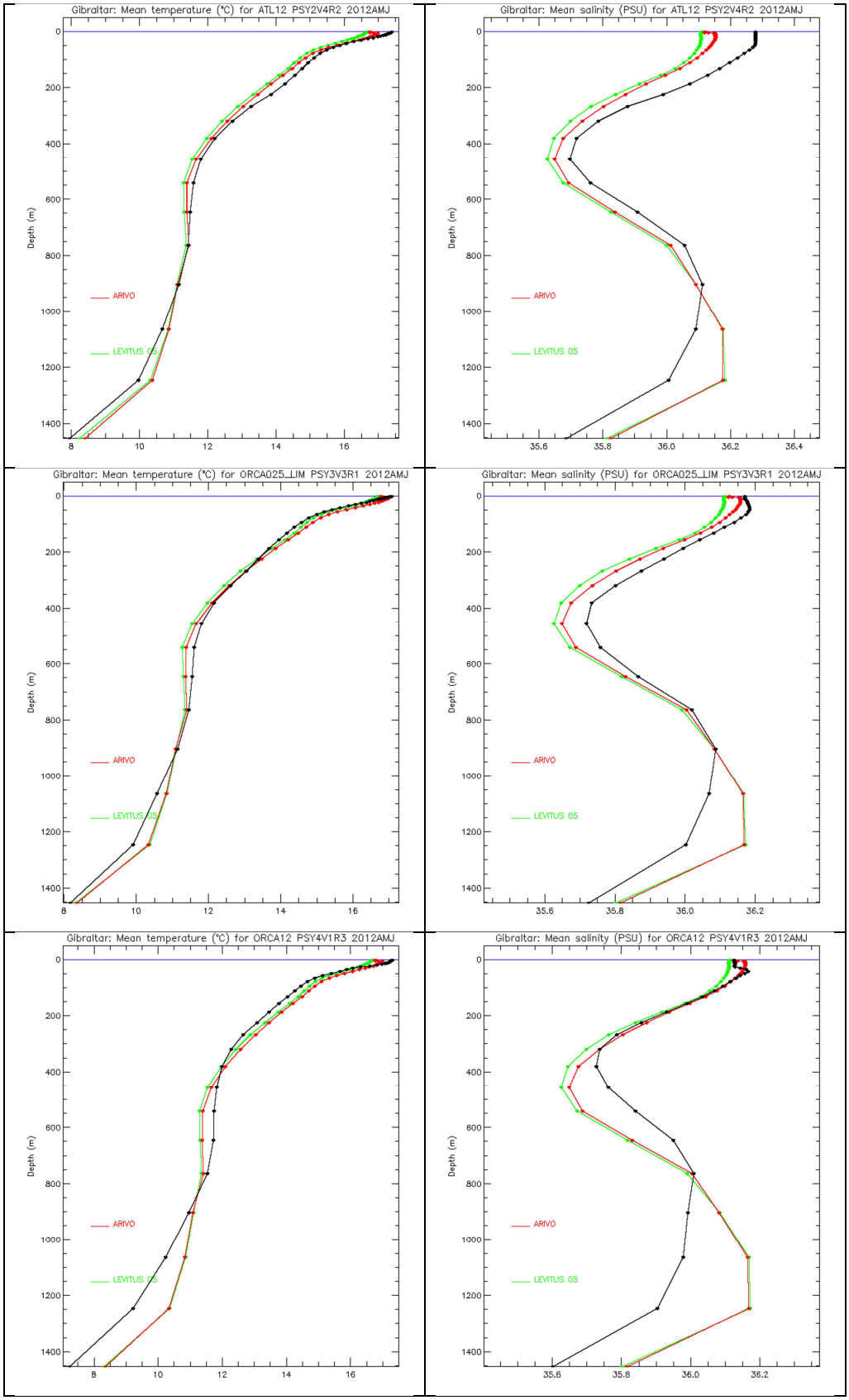

Figure 58: Comparisons between AMJ 2012 mean temperature (°C, left panel) and salinity (psu, right panel) profiles in PSY2V4R2, PSY3V3R1 and PSY4V1R3 (from top to bottom, in black), and in the Levitus WOA05 (green) and ARIVO (red) monthly climatologies.

VII.4. Sea Ice extent and area

The time series of monthly means of sea ice area and sea ice extent (area of ocean with at least 15% sea ice) are displayed in Figure 59 and compared to SSM/I microwave observations. Both ice extent and area include the area near the pole not imaged by the sensor. NSIDC web site specifies that it is assumed to be entirely ice covered with at least 15% concentration. This area is 0.31 million square kilometres for SSM/I.

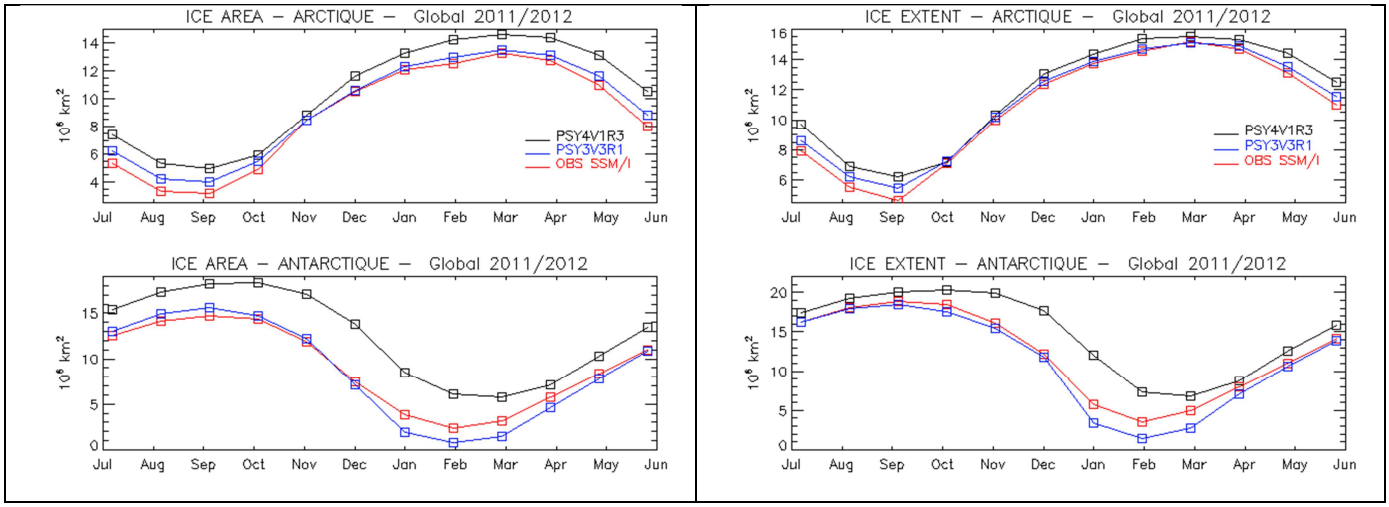

Figure 59: Sea ice area (left panel, 10^6 km2) and extent (right panel, 10^6 km2) in PSY3V3R1(blue line), PSY4V1R3 (black line) and SSM/I observations (red line) for a one year period ending in AMJ 2012, in the Arctic (upper panel) and Antarctic (lower panel).

These time series indicate that sea ice products from PSY4V1R3 are generally less realistic than PSY3V3R1 products. This is partly due to the use of two different dynamics in the two models. PSY4V1R3 sea ice cover is overestimated throughout the year. The accumulation of multiannual Sea Ice in the Central arctic is overestimated by the models and especially by PSY4V1R3 all year long (see Figure 36). PSY4V1R3 overestimates the sea ice area and extent in boreal summer, while PSY3V3R1 ice area and extent are slightly underestimated. In boreal winter, PSY3V3R1 performs very well, with respect to observations.

VIII Impact of the loss of Envisat on PSY3V3R1's performance

This section briefly describes a study that summarizes the impact on Mercator Ocean analysis and forecasting systems of the loss of the ENVISAT SLA data, and the temporary loss of Jason1 data in the beginning of the year 2012. This study shows the necessity of observing system experiments (OSEs and OSSEs) to correctly estimate the potential impact in terms of accuracy change for the users' applications. The need for a growing sustainable global ocean observing system is confirmed.

VIII.1. Introduction

The unavailability of Jason-1 (since mid-February 2012) and the recent loss of Envisat (8 April 2012) have significantly reduced the SLA coverage. Even if Cryosat-2 observations have since been added in the Mercator Ocean assimilation systems, the current coverage is far coarser than it was before, as can be seen on Figure 60. The aim of the study was to identify and quantify the actual degradation of Mercator Ocean system's quality after the loss of the two altimeters.

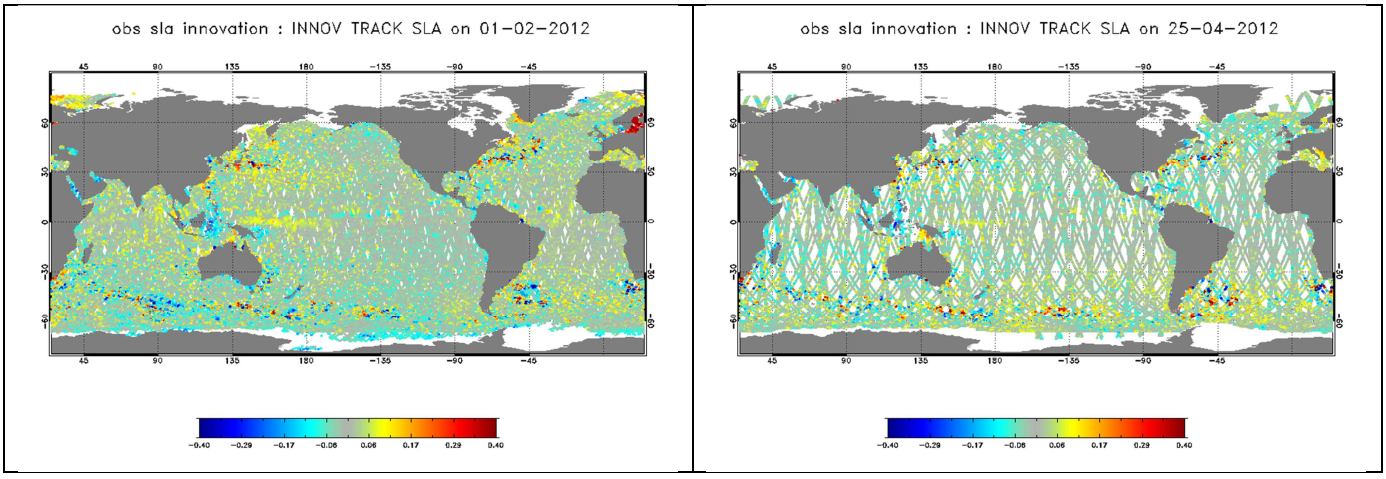

Figure 60: SLA innovations along tracks, with Jason-1, Jason-2 and Envisat altimeters (left) in February 2012, and the current configuration Jason-2 and Cryosat-2 (right).

First, operational diagnostics covering several months before and after the loss of Envisat were examined. Mean and RMS errors in salinity and temperature, as well as altimetry and SST assimilation scores did not exhibit any signal that could be for certain attributed to the lack of SLA measurements (not shown). An estimation of the intensity of the mesoscale activity did not display any slowing down and the mixed layer depth estimation did not show any clear degradation with respect to previous years (not shown). It was thus necessary to conduct OSEs in order to assess the impact of the number of altimeter data sources on an analysis and forecast system accuracy. In such studies, a reference run where all available observations are assimilated gives an absolute reference to compare with other experiments where one or more data sources are not assimilated. Conclusions of such studies highly

depend on the analysis system, the prescribed error and the model configuration and resolution.

VIII.2. OSEs with the Mercator systems

Three PSY3V3 simulations have been run for 4 weeks from August 11th 2010 to September 9th. The only differences between those simulations were the assimilated satellites (see Table 5). In situ and SST observations were assimilated as usual. Model misfits to the Envisat and Jason-1 SLA were still computed for diagnostic purposes. The goal is to identify the changes in the analysis when one (Envisat) or two (Envisat and Jason-1) are removed.
The diagnostics were mainly performed in the observation space. These type of diagnostics was considered as a good reference for analysis and forecast error estimation.

	Jason 1	Jason 2	Envisat
Run 1	**x**	**x**	**x**
Run 2	**x**	**x**	**no**
Run 3	**no**	**x**	**no**

Table 5: which SLA are assimilated?

Differences in the ocean state estimation on temperature at 300m are presented in Figure 61.

Changes from run 1 to run 2 (Envisat is removed) are restricted to small scale structures located in regions of strong eddy activity: western boundary currents, circumpolar current, confluence zone and Agulhas region. There is no significant change in the tropics. Comparisons with the ARGO temperature observations cannot help to measure these small changes. The spatial array of SLA tracks from Jason 1 and 2 seems sufficient to control all of the model scales in the different regions, except in regions where eddies dominate the ocean dynamics. Smaller scale structures require a denser observation array to be estimated.

Changes from run 1 to run 3 (only Jason-2 is assimilated) are far stronger: the SSH differences reach at least 2 cm almost everywhere (not shown). At 300m temperature differences reach 0.5 to 1°C locally. For our experiment and in our configuration, we can already establish that there is a great qualitative drop when we decrease the number of SLA sources from 2 to 1, even greater than from 3 to 2.

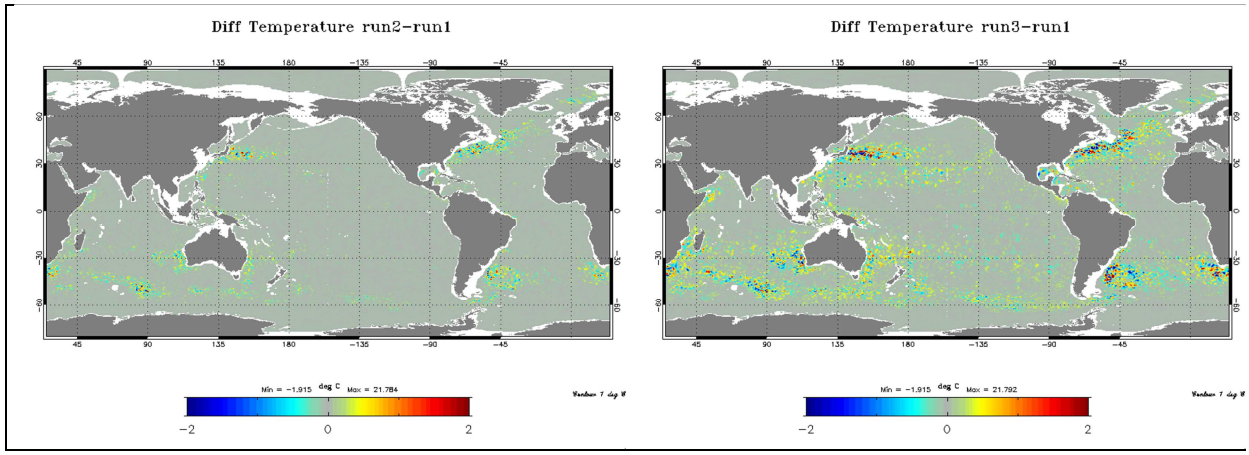

Figure 61: Temperature difference near 300m (°C) between run2 and run1 (left) and between run3 and run1 (right) on September 2nd, 2010 (colorbar is from -0.1 to 0.1 meters).

It is quite challenging to know which run is closer to the "true" ocean state from those figures. One way to answer is to compute the differences between observations and their model counterparts, in the three runs. The differences should be within the error bar to consider the simulation as successful for a given data type comparison.
This has been done in the study, for different observed variables: SLA misfit statistics have been computed as well as salinity and temperature mean and RMS misfits on profiles, and followed along the run period. In global mean and in most of the regions, the impact is weak but it is visible and tends to deteriorate when one or two satellites are assimilated instead of three (not shown). A longer simulation (a few months) would probably have shown a greater impact. Consequences can be seen at different depth for both temperature and salinity: the SSH data gives information on the T and S variables integrated vertically on the water column. For SLA misfit statistics specifically, we reach the following conclusion: the transition from 3 to 1 SLA source causes a decrease in the system performances of about 10 to 15%.

VIII.3. Conclusions

Constraining the Mercator system PSY3V3 with 2 satellites instead of 3 does not lead to large changes. A third satellite such as Envisat, with a larger instrumental error than the others, does not impact a lot the ocean estimation which already benefits from other information from the model forecast, in situ, SST data and the 2 Jason satellites whose tracks are complementary and offer a homogeneous coverage. The impact of the removal of Envisat is visible only in regions dominated by a strong eddy activity: small scale structures require denser observation coverage to be properly estimated.

From the literature, reducing the number of satellite to only one should lead to a much larger impact. It is in agreement with our results obtained when only Jason 2 is available. The quality of the analysis is clearly degraded and even the SLA misfit to the remaining altimeter is not as good as with 2 or 3 satellites. The system is not optimal any more and tends to drift away in time.

Those results cannot be extended to the Cryosat case (DR3) which has a very different "groundprint" leaving large regions free of data, more precisely larger than the model scale and analysis scale.

All the studies presented here are based on assimilation of SLA data in a numerical model in addition to other data sets. The results differ from the impact studies in the context of 2D mapping of SLA (by Pujol et al, 2012) where large errors were diagnosed following the loss of Envisat. Our results show that the Mercator Ocean global forecasting system is less demanding on data. The dynamical model brings useful information, and ensures spatio-temporal continuity when 2 satellites like Jason1 and 2 are available. This does not demonstrate yet that more than 3 satellites are needed to obtain accurate results, at least in the ¼° system PSY3, but it can be inferred from earlier results with PSY2 that 3 or more satellites are indeed necessary to obtain the nominal level of surface accuracy (SLA, currents, possibly MLD) in higher resolution system. When only one satellite constrains PSY3 or PSY2, the equilibrium of the entire system is lost. The combination of Jason 1 and 2 seems in fact to be optimal for PSY3. This can be due to the fact that the number of "efficient observations" at one given analysis location is probably reached. The prescribed error levels are currently under evaluation as some recent diagnostics (Desroziers, 2005) show that more information could be derived from the same number of observations in some regions.

Future work includes more specific diagnostics not only based on statistics but also on spatial structure identification (filaments), mixed layer depth characteristics, spatial scale analysis and observation efficiency (DFS). Such experiments should also be done in the 1/12° system, PSY2V4.

references

Pujol M.-I., G. Dibarboure, P.Y. Le Traon and P. Klein. Using high resolution altimetry to observe mesoscale signals. J. Atmos. Oceanic Technol., in press

G. Desroziers, L. Berre, B. Chapnik, P. Poli, Diagnosis of observation, background and analysis-error statistics in observation space, Quarterly Journal of the Royal Meteorological Society, Volume 131, Issue 613, pages 3385–3396, October 2005, Part C.

I Annex A

I.1. Table of figures

II Annex B

II.1. Maps of regions for data assimilation statistics

II.1.1. Tropical and North Atlantic

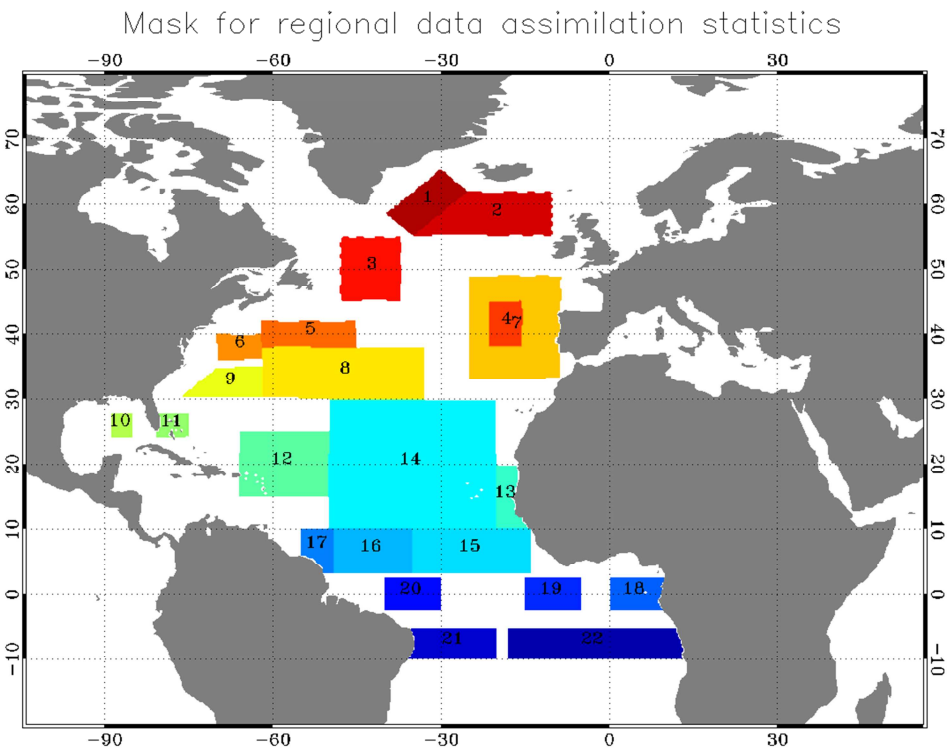

1	Irminger Sea
2	Iceland Basin
3	Newfoundland-Iceland
4	Yoyo Pomme
5	Gulf Stream2
6	Gulf Stream1 XBT
7	North Medeira XBT
8	Charleston tide
9	Bermuda tide
10	Gulf of Mexico
11	Florida Straits XBT
12	Puerto Rico XBT
13	Dakar
14	Cape Verde XBT
15	Rio-La Coruna Woce
16	Belem XBT
17	Cayenne tide
18	Sao Tome tide
19	XBT - central SEC
20	Pirata
21	Rio-La Coruna
22	Ascension tide

II.1.2. Mediterranean Sea

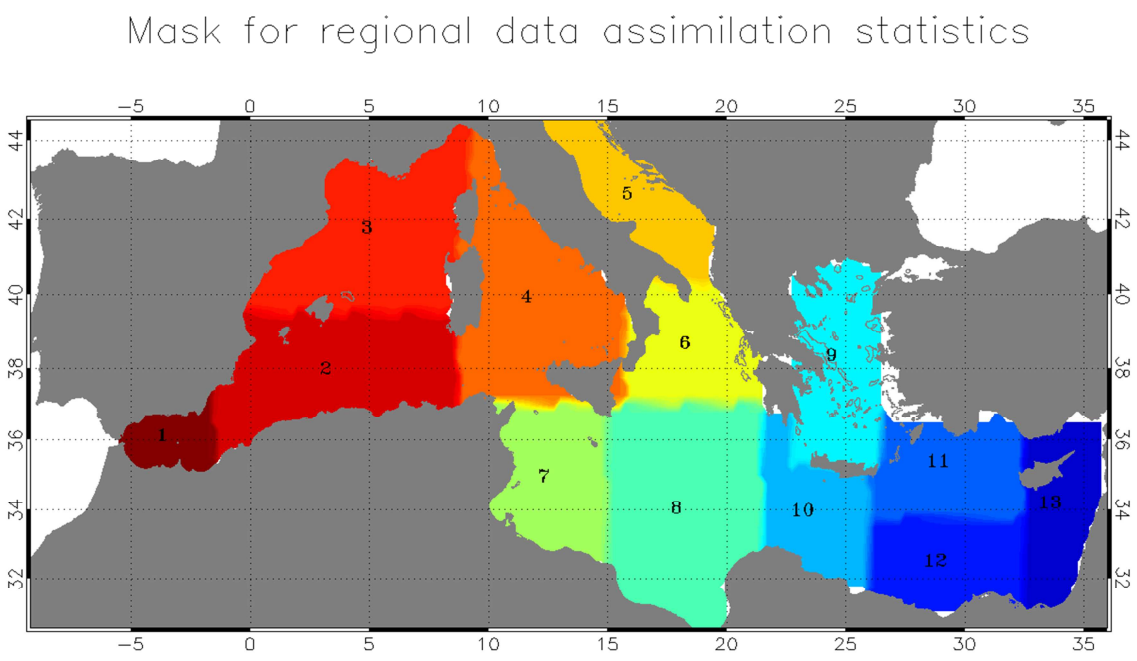

1	Alboran
2	Algerian
3	Lyon
4	Thyrrhenian
5	Adriatic
6	Otranto
7	Sicily
8	Ionian
9	Egee
10	Ierepetra
11	Rhodes
12	MersaMatruh
13	Asia Minor

II.1.3. Global ocean

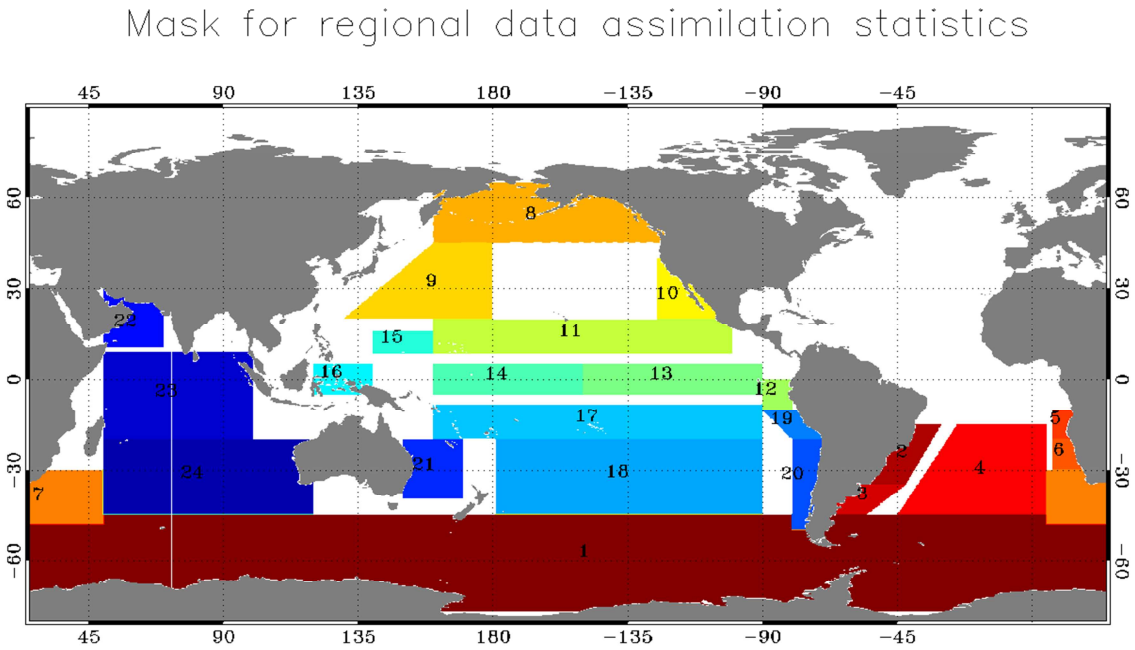

1	Antarctic Circumpolar Current
2	South Atlantic
3	Falkland current
4	South Atl. gyre
5	Angola
6	Benguela current
7	Aghulas region
8	Pacific Region
9	North Pacific gyre
10	California current
11	North Tropical Pacific
12	Nino1+2
13	Nino3
14	Nino4
15	Nino6
16	Nino5
17	South tropical Pacific
18	South Pacific Gyre
19	Peru coast
20	Chile coast
21	Eastern Australia
22	Indian Ocean
23	Tropical indian ocean
24	South indian ocean

III Annex C

III.1. Quality control algorithm for the Mercator Océan drifter data correction (Eric Greiner)

Before estimating the bias, it is essential to conduct a quality control. We must consider an individual monitoring of buoys, and a comparison with the geostrophy and windage. In real time, this is not possible, and I propose below a simple test developed by position (date by date) which involves only the mean wind (2 days) and the buoy drift. Basically, we found drifters where drift is close to argue between 0.2 and 3% of the wind (almost the same direction with a drag corresponding to a loss of drogue). For these buoys, if the contamination is real, then the error due to the wind is important with respect to current real at 15m depth. We test different values of windage (wind effect for a fraction of a given wind between 0.2% and 3%). If a questionable observation is found for a given windage, we estimate a correction. We apply at the end an average correction QC (windage among all acceptable). We although increase the error of observation. Note that in delayed time, we could correct all the data from the buoy, at least in a 10-day window. **Note however that a buoy that has lost its drogue can give a good measure if the wind is low**

- **No anomaly : slippage correction of 0.07% of the 10m wind speed**
- **Windage > 0.2% or < 3% correction of 1% of windage**

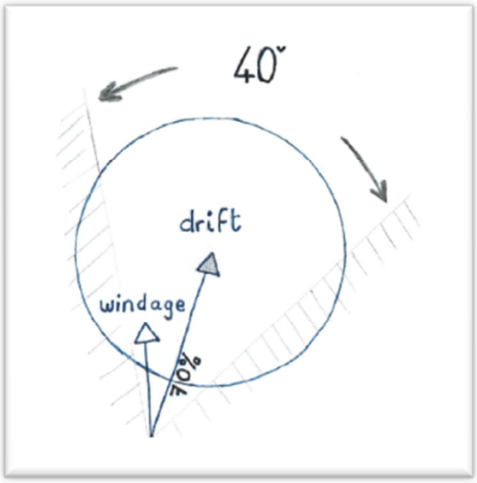

Figure 62 : illustration of QC: Quality test example chosen for windage (eg. 1%) we reject or correct a drift that differs little from the windage (less than 70% of the drift angle <40 °)

Note that a correction of more than 3% is not normally possible (construction of the buoy). This may correspond to breaking waves and swell. Between 2% and 3%, there is ambiguity between Stokes and windage. In other words, it is likely that beyond 2%, we eliminate all or part of the effect of waves and swell. If waves and swell are not aligned with the mean wind (swell remote for example), then the correction will be approximate. Ideally, you should use the Stokes drift from a wave model like Wavewatch3.

When calculating the equivalent models with AOML positions, which were filtered to remove 36h gravity waves and reduce positioning errors, we must :

- **add 0.07% wind averaged over 48h 10m : slippage correction**
- **windage correction and modify the error**